Stony Brook University

Transverse Movements of the Components of the Lipid Bilayer

A Dissertation Presented

by

Jamie LeBarron

to

The Graduate School

in Partial Fulfillment of the

Requirements

for the Degree of

Doctor of Philosophy

in

Physiology and Biophysics

Stony Brook University

December 2016

Stony Brook University

The Graduate School

Jamie LeBarron

We, the dissertation committee for the above candidate for the

Doctor of Philosophy degree, hereby recommend

acceptance of this dissertation.

Dr. Erwin London – Dissertation Advisor
Professor Dept. of Biochemistry and Cell Biology

Dr. Mark Bowen - Chairperson of Defense
Associate Professor Dept. of Physiology and Biophysics

Dr. Suzanne Scarlata – Committee Member
Professor Dept. of Physiology and Biophysics

Dr. David Thanassi – Committee Member
Professor and Interim Chair Dept. of Molecular Genetics
Stony Brook University

This dissertation is accepted by the Graduate School

Nancy Goroff

Interim Dean of the Graduate School

Abstract of the Dissertation

Transverse Movements of the Components of the Lipid Bilayer by

Jamie LeBarron

Doctor of Philosophy

in

Physiology and Biophysics

Stony Brook University

2016

Cell membranes are a complex mixture often composed of approximately equal parts lipid and protein molecules. Lipids are amphipathic, having polar headgroups that prefer to associate with water and hydrophobic tails that self-associate away from water. As a result, the lipids in cell membranes exist in the form of a lipid bilayer, with lipid polar headgroups facing outwards towards water and tails grouped together in the middle. Proteins embedded in this bilayer facilitate the movement of molecules across this barrier. The molecules that form the membrane have an asymmetric distribution, with different lipids being preferentially found on one side of the bilayer or the other and membrane proteins having a definite, defined orientation. In this work, we investigated how lipid and protein structure either assist or hinder their movement across the lipid bilayer. Using simple peptides as models for proteins, we have shown that peptides accelerate the transleaflet movement (flip-flop) of lipids across the lipid bilayer in a time- and sequence-dependent manner. We also investigated the effect of polar amino acid residues located in the membrane, and the effect of different types of lipids of the rate of flip-flop. In a second study, we investigated what polar sequences at the ends of hydrophobic peptides were able allow the peptide to move across membranes, or retarded such movements. We found that peptides with relatively large and polar sequences attached at their ends were able to pass through a biologically relevant membrane rapidly, i.e. in less than 10 sec. The amount of cholesterol limited peptide movement across the bilayer, but even then only at a detectable level for the peptide with the longest, and most polar end sequence. These results have implications membrane protein maturation, and mode of membrane penetration for certain toxins, and for control of protein and lipid localization in our new asymmetric membrane preparations, which mimic cell membranes more closely than prior artificial membranes.

Dedication Page

I would like to thank ….

The Committee members and Dr. Erwin London, their tolerance.

My lab mates, past & present; for teaching me what I needed to know, and then those who made me feel smart when I taught them

Mel Bonnette, Thanks for everything

Various friends from LI, also past and present, who I enjoyed board games with, or panic studying, or movies, or *moving,* or a little B &E.

Everyone at home, who has tolerated me trying to accomplish this crazy thing.
In no particular order:

Mom & Dad

Grandmas & Grandpas :/

More relatives than I can remember (the girls, their kids, aunts and uncles, etc)

Dr. John Paige & Chris Finn

And of course my girlfriend, Ana, for **tolerating** me, and giving me a swift kick from time to time.

Frontispiece

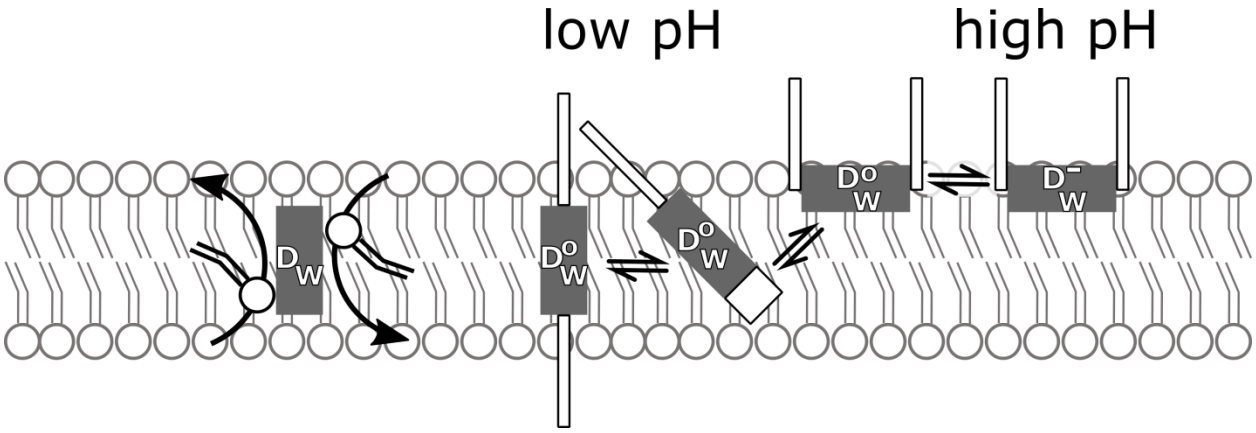

Table of Contents

List of Figures

List of Tables

List of Abbreviations

1/10 PBS	1 mM Na_2HPO_4, 15 mM NaCl
chol	cholesterol
DAG	diacylglycerol
DEiPC	1,2-dieicosenoyl-*sn*-glycero-3-phosphocholine
DEuPC	1,2-dierucoyl-sn-glycero-3-phosphocholine
DMoPC	1,2-dimyristoleoyl-*sn*-glycero-3-phosphocholine
DOPC	1,2-dioleoyl-*sn*-glycero-3-phosphocholine
DOPG	1,2-dioleoyl-sn-glycero-3-phospho-(1'-rac-glycerol)
DPoPC	1,2-dipalmitoleoyl-*sn*-glycero-3-phosphocholine
ER	endoplasmic reticulum
HPLC	High-Pressure Liquid Chromatography
LUVs	large unilamellar vesicles
MALDI-TOF	matrix assisted laser desorption ionization-time of flight
MLVs	multi-lamellar vesicles
Mol%	molar fraction
N_0K_2-flanked	KKLALALLLDWLLLLALALKK
N_2K_2-flanked	NNKKLALALLLDWLLLLALALKKNN
N_6K_2-flanked	NNNNNNKKLALALLLDWLLLLALALKKNNNNNN
NaDt	$Na_2S_2O_4$
NBD-PC	1-acyl-2-(6-[(7-nitro-2-1,3-benzoxadiazol-4-yl)amino]hexanoyl)-sn-glycero-3-phosphocholine
$p(LA)_6$	KKGLALALAWLALALAKKA
PBS	10 mM Na_2HPO_4, 150 mM NaCl

PC	phosphatidylcholine
PE	phosphatidylethanolamine
pL_{14}	KKGLLLLLLLWLLLLLLLKKA
pL_{15}(D10)	KKLLLLLLLDWLLLLLLLKK
pL_9A_6(D10)	KKLALALALDWLLALALALKK
PM	plasma membrane
Polio-flanked	KLFAGHQLALALALDWLALALALKLFAGHQ
POPC	1-palmitoyl-2-oleoyl-sn-glycero-3-phosphocholine
POPE	1-palmitoyl-2-oleoyl-sn-glycero-3- phosphatidylethanolamine
POPS	1-palmitoyl-2-oleoyl-sn-glycero-3- phosphatidylserine
PS	phosthatidylserine
SM	sphingomyelin
SUVs	small unilamellar vesicles
TFA	trifluoroactetic acid
TM	transmembrane
Tris	$(HOCH_2)_3CNH_2$

Acknowledgments

The text of this dissertation in part is a reprint of the materials as it appears in

Biochimica et Biophysica Acta (BBA) – Biomembranes
&
Langmuir

The co-author listed in the publications directed and supervised the research that forms the basis for this thesis or dissertation.

Permissions have been obtained from the appropriate individuals.

Chapter 1: Introduction

The cell is defined as the smallest thing that is alive. In eukaryotic cells the plasma membrane forms the barrier of what the cell is and controls, and what is the exterior environment. Nutrients and waste products must cross this barrier, along with signals to and from the environment. Proteins that are embedded into the plasma membrane allow these signals to cross, and also allow the cell to control the flow of nutrients and waste. Concomitant with these diverse functions that must be performed; the plasma membrane is appropriately complex.

The eukaryotic plasma membrane functions as a barrier in two primary ways. The first is it has lipid bilayer. In fact, it is the thickest membrane in the cell, with the highest amount of sphingomyelin (SM) and almost half of lipids being cholesterol (see below). It is known that as the percentage of cholesterol in a membrane increases, the membrane thickness increases (Hung *et al.*, 2007) and the fluidity of the membrane decreases (de Kroon *et al.*, 2013; Engberg *et al.*, 2015; Hung *et al.*, 2007; Stachowiak *et al.*, 2012). These properties likely make it a stronger barrier. The second way it acts as a barrier is that it is approximately half protein, by weight. The topology and organization of most membrane proteins suggests that the hydrophilic domains of these proteins likely serve as a shell, preventing direct access to lipids (Stachowiak *et al.*, 2012; van Meer *et al.*, 2008).

In addition, both membrane lipids and proteins have the capability to signal across membranes. Protein-protein interactions in which the membrane is involved are well-documented, whether it be for G-protein coupled receptors (Munk *et al.*, 2016), receptor tyrosine kinases (Delos Santos *et al.*, 2015), or physical contact with other cells (Alanko & Ivaska, 2016). Lipid signaling across membrane is less well characterized. However, the behavior of phosphatidylserine (PS) is interesting in this regard. Under normal circumstances PS is known to reside only in the inner leaflet of the bilayer (Balasubramanian & Schroit, 2003). One of the best characterized lipid based signal is that of transleaflet movement, or flip-flop, of PS from the inner to the outer leaflet. Although this movement was first described as a pro-

apoptotic signal, cellular response to PS flip-flop can have diverse results involving blood coagulation, bone and neuronal remodeling, or egg fertilization (Bevers & Williamson, 2016). Other signaling cascades propagated by lipids have been categorized including ceramide (Mencarelli & Martinez-Martinez, 2013), lysophosphatidic acid (Sheng *et al.*, 2015), and phosphoinositides (Waugh, 2015).

Eukaryotic lipid synthesis and localization

The fact that lipid signaling can involve movement of lipids across the bilayer raises the question: how are lipids synthesized, organized and localized to one or another leaflet of the membrane in the first place? All lipids are amphipathic in that they have both hydrophilic headgroups and hydrophobic regions. The lowest energy state of these amphipathic molecules is two layers of lipids with a hydrophobic core and headgroups interacting with water; the lipid bilayer. Even the homogenous "fluid" of the classical fluid-mosaic model (Singer & Nicolson, 1972) is recognized as being comprised of thousands of chemically distinct lipids (Sud *et al.*, 2007). However, the mammalian membrane is primarily composed of four "structural" lipid types (SM, PS, phosphatidylcholine, phosphatidylethanolamine) (van Meer *et al.*, 2008) plus cholesterol. While these lipids form both leaflets, in different amounts, lipids are synthesized asymmetrically on the endoplasmic reticulum (ER). The proteins responsible for lipid synthesis are typically tethered to the membrane with the enzymatic domains located only in the cytosol (see below and reviewed in (van Meer *et al.*, 2008)).

The most prevalent type of lipid (~50%) in eukaryotic cells is phosphatidylcholine (PC) (Daleke, 2008; Takamori *et al.*, 2006). PC is asymmetrically distributed across the plasma membrane, with it primarily being found on the outer leaflet (Daleke, 2008). PC's zwitterionic headgroup causes it to not contribute to net charge on a lipid leaflet, while the size of its headgroup leads to preferential interactions with cholesterol (see below and Figure 1.1). Most *de novo* synthesis of PC begins with synthesis of diacylglycerol (DAG) (Reviewed in (Bell & Coleman, 1980)). The enzyme that forms DAG, which serves as a checkpoint for lipid synthesis,

has been shown to strongly bind to cytosolic leaflet of the ER (Han *et al.*, 2006). If later lipids are to be unsaturated, the DAG molecule that they are composed of must be de-saturated. This function has been localized to the ER (Heinemann & Ozols, 2003), and its structure indicates that the reaction center for the de-saturation reaction faces the cytosolic leaflet (Bai *et al.*, 2015). Possibly to match the location of DAG synthesis, the enzymes that synthesize PC are found on the cytosolic leaflet in either the ER or Golgi (Henneberry *et al.*, 2002). Therefore, PC synthesis is asymmetric with respect to the bilayer, with both acyl chain and PC headgroup synthesis occurring preferentially in the cytosolic leaflet of the ER.

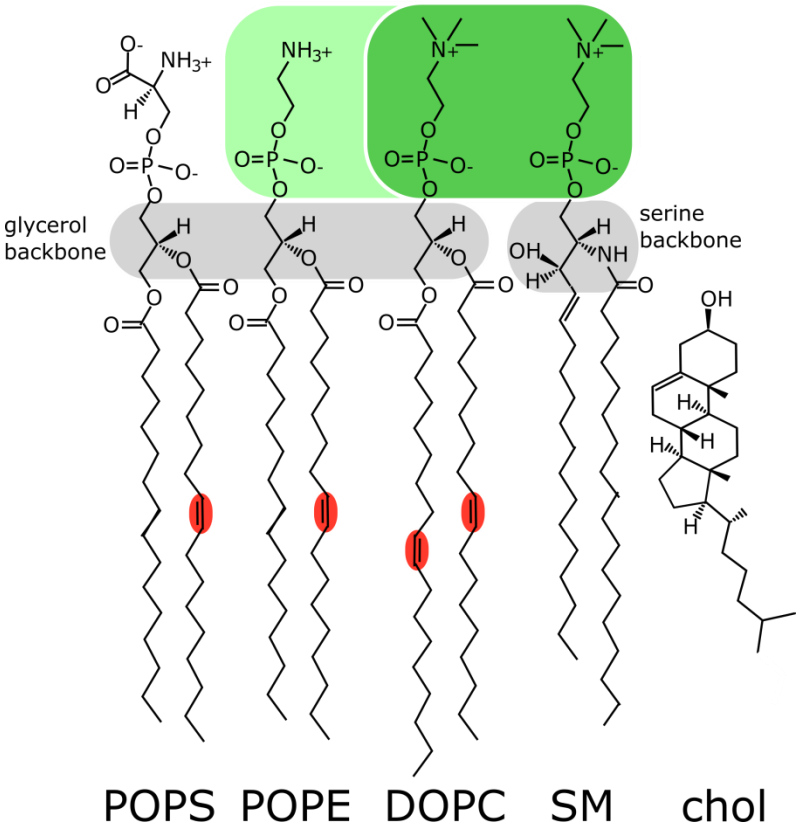

Figure 1.1: Examples of eukaryotic structural lipids and cholesterol. Electrically neutral lipid headgroups are highlighted in green, large phosphatidylcholine headgroups highlighted in dark green. Cis double bonds in acyl chains of lipids highlighted in red. Backbones for each lipid (either glycerol or serine) are highlighted in grey. Lipids depicted are: POPS, 1-palmitoyl-2-oleoyl-sn-glycero-3- phosphoserine; POPE, 1-palmitoyl-2-oleoyl-sn-glycero-3-phosphoethanolamine; DOPC, 1,2-dioleoyl-*sn*-glycero-3-phosphocholine; SM, sphingomyelin (representative structure of SM from porcine brain); chol, cholesterol.

Phosphatidylethanolamine (PE) is the second most prevalent structural lipid, composing of roughly one quarter of all lipids in eukaryotic membrane (Zinser *et al.*, 1991). Unlike PC, PE is found more in the inner leaflet of the eukaryotic PM (Daleke, 2008). Previous work has suggested that the presence of PE in the inner leaflet may have a stabilizing effect for lipids in terms of preventing movement of lipids from one leaflet to the other (Kol, van Laak*, et al.*, 2003; Son & London, 2013b). The PE headgroup shares structural and electrical similarities with PC. However, is lacks the three methyl groups of PC (Fig. 1.1), and does not have the preferential interactions with cholesterol that PC does (Engberg *et al.*, 2015; Vermeer *et al.*, 2007). The structural similarities between PE and PC are reflected by PE synthesis being performed by a subset of the enzymes that forms PC (Henneberry *et al.*, 2002). The overlap between enzymes responsible for PC and PE synthesis means that PE synthesis occurs asymmetrically in a fashion similar to PC, in the cytosolic leaflet of the ER.

Phosphatidylserine (PS) is the most prevalent negatively charged lipid in eukaryotic membranes (Daleke, 2008; Takamori *et al.*, 2006). Serine itself is zwitterionic, so that with the phosphate from the donor lipid PS has a net negative charge. PS is usually located on the inner leaflet of eukaryotic PM (Daleke, 2008). However, it can be found on the outer leaflet of several types of cancerous cells (Ran *et al.*, 1998; Rao *et al.*, 1992; Utsugi *et al.*, 1991). When it is found on the outer leaflet of normal cells PS can be a signal for blood coagulation (Bevers *et al.*, 1983), and apoptosis (Fadok *et al.*, 1992). PS is formed when the headgroup of either PC or PE is exchanged for the amino acid serine (Stone *et al.*, 1998; Stone & Vance, 1999). PS synthase in mammals has been localized to specific regions of the ER (Stone & Vance, 2000). Although no structure for PS synthase has yet been solved, the orientation of other lipid synthases suggests that the PS synthesis occurs on the cytosolic side of the ER membrane. In addition, the fact that ER and mitochondria share PE, the precursor of PS, in a fashion involving the apparent interaction between ER and mitochondrial membranes (Stone & Vance, 2000), also suggests that the PS synthesis occurs on the cytosolic side of the ER membrane.

Sphingomyelin (SM) may serve a similar structural role in eukaryotic plasma membranes as PC. Like PC, SM is preferentially found on the outer leaflet of the PM (Daleke, 2008), is

zwitterionic, and has an identical headgroup as PC which results in a similar favorable interaction with cholesterol ((J. Huang & Feigenson, 1999)and Figure 1.1). Because SM uses serine as a backbone, it does not utilize DAG in its synthesis, and uses a dedicated biosynthesis pathway separate of the other structural lipids (reviewed in (Futerman & Riezman, 2005)). There are many different enzymes in SM synthesis, and SM intermediates are asymmetrically synthesized. Seven enzymatic steps in SM synthesis have been localized in terms of leaflets, with four steps occurring on the cytosolic leaflet (Delon *et al.*, 2004; Mandon *et al.*, 1992; Michel & van Echten-Deckert, 1997; S. Yasuda *et al.*, 2003) and three in the lumen (Kihara *et al.*, 2003; Sprong *et al.*, 1998; Yamaoka *et al.*, 2004) of the ER or Golgi body. The synthesis of SM is an excellent example of the importance of lipid asymmetry, and how controlled lipid transleaflet diffusion (to move the products along the pathway) is required for homeostasis.

Cholesterol, the remaining major component of eukaryotic membranes, is electrically neutral. Its polar headgroup is only a single hydroxyl, the smallest headgroup of the structural lipids (Figure 1.1). Membranes of PC have been shown to tolerate up to 60 mol% of cholesterol (J. Huang & Feigenson, 1999). Cholesterol is believed to be located in both leaflets of membranes, and has been claimed to be concentrated slightly in the cytosolic leaflet (Mondal *et al.*, 2009). The umbrella model of cholesterol interactions states that the hydrophilic portion of cholesterol (a single hydroxyl group) does not offer enough protection for the rest of the molecule from water. To minimize unfavorable interactions between the polar water and the hydrophobic portion of cholesterol, PC or SM headgroups reorient to protect the cholesterol from the water (like an umbrella) (J. Huang & Feigenson, 1999). PC and SM membranes thicken upon addition of cholesterol, as extended acyl chain conformations that make room for cholesterol form (Engberg *et al.*, 2015; Hung *et al.*, 2007; Leftin *et al.*, 2014; Vermeer *et al.*, 2007). While PC and SM have the same headgroups, SM is believed to associate with cholesterol even better because it tends to be more saturated (fewer on no double bonds) (Futerman & Riezman, 2005). Saturated acyl chains take up less space (Kucerka *et al.*, 2005), allowing cholesterol to fit under the headgroup more easily.

Because of its unique structure the synthesis of cholesterol is distinct from that of the other structural lipids. Direct synthesis of cholesterol from acetyl-CoA requires a minimum of 21 separate steps, along two alternate pathways/branches, to form its rigid planar four-member ring and eight carbon acyl chain tail (L. J. Sharpe & Brown, 2013). Regulation of some cholesterol synthesis enzymes has been shown to involve their movement off the ER membrane. The last enzyme in the cholesterol pathway (DHCR24) relocates to the nucleus under either reactive oxygen species or oncogenic stress stimulus (Wu *et al.*, 2004). Enzymes from each branch of cholesterol synthesis have been shown to relocate from ER membrane to lipid droplets in response to an accumulation of free fatty acids (Hartman *et al.*, 2010; Ohashi *et al.*, 2003; Wan *et al.*, 2007). The ability of these enzymes to relocate in this fashion indicates that they are on the cytosolic leaflet of the ER, indicating that at least these steps of cholesterol synthesis occur asymmetrically.

Spontaneous lipid flip-flop

As the discussion above indicates, lipid biosynthesis takes place asymmetrically across the lipid bilayer, and lipids are often asymmetrically distributed. However, the leaflet on which lipid synthesis occurs and the final location of lipids is not always the same. This requires that lipids move across membranes. There remains considerable uncertainty about how lipid asymmetry is maintained and destroyed. Asymmetry should be limited by the transverse diffusion of lipids (flip-flop), i.e. the rate at which lipids spontaneously flip across the lipid bilayer (Figure 1.2). As membrane asymmetry is so integral to the cellular membrane (see above), the quantification of lipid flip-flop has been addressed in a number of studies using various techniques. One approach used is lipids are fluorescently labeled, and allowed to flip-flop for a given time, and then the fluorescence on the outside of the membrane is destroyed. The remaining fluorescence is the amount of lipid that flip-flopped over the given time (McIntyre & Sleight, 1991). Using the protection assay and vesicles made of egg PC:egg PG it has been found that lipid flip-flop is highly dependent on headgroup, with flip-flop half times of ~ 1 hr (PE) to > 2 days (PC) (Matsuzaki *et al.*, 1996). The composition of the lipid membrane that the labeled lipid is embedded in, has also been investigated. As the degree of unsaturation

increases in a lipid membrane, the labeled lipid increases its flip-flop rate as well (Armstrong *et al.*, 2003). Similar behavior was found in when one lipid leaflet was fully saturated SM, and the other leaflet was composed of PC with varying degrees of unsaturation. This indicates that these findings are not artifacts of the use of labeled lipids, and can occur in asymmetric membranes (Son & London, 2013a).

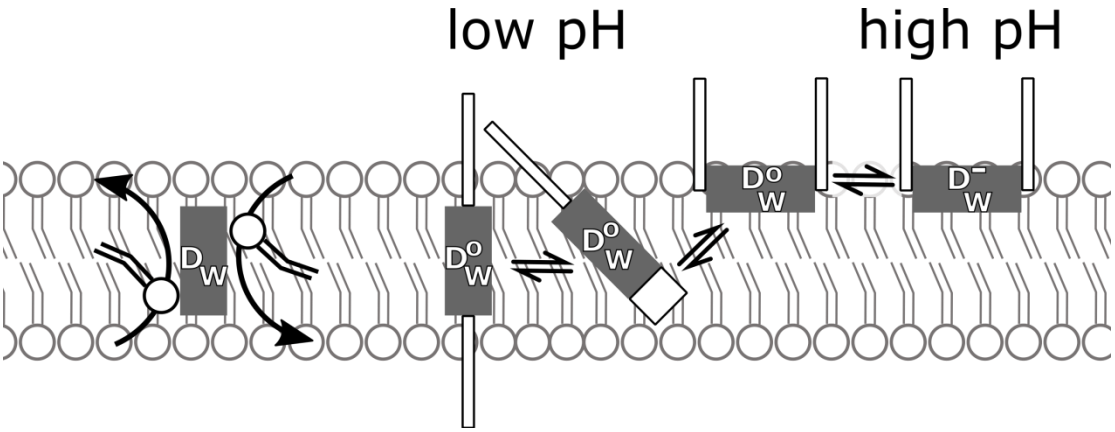

Figure 1.2: Schematic of the transverse movements of polar molecules through an idealized lipid bilayer. Hydrophobic peptide of the type studied in this thesis forming a TM helix is shown as a grey cylinder, with Trp and Asp with charge state shown. **Left:** schematic representation of lipid molecules diffusing through the bilayer (flip-flop) with polar headgroups shown as white circles that can interact with a TM helix. **Center and right:** Peptide TM to membrane associated non-TM interconversion. Skinny white rectangle represents polar juxtamembrane (JM) residues in an extended configuration. White square represents JM residues in a helical configuration.

The exact conformation of lipids during flip-flop is unknown. Lipid flip-flop requires that the hydrophilic portion of the molecule necessarily passes through the hydrophobic core of the membrane (Figure 1.2). For a hydrophilic headgroup to pass through a membrane it must either be dehydrated or the bound water must also cross the bilayer. Either option is energetically unfavorable, which is one likely reason spontaneous flip-flop can be so slow (i.e. with a half time on the order of days) in simple lipid bilayers (discussed above and (Dicorleto & Zilversmit, 1979 ; Rothman & Dawidowicz, 1975; Sapay *et al.*, 2010; Son & London, 2013a, 2013b)). Labeled lipids have been shown to flip-flop faster if attached to a smaller headgroup

lipid than when attached to a larger headgroup lipid, regardless of the remaining vesicle composition, which may indicate that smaller headgroups are easier to dehydrate or bind to water in the bilayer, or perhaps need to bind less water in the first place (Kol, van Laak*, et al.*, 2003).

Lipid flip-flop in different lipid compositions have also been investigated using planar-supported lipid bilayers. This technique adsorbs one leaflet of a lipid bilayer onto the sensing surface, typically with some molecular cushion between the lipid and the surface. Later, the other leaflet of the bilayer is added to the first, resulting in a flat supported bilayer without curvature. Results from this technique (Brown & Conboy, 2013; Liu & Conboy, 2005) suggest headgroup labeled lipids flip-flop at a much slower rate than natural lipids, which might be expected when a lipid has a large headgroup. It was also found that lipids with acyl chains shorter than the remaining lipids flip-flop faster than the typical lipid. Increasing the amount of short chain lipid increased its own flip-flop rate, but the remaining lipids were undisturbed (Brown & Conboy, 2013; Liu & Conboy, 2005). It was also found that the quantitative half times for PC lipids was consistently found to be ~ 2 hr, much faster than vesicle based experiments. Besides an effect from the planar nature of these samples, there is no obvious explanation why flip-flop rates using these different experimental systems should be so different. One possibility is that planar bilayers have more packing defects than vesicles.

Interestingly, unlike the case with vesicles, this technique allows control of lateral pressure between lipids during experiments. It was found that at lower lateral pressure, the rate of flip-flop increased dramatically. This may involve water penetration into the bilayer. It was proposed that the lower pressure allowed deeper invasion of water into the membrane, possibly a result of their being more disordered lipids (Anglin *et al.*, 2010), and it has been proposed in a study by a different group that the barrier to flip-flop is decreased by transient water pore formation (Sapay *et al.*, 2010). If more disordered lipids create a long-lived water defect due to their looser packing, this may accelerate flip-flop because the lipid headgroup no longer needs to desolvate. This may explain the observation of faster flip-flop in bilayers with highly unsaturated lipids, which pack loosely (Armstrong *et al.*, 2003; Son & London, 2013a).

Additional evidence supports the proposal that packing/order of the lipid is relevant. Inclusion of cholesterol into various membranes has been shown to decrease lipid flip-flop rate (Kol, van Laak*, et al.*, 2003; Langer & Langosch, 2011). While increasing cholesterol content thickens the membrane (Hung *et al.*, 2007), the increase in lipid packing may have a stronger effect (Bhattacharya & Haldar, 2000; Hung *et al.*, 2007; Kol, van Laak*, et al.*, 2003; Leftin *et al.*, 2014; T. Yasuda *et al.*, 2015). These properties may partly explain why to prevent unwanted molecules entering the cell, the plasma membrane is the thickest and most tightly packed of the eukaryotic membranes (Pogozheva *et al.*, 2014), containing the highest cholesterol content (Pomorski & Menon, 2006).

With regard to the role of packing defects, it is interesting that another exception to the typically slow flip-flop rate of lipids is near the melting temperature (Tm), the temperature where a lipid transition between gel and disordered state of a pure lipid occurs. Using the fluorescence protection assay described previously, the flip-flop rates of vesicles of different lipid compositions were investigated at various temperatures. The least amount of fluorescence protection always occurred if the flip-flop occurred at the Tm of the lipids forming the vesicle. This acceleration of flip-flop is thought to be due to an increase of packing defects at Tm (John *et al.*, 2002). The sharp minimum in protection disappears when lipid compositions are no longer composed of a single lipid, whether that be from addition of cholesterol or using natural lipids with variable acyl chain length. Thus, while this work gives insight into biophysical properties, cellular membranes are complex mixtures, and therefore do not exhibit sharp thermal transitions that might be needed for such defects to form.

Consequences of loss of membrane asymmetry

Flip-flop in cells can be either beneficial or destructive, depending on various factors, hence the typical tight regulation of it in living cells. While the cell spends energy creating and enforcing asymmetry, equilibration of leaflet composition to destroy asymmetry is also tightly controlled and can be a part of normal cellular homeostasis. Movement of PS to the outer leaflet, by scrambling of lipids across the membrane, has been shown to be indicative of

differentiating myotubes (Sessions & Horwitz, 1983; van den Eijnde *et al.*, 2001). A classic outcome of PS movement to outer leaflet of cells is that as a pro-apoptotic signal (Fadok *et al.*, 1992; Martin *et al.*, 1995). Interestingly, the macrophage response to the apoptotic cells also involves PS scrambling on the macrophage (Callahan *et al.*, 2000; Fadok *et al.*, 2001).

Membrane proteins can actively accelerate lipid flip-flop

Clearly, tightly regulated lipid asymmetry must involve more than just spontaneous lipid flip, and the presence of TM proteins can greatly alter the lipid flip-flop rate (Figure 1.2). After lipid synthesis, primarily in the ER and Golgi body (see above), the eukaryotic cell uses considerable resources creating and maintaining the proper lipid asymmetry. The proteins responsible for maintaining, and sometime eliminating this asymmetry have been classified into “flippases” (proteins performing transbilayer lipid movement of lipids to the cytoplasmic leaflet), “floppases” (proteins moving lipids to the exofacial or luminal leaflet), or “scramblases” (which accelerate movement from a lipid from the leaflet of in which its concentration is highest to the other leaflet) (Daleke, 2003).

The best characterized flippases are the P4-ATPases, which have been shown to constitutively enhance asymmetry by moving PS lipids from the exofacial leaflet of the plasma membrane to the cytosolic leaflet (Tang *et al.*, 1996). Homologs have been found in higher organisms (Darland-Ransom *et al.*, 2008; Lenoir *et al.*, 2007), and the flippase activity is markedly increased in Golgi body (Muthusamy *et al.*, 2009), where lipid asymmetry is known to become more stringent. Mutations in a human protein in this class, ATP8B1, are known to cause two different forms of cholestatic disease as well as intrahepatic cholestasis of pregnancy (Folmer *et al.*, 2009). Missense mutations limited protein delivery at certain points, with disease severity correlating with degree of protein expression at plasma membrane (Folmer *et al.*, 2009). Although the physiological mechanisms are not completely mapped, it appears that these three diseases are caused by dysregulation of lipid asymmetry.

In contrast, scramblases are ATP-independent TM proteins that, as noted above, allow lipids to diffuse across leaflets down their concentration differential. These proteins destroy

asymmetry. One protein in this class, PLSCR1 has been shown to scramble various lipids, but when activated *in vivo* the net result is movement of PS to the outer leaflet (reviewed in (Kodigepalli *et al.*, 2015)). Other factors, such as interaction with specific proteins or lipid charge gradients could also influence asymmetry.

Simple TM helices can also accelerate lipid flip-flop

While the destruction of lipid asymmetry may sometimes be beneficial, lipid flip-flop is often destructive when it is caused by toxins, some of which are simple TM helices. Alamethicin is a well characterized helical toxic peptide from fungus. It has been shown to adsorb onto lipid membranes, and when a voltage pulse is applied lipid asymmetry is destroyed as flip-flop is accelerated through pores (Hall, 1981). Once formed, these alamethicin pores have been shown to be large, oligomeric and long-lasting (Wiedman *et al.*, 2013). Melittin, from bee venom, is another helix-forming peptide that has been shown to accelerate lipid flip-flop, but not through barrel stave pores as with alamethicin (Wiedman *et al.*, 2013). Instead, it is thought that melittin works as a monomer and reduces the effective thickness of the membrane, therefore accelerating lipid flip-flop (Anglin & Conboy, 2009)**.** Magainin 2 is a toxic peptide used defensively by some frogs, and because of dye efflux, is thought to form pores (Matsuzaki *et al.*, 1995). Because of the similarity of lipid flip-flop rates and dye movement (Matsuzaki *et al.*, 1996) and measurement of peptide orientation (Yang *et al.*, 2001) it is thought both magainin and melittin form pores composed of both peptide and lipids. These peptides are generally being investigated as cancer drugs (Biswas *et al.*, 2012), indeed some are found to be particularly specific to cancer cells due to higher exofacial PS (Leite *et al.*, 2015). The development of membrane toxins in such a wide variety of organisms argues their efficacy, and a shared molecular mode of action. It is possible that lipid flip contributes to this.

The ability to eliminate membrane asymmetry through flip-flop has also been seen in model hydrophobic peptides. To investigate peptide accelerated lipid flip-flop, the Leu-Ala repeat peptide is often used. This class of peptides has a hydrophobic TM region of repeating Leu-Ala

repeats, possibly with a polar residue in the middle, and hydrophilic residues at both peptide termini. A version with Trp at both termini (WALP) was shown to differentially accelerate flip-flop of fluorescently labeled lipids. Lys flanked residues accelerated flip-flop less. Similar to previous results (Kol, van Laak*, et al.*, 2003), flip of lipids with small charged headgroups were accelerated more than PC (Kol, van Laak*, et al.*, 2003). Research with His and Lys flanked peptides were shown to be less successful at lipid flip flop than Trp flanked (Kol *et al.*, 2001; Kol, van Laak*, et al.*, 2003). These peptides were TM and alpha helical, and loss of the TM region resulted in lack of peptide flip-flop. As long as the TM region is a minimum thickness, increasing its length had no effect on lipid flip-flop (Kol *et al.*, 2001). Work with a similar Leu-Val repeat indicated that TM regions too short for a membrane (negative hydrophobic mismatch) increased lipid flip flop, but also showed positive hydrophobic mismatch didn't effect lipid flip flop (Poschner *et al.*, 2010).

Both toxic and non-toxic peptides include hydrophobic residues in the center of TM regions, so the effect of their sequence has been investigated. Simple model peptides that include polar residues in the TM region and peptides with negative mismatch relative to the membrane bilayer accelerated lipid flip-flop (de Planque *et al.*, 2002; de Planque *et al.*, 1998; Kaihara *et al.*, 2013; Poschner *et al.*, 2010). In a peptide with positive mismatch, which was shown to not effect lipid flip-flop, the presence of either a positive or negative charge in the peptide accelerated flip-flop of both POPC and fluorescently labeled lipid (Kaihara *et al.*, 2013). Peptide accelerated flip-flop is not an artifact of model peptides having highly artificial sequences; it has been demonstrated for various natural sequences as well. The TM region of leader peptidase also induces flip-flop (Kol, van Dalen*, et al.*, 2003; Langer & Langosch, 2011; Langer *et al.*, 2013). While not their primary function, the much larger potassium channel KcsA (Kol, van Dalen*, et al.*, 2003; Langer & Langosch, 2011; Langer *et al.*, 2013), and opsins (Abell *et al.*, 2007; Goren *et al.*, 2014; Menon *et al.*, 2011) have also been reported to help destroy lipid asymmetry. These results support the hypothesis that accelerating lipid flip-flop is a common (but perhaps not universal) property of TM proteins (Kol *et al.*, 2001).

Membrane protein synthesis and insertion

Membrane proteins also cross lipid bilayers. To insert properly, most membrane proteins are passed to the translocon as they are synthesized by the ribosome (Cymer *et al.*, 2015; Denks *et al.*, 2014). The translocon is itself a multi-pass membrane protein of 10 TM helices arranged in a sideways "pacman" shape; with the hydrophobic "mouth" inside the membrane and the corners of the mouth forming a more hydrophilic pathway across the membrane (Breyton *et al.*, 2002). When membrane proteins are not being synthesized, it is believed that the cytosol and ER lumen remain separated by blocking the hydrophilic path at either end (Denks *et al.*, 2014; Tam *et al.*, 2005; Tanaka *et al.*, 2015). As nascent helices pass through the translocon, they may take two pathways. If the nascent helix is hydrophobic it may it may populate the hydrophobic crack (Tanaka *et al.*, 2015), leading to the opening of the lateral gate directly into the hydrophobic core of the membrane. If the nascent protein is hydrophilic, the plug of the translocon moves aside to allow the pre-protein to enter the ER lumen (Tam *et al.*, 2005). It is this hydrophilic pathway that extracellular hydrophilic loops that link TM helices likely follow. An alternate model for the movement of hydrophobic TM helices has been suggested, that proposes the lateral gate not as an all-or-nothing mechanism, but to provide a space for hydrophobic helices to "pop out" to the interface layer between the hydrophobic core and bulk water (De Marothy & Elofsson, 2015). This model is consistent with the experimental data, and is more conducive to recent results showing post-translational membrane protein topology changes (discussed below). Regardless of which model is correct, the translocon provides some pathway for peptides to enter and/or cross the membrane.

Maturation of membrane protein conformation can involve transmembrane movements of polar sequences

The folding of membrane proteins is regarded as a two-step process; the first step being the insertion of hydrophobic helices into the membrane (as discussed above) and the second step being any subsequent steps required to obtain a functional protein (Cymer *et al.*, 2015). One of

those maturation steps can involve topological rearrangements of the membrane protein, as has been shown for aquaporin 1 (AQP1). Initial experiments of AQP1 synthesis and topology using C-terminal deletion mutations resulted in a model of the protein that had four TM helices (Skach *et al.*, 1994). This was in conflict with both previous work and experiments that probed AQP1 topology using an epitope tag which resulted in showing the protein with six TM helices (Preston *et al.*, 1994). Later work using both large (142 residue) and small (14 residues) epitope insertions into AQP1 indicated that AQP1 initially only has four TM helices, but later matures into the canonical six TM form (Lu *et al.*, 2000). This change in topology requires significant post-translational topological changes including one TM helix flip, insertion of two helices into the membrane, and flipping of two hydrophilic extracellular loops across the membrane.

Another example of topological changes by movement of hydrophilic residues through the bilayer is linked to the natural functioning of the small multi-drug resistance protein EmrE. This membrane protein has four TM helices and can render *E. coli* resistant to small positively charged aromatic toxins (Schuldiner, 2009). Crystal structures confirmed that EmrE forms an anti-parallel homodimer (Chen *et al.*, 2007). Because it operates in an anti-parallel organization, this implies that the EmrE protein chain enters the ER membrane from one side (the cytosolic side with the ribosome), then ~50% of the protein molecules reverse topology. This topological change involves flipping four hydrophobic helices in the membrane, and passing three hydrophilic loops and two hydrophilic termini completely through the hydrophobic membrane (Chen *et al.*, 2007). Topological changes to EmrE have been shown to be so labile that single charged residues at the end of an artificial fifth helix appended to EmrE was shown to be able to affect the topology of the entire protein (Seppala *et al.*, 2010). It now appears that this dual topology forms co-translationally only while EmrE is still being passed through the translocon, not after (Woodall *et al.*, 2015).

In contrast to the examples discussed above, half of each molecule of *E.coli* lactose permease (LacY) has been shown to be able to completely reorient in the membrane (including hydrophilic loops crossing the membrane) even without the translocon present. LacY utilizes the high extracellular concentration of H^+ to pump a galactoside into the cell. LacY has two

domains of six TM helices arranged in a pseudosymmetrical fashion, with the binding sites for both ligands located in the cleft between protein halves (Guan & Kaback, 2006). Development of an *in vitro* system showed that the proper topology, but not membrane insertion, of the first half of LacY was dependent on the presence of PE lipid in the target membrane. More importantly, the proper topology of already inserted LacY developed after PE was synthesized (Bogdanov & Dowhan, 1998). Therefore, the rearrangement of six TM helices and several hydrophilic loops through the membrane was induced by the addition of PE. The assistance of other membrane proteins (e.g. translocon) could not be ruled out in those studies (Bogdanov & Dowhan, 1998), but the development of *in vitro* methods of delivering lipids to vesicles (Cheng & London, 2011; Cheng *et al.*, 2009) containing purified LacY, showed in a later study that the same topographical rearrangements could be induced by changing the lipid composition in the lipid vesicles, eliminating the possible involvement of other proteins in LacY rearrangement (Vitrac *et al.*, 2013; Vitrac *et al.*, 2015). The influence of PE on topology is not unique to lactose permease, PE has been shown to affect topology of γ-aminobutyric acid permease (Zhang *et al.*, 2005) and phenylalanine permease (Zhang *et al.*, 2003). Considering the antiparallel homodimer drug pump, and the influence of PE on the topology of several permeases, the hydrophobic core of the membrane is not the barrier to hydrophobic loops it was once considered.

Protein toxin insertion can involve transmembrane movements

While the translocation of hydrophilic portions of proteins through the hydrophobic core of a membrane can be required for protein maturation immediately after biosynthesis, in the case of protein toxin action during infection it can also occur long after protein synthesis. Protein toxins may bind to many different membrane proteins, but it often the toxin protein itself that breaches the host membrane (Williams & Tsai, 2016). The heavy chain of *Clostridium botulinum* neurotoxin has been shown to form pores in PE:PC membranes, and subsequently the enzymatic activity of the light chain is found in the opposing side of the membrane (Koriazova & Montal, 2003). These results indicate that not only was a least part of the heavy chain able to cross the membrane, but it was able to also deliver the light chain as well. From a detailed

comparison, it appears that *C. tetanus* toxins share many similarities in domain architecture and method of cellular intoxication with the toxin from *C. botulinum* (Pirazzini *et al.*, 2016).

The *Bordetella pertussis* toxin (CyaA) also has a protein domain organization similar to that of *C. botulinum* toxin; three domains that are independently responsible for receptor binding, translocation across the membrane, and an enzymatic domain. Experiments with purified CyaA on a tethered bilayer of model lipids have shown that the only requirements for enzymatic activity to cross the membrane are a typical eukaryotic transmembrane potential and the presence of calmodulin of the side of the membrane opposite that from which CyaA inserts (Veneziano *et al.*, 2013).

In yet one more example, the structure of diphtheria toxin from *Corynebacterium diphtheriae* has a similar domain organization as the previously discussed toxins(Choe *et al.*, 1992), and shows similar overall insertion behavior. As shown by release of trapped fluorescently labeled dextrans of various sizes, pores were created in model vesicles by purified diphtheria toxin, a step that necessarily requires the insertion of TM helices into membranes (Figure 1.2) (J. C. Sharpe & London, 1999). Mutational experiments have shown that helices 8 & 9 likely are driving insertion of protein into the membrane (Lai *et al.*, 2008). The pH dependence of diphtheria T domain insertion was later at least partly localized to acidic residues in helices 8 & 9 (Ghatak *et al.*, 2015).

pH low insertion peptide (pHLIP): A bacteriorhodopsin TM helix as a model for peptide insertion and translocation of JM groups

The toxins above often require acidification in endosomes or lysosome to insert themselves, and the delivery of a large protein payload across a cellular membrane. The acidification affects the ionization state of acidic residues determining insertion into membranes (discussed above and (Jiang *et al.*, 2015; Pirazzini *et al.*, 2016)). A simpler model following this process was discovered in studies of the third helix of bacteriorhodopsin, which can be water soluble, but also can interact with lipid vesicles. Importantly, a peptide with the sequence of helix 3

reversibly inserted itself into vesicles when the pH was lowered to ~pH 6 (Hunt *et al.*, 1997). This simple peptide can be used to investigate how some toxins work, and how peptide sequence affects peptide interconversion between soluble and membrane-inserted states. This peptide was renamed pHLIP (pH low insertion peptide). Interestingly, at low pH, pHLIP could insert across intact cell membranes and deliver two different hydrophilic dyes and peptide nucleic acids across membranes of various types of cells (Reshetnyak *et al.*, 2006). Subsequent research into pHLIP has addressed both the size/polarity of the cargo that can be delivered across a membrane and the relevance and function of the residues of pHLIP on its properties.

Close studies of pHLIP have addressed how an individual peptide can self-translocate, and the importance of certain residues to this activity. pHLIP insertion into membranes from solution was composed of at least two steps. The first step is at neutral pH is when unstructured peptide binds to the membrane but remains unstructured. The second step being upon acidification pHLIP rapidly forms an alpha helix and at the same time translocates the C-terminal residues (Reshetnyak *et al.*, 2008). A conservative change of Asp to Asn in the inserting end of pHLIP was shown to severely limit translocation. This reduction was postulated to be due to the loss of the protonation of the Asp that gave the pH dependent response (Andreev *et al.*, 2007). To confirm this hypothesis Asp in TM region were changed to either hydrophobic Ala or acidic Glu. Single mutations of Asp to Ala were still responsive to pH change, but decreased amounts of monomeric peptide in water. Mutation of either TM Asp to Glu caused the peptide to insert across membranes at more neutral pH. While a Glu double mutation caused the peptide to always be helical, thus decreasing insertion across membranes. While the Asp residues were required for TM insertion, they also were important to maintain peptide in random coil and stay monomeric in solution. When mutant peptides were helical in solution, they showed decreased ability to insert TM across a membrane (Musial-Siwek *et al.*, 2010). The function of Asp residues in the membrane-inserted C-terminus was also investigated. Aggregation in solution was generally decreased by inserting a Gly into the most hydrophobic stretch of pHLIP. Similar to Glu substitutions, changing TM Asp to His shifted pH of peptide insertion to pH closer to that of His. His containing peptides increase binding cooperativity and decreased reversibility of pHLIP insertion (Barrera *et al.*, 2011). Depending on Asp initial placement in the sequence,

the movement of TM Asp either towards the hydrophobic core or bulk water had different impacts on pHLIP behavior. Placement of Asp in the TM portion closer to the C-terminus, therefore earlier to insert, induced aggregation of pHLIP regardless of direction of Asp placement. In the N-terminus portion of TM, movement of Asp "up" from the hydrophobic core resulted in peptide that inserted at lower pH, closer to the pH of Asp side chain in bulk water. While movement of the same TM Asp "down", or deeper into the membrane, resulted in peptide insertion at higher pH than WT pHLIP (Fendos *et al.*, 2013). This likely reflects the ease of protonation of Asp side chains in more hydrophobic environments, a finding this lab has also described (see below). These results show that the importance of pHLIP staying monomeric before lipid binding, and that ionizable residues help determine the insertion pH of pHLIP, which is heavily dependent on the location of residues in target membrane.

In addition to pHLIPs ability to self-insert into cellular membranes, its ability to carry relatively large and polar cargoes into cells have made it a focus of research. pHLIP can use the natural acidity of cancer cells to target the translocation of hydrophilic dyes across cellular membranes, but not that of normal cells (Andreev *et al.*, 2007). Investigating the steps of pHLIP insertion, from bulk water to TM, revealed that the ionizable residues that translocate across membranes to the interior of the cell, are not required for insertion. These JM residues create an intermediate insertion step that is not required for pHLIP insertion, and a large number of these residues can prevent eventual insertion (Karabadzhak *et al.*, 2012). In an effort to determine the maximum polarity or charge of cargo that pHLIP can deliver, four different cyclic peptides were attached to the C-terminus of pHLIP and these were tested for cellular penetration. At low pH either four cyclic Asp or four cyclic Ser were able to be inserted by pHLIP into cancerous cells, but similar arrangements of Asn or Arg were not (Thevenin *et al.*, 2009). Although when added to bulk solution outside the cell, the bicyclic octapeptide toxin alpha-amanitin cannot cross cell membranes by itself, when attached to pHLIP via a reducable linker, the toxicity of alpha-amanitin was dramatically increased in four different cancer cell lines (Moshnikova *et al.*, 2013). As an extreme example of pHLIP ability to deliver cargo across membranes, pHLIP was conjugated to gold-europium complex ~13 nm in diameter. Multiple peptides were bound to the complex, and pHLIP was able to deliver the metal complex inside

human platelets (Davies *et al.*, 2012). The ability of pHLIP, and its derivatives, to deliver hydrophilic markers and drugs to within cells, particularly sick (Sosunov *et al.*, 2013) or cancerous ones, may prove vital to practical applications of pHLIP.

This type of behavior has also been seen with other peptides. For example, changes in pH were shown to alter the charge state of His residues, which allowed a model peptide to switch between an orientation that is TM and in-plane to the lipid membrane (Bechinger, 1996). At intermediate pH, a mixture of both forms was detected with NMR (Bechinger, 1996). Other examples studied in our lab are described below.

Membrane thickness can influence hydrophobic helix insertion

Hydrophobic mismatch is when the TM portion of a helix does not match the hydrophobic thickness of the membrane it's in. Positive mismatch is when the peptide is longer than the hydrophobic thickness of the membrane. Under positive mismatch, hydrophobic peptides can only "fit" within the hydrophobic core of the membrane by adapting a tilted configuration. This angled configuration induces significant orientational and conformational disorder for both peptide and lipids. When there is too much negative mismatch, a peptide adopts in-plane orientations in which it is membrane inserted, but no longer TM (Harzer & Bechinger, 2000). Switching between these two states involves movement across the bilayer, including translocation of JM residues, as is described below.

Mismatch can also induce changes in lipid conformation. Hydrophobic mismatch effects on lipids have been examined with WALP peptides, which as noted above are simple Ala-Leu repeats with two Trp on each terminus. In response to WALP peptides with positive (longer) mismatch, membranes have been shown to thicken in an attempt to match the length of the peptide. The thickening occurs primarily through alteration of the local order of acyl chain carbons, with the change in order being greatest for carbons closest to the lipid headgroups. Lipid membranes are found to respond more strongly (thicken) in response to a positive mismatch than thin in response to shorter peptides (de Planque *et al.*, 1998). The membrane response to positive mismatch was found to be highly dependent on sequence. Peptides with

aromatic residues (Trp, Phe and to a lesser extent Tyr) flanking the hydrophobic region caused the membrane to thicken much more than when the peptide was flanked by Lys, Arg or His. This illustrates that interactions in the interfacial region can contribute to peptide/lipid interactions (de Planque *et al.*, 2002). The dominant force in terms of lipid thickness for these simple peptide/lipid systems is to locate the Trp residues at the interfacial region. Lipid membrane thicknesses matched the Trp position, even when these Trps where close to the center of Ala-Leu peptides. This peptide/lipid arrangement exposed Ala-Leu repeats out of the hydrophobic core of the membrane (de Planque *et al.*, 2003).

Lab work leading to investigation of movement of JM sequences across membranes

Using fluorescence techniques our lab has investigated the effects of changes in hydrophobic mismatch between peptides and membranes. When they located are in an otherwise very hydrophobic polyLeu sequence, both Trp and Asp are tolerated inserted deeply within membranes (Caputo & London, 2003a, 2003b; Krishnakumar & London, 2007a; Lew *et al.*, 2000; Ren, Lew*, et al.*, 1999; Ren *et al.*, 1997; Shahidullah & London, 2008). Trp fluorescence (λ max) was found to correspond almost linearly with its position in the peptide sequence, and its depth in the membrane (Caputo & London, 2003a, 2003b; Lew *et al.*, 2000; Ren *et al.*, 1997). This can be used to monitor peptide location, because when the peptide is TM, Trp λ max is at shorter wavelengths than when the peptide moves across the bilayer and forms a non-TM state that is not deeply inserted (Caputo & London, 2003a, 2003b, 2004; Krishnakumar & London, 2007a, 2007b; Lew *et al.*, 2000; Ren, Lew*, et al.*, 1999; Ren *et al.*, 1997; Shahidullah & London, 2008). The Asp allows such peptides to show pH-dependent behavior, because the TM form is not stable at high pH, at which the Asp is unprotonated (Caputo & London, 2004; Krishnakumar & London, 2007a; Lew *et al.*, 2000).

Using hydrophobic peptides with one Trp and one Asp, our lab found that thickening a bilayer by *in situ* decane addition, or preparation with increasing amounts of cholesterol, resulted in negative mismatch as described above that promoted conversion of the TM state to

one parallel to the membrane surface, i.e. in which the peptide crossed the lipid bilayer(Ren *et al.*, 1997). In both states the peptides maintained their helical structure (Ren *et al.*, 1997). Peptides with other polar residues in the middle of polyLeu sequences showed similar behavior when hydrophobic mismatch was varied by using lipids various length acyl chains(Caputo & London, 2003a). With the addition of decane, both peptides with either a central Asp or with two central Pro exhibited a λ max change of ~ 10 nm, suggesting that a significant fraction of these peptides transitioned from TM to a non-TM state when the membrane was thickened (Caputo & London, 2003a; Ren *et al.*, 1997). This peptide movement to non-TM state requires the movement of two JM Lys to be moved through the hydrophobic core of the membrane.

Our lab's previous work had shown that peptides containing Asp in a central position are more sensitive to negative hydrophobic mismatch than those peptides without an Asp (Ren *et al.*, 1997). Considering this, the lab investigated if the effects of hydrophobic mismatch could be altered through use of Asp residues in various positions in polyLeu peptides. Peptides with Asp positioned in the sequence closer to bulk water when in a TM state had a pH of insertion lower, closer to normal pKa of Asp, than peptides with Asp deep in the hydrophobic core. This is similar to results found for pHLIP peptides (Barrera *et al.*, 2011; Fendos *et al.*, 2013). The peptides interconverted between TM and non-TM states at pH values that depended on the placement of the Asp and hydrophobic thickness. An Asp residue that was placed close to the end of the hydrophobic sequence decreased the effective hydrophobic length of the peptide, increasing negative mismatch in thicker bilayers, and thus favoring conversion to the non-TM state. This conversion could again occur despite two Lys residues at each peptide terminus (Caputo & London, 2004).

The lab also investigated if analogous behavior could occur in TM sequences that were even less hydrophobic. A sequence of Leu-Ala repeats was used as the hydrophobic sequence, similar to WALP peptides (de Planque *et al.*, 2003; de Planque *et al.*, 2002; de Planque *et al.*, 1998). For a given polar residue in a few residues from the edge of TM region, changing sequence from polyLeu to Leu-Ala repeats resulted in fewer peptides in the TM configuration, consistent with an increased negative mismatch. For peptides with Glu, Asp and His in the sequence, at a pH

where the residue was uncharged a larger fraction of peptides were reported TM, i.e. the effect of such residues on mismatch was less when they were uncharged(Krishnakumar & London, 2007a).

The lab next investigated the behavior of Asp-containing sequences with different Leu to Ala ratios in the TM sequence and with the Asp near the center of the hydrophobic sequence. It was shown that as hydrophobicity decreases (increasing number of Leu to Ala substitutions), peptide with an uncharged Asp became more sensitive to negative hydrophobic mismatch, showing decreased formation of the TM state at lower hydrophobicity. A charged Asp (higher pH) prevented formation of the TM state at any membrane thickness. When as little as 30% negative lipid was included in vesicles peptide insertion in a TM state was more stable, likely due to electrostatic interactions between JM Lys and the anionic lipids. This electrostatic interaction was confirmed by using short (L12) peptides with juxtamembrane (JM) ionizable His residues; peptides were TM only at pH where His was positively charged and when negative lipid was in the membrane (Shahidullah & London, 2008).

Motivation for studies of lipid and peptide movements across bilayers in this thesis

The movement of lipids and peptides across bilayers are the subjects investigated in this thesis. In the future, the London lab wishes to use artificial asymmetric unilamellar vesicles to study protein-lipid interaction. To determine what applications of asymmetric vesicles to studies of lipid-protein interaction are practical, we started by examining the membrane behavior of hydrophobic alpha helices, the main structural element in most membrane proteins. We first examined how hydrophobic peptide-accelerated flip-flop was affected by peptide sequence and vesicle composition. This is crucial, because flip-flop destroys asymmetry, so only peptides that maintain asymmetry can be studied. In addition, for studies of membrane proteins or hydrophobic helices in asymmetric membranes to be most informative, the orientation of the protein relative to the lipid must be known, as it will

determine which amino acid residues are interacting with which lipids. To know peptide orientation we have to know whether or not hydrophobic helices can spontaneously flip orientations in lipid bilayers. In theory, this could be prevented if the helix were flanked by hydrophilic residues that cannot cross membranes. Thus, it is important for studies with asymmetric vesicles to know what hydrophilic amino acid sequences results in a fixed helix orientation vs. one that is equilibrating between N and C terminus outside orientation. To examine this, we investigated the effect of JM hydrophilic sequences attached to membrane-inserted hydrophobic helices on the ability of the helices to interconvert between different orientations.

Chapter 2: Materials and Methods

Materials

All lipids and cholesterol were purchased as chloroform solutions from Avanti Polar Lipids (Alabaster, AL). Lipid abbreviations and scientific names are as follows: POPC, 1-palmitoyl-2-oleoyl-sn-glycero-3-phosphocholine; DOPG, 1,2-dioleoyl-sn-glycero-3-phospho-(1'-rac-glycerol); DMoPC, 1,2-dimyristoleoyl-*sn*-glycero-3-phosphocholine; DPoPC, 1,2-dipalmitoleoyl-*sn*-glycero-3-phosphocholine; DOPC, 1,2-dioleoyl-*sn*-glycero-3-phosphocholine; DEuPC, 1,2-dierucoyl-sn-glycero-3-phosphocholine; DEiPC 1,2-dieicosenoyl-*sn*-glycero-3-phosphocholine; NBD-PC, 1-acyl-2-(6-[(7-nitro-2-1,3-benzoxadiazol-4-yl)amino]hexanoyl)-sn-glycero-3-phosphocholine; chol, cholesterol. NBD-PC was typically stored in ethanol at -20°C, with the concentration determined via absorbance on a Beckman DU-650 spectrophotometer using a molar extinction coefficient of 21,000 cm^{-1} M^{-1} at 465 nm. All lipids were stored at -20°C until use.

Glacial acetic acid was purchased from Pharmco-Aaper (Shelbyville, KY). High-Pressure Liquid Chromatography (HPLC) acetonitrile was purchased from Avantor Performance Materials (Center Valley, PA). Tris base was obtained from Roche (Nutley, NJ). Hydrochloric acid was purchased from Fischer Scientific (Pittsburgh, PA). Phosphate buffered saline (PBS, 10 mM Na_2HPO_4, 150 mM NaCl) at pH 7.5 unless otherwise pH adjusted, was purchased from Biorad Laboratories (Hercules, CA). pH was measured with a Radiometer Copenhagen PHM 64 pH meter from The London Company (Cleveland, OH) using a Calomel electrode from Hach Lange Sensors (Vaulx-en-Velin, France). Acrylamide was purchased from Serva (Heidelberg, Germany). Glacial acetic acid was purchased from Pharmco-Aaper (Shelbyville, KY). Tris base was obtained from Roche (Nutley, NJ). Hydrochloric acid was purchased from Fisher Scientific (Pittsburgh, PA). Sodium hydroxide (NaOH) was purchased from Mallinckrodt Baker (Phillipsburg, NJ). All other chemicals (isopropanol, trifluoroacetic acid(TFA)) were obtained from Sigma-Aldrich (St. Louis, MO).

Unpurified peptides were purchased either from W.M. Keck Small Scale Peptide Synthesis Facility (New Haven, CT) or from Anaspec (San Jose, CA). Peptide abbreviations and sequences

are as follows: pL_{14}, KKGLLLLLLLWLLLLLLLKKA; pL_{15}(D10), KKLLLLLLLDWLLLLLLLKK; $p(LA)_6$, KKGLALALAWLALALAKKA; pL_9A_6(D10),KKLALALALDWLLALALALKK; N_0K_2-flanked peptide, KKLALALLLDWLLLLALALKK; N_2K_2-flanked peptide, NNKKLALALLLDWLLLLALALKKNN; N_6K_2-flanked peptide, NNNNNNKKLALALLLDWLLLLALALKKNNNNNN; Polio-flanked peptide, KLFAGHQLALALALDWLALALALKLFAGHQ. Except for the polio-flanked peptide, which was unblocked, all peptides were blocked on their N-terminus with an acetyl group and C-terminus with an amide group. Peptides were suspended in water, and isopropanol was titrated until peptides dissolved, typically at ~30-45% (by volume) isopropanol. Peptides were stored at this isopropanol:water ratio at 4°C until use. Peptide concentrations were determined at an absorbance of 280 nm on a Beckman (Indianapolis, ID) DU-650 spectrophotometer using the extinction coefficient of Trp as 5,560 cm^{-1} M^{-1}.

For work discussed in Chapter 3, peptides were purified following a modification of the procedure outlined in (Lew & London, 1997). Solvent A was purified water including 0.5% TFA, Solvent B was 90% isopropanol, 10% acetonitrile and 0.5% TFA. (Solvent solutions are reported in terms of percent by volume.) Unpurified peptides were suspended in water, and isopropanol was titrated until peptides dissolved. Peptide (~1 mg/ml) was loaded on a Rainin-Dynamax HPLC running in reverse phase controlled by Apple Macintosh PowerPC computer. An analytical C18 column (25 cm, 4.6 mm inner diameter) was used with a sample size of no larger than 400 µl. Typically, the peptides dissolved in 20-30% isopropanol and eluted at ~50% solvent B. Individual peaks were collected, and peptide purity was confirmed by matrix assisted laser desorption ionization-time of flight (MALDI-TOF) mass spectrometry at the Center for Analysis and Synthesis of Macromolecules (Stony Brook, NY). Peptide fractions used were 85-95% pure (any impurities had little if any activity, see below). Appropriate peak fractions were dried under vacuum, and resuspended with a minimum volume of isopropanol:water at the same ratio that eluted the peptide off of the HPLC column. TFA from purified peptides was removed with a protocol modified from (Andrushchenko *et al.*, 2007). To do this, HCl was added to the resuspended peptides to 50 mM, and the samples were then flash frozen and lyophilized. Resuspension, addition of HCl, and lyophilzation were repeated two more times. Final stock peptide concentration was determined using absorbance at 280 nm with a molar extinction

coefficient of 5,560 cm^{-1} M^{-1} (Trp) on a Beckman (Indianapolis, IN) DU-650 absorbance spectrophotometer. Peptides were stored in the same isopropanol:water ratio that eluted each peptide off the column at 4°C until use.

For the work discussed in Chapter 4, peptide purity was determined by MALDI-TOF mass spectrometry at Center for Analysis and Synthesis of Macromolecules (Stony Brook, NY) and was determined to be 70-88% pure. To check if purity influenced results, crude N_2K_2 peptide (72% pure) was purified via reverse-phase HPLC and TFA removed as previously (LeBarron & London, 2016) using a modified protocol of (Andrushchenko *et al.*, 2007). No difference in behavior between purified and crude peptide was noted.

Methods

Vesicle Preparation

Ethanol dilution small unilamellar vesicles (SUV) were prepared using a procedure modified from (Batzri & Korn, 1973). Lipid stock concentration was determined via dry weight. For each sample, the stock solutions of lipids (in chloroform), peptides (when used) and NBD-PC (in ethanol) were warmed to room temperature, and then the desired aliquots of each were removed and mixed in glass culture tubes. Samples were dried for 10 min under a nitrogen stream, and then dried under high vacuum for 1 h. Samples were placed in 70°C water bath for 10 min, then dissolved in 12 µl room temperature ethanol. Ethanol dissolved samples were vortexed while adding 788 µl of 70°C PBS (10 mM Na_2HPO_4, 150 mM NaCl), pH 7.5, or PBS pH adjusted to about 4 or 10 with either NaOH or acetic acid, respectively (pH adjustment involved <1% dilution of PBS, see below). When noted, vesicles also included 40 mol% cholesterol. Samples were allowed to return to room temperature before use. If NBD-PC was included, the samples were generally covered to prevent exposure to light. Unless otherwise noted final total lipid concentration was 200 µM. Vesicle size was calculated using a DynaPro Dynamic Light Scattering machine from Protein Solutions (Lakewood, NJ) running DYNAMICS software version 5.25.44. SUVs used in Chapter 2 were determined to have an average hydrodynamic radius and range of 300 ± 100 Å, and a polydispersity of 25-40%, while in Chapter 3 vesicles containing

the N_2K_2-flanked peptide and N_2K_6-flanked peptide fell in the size range for large unilamellar vesicles (LUV) (see Table A.1 in Appendix).

Multi-lamellar vesicles (MLVs) were prepared using a modified procedure from (Ahmed *et al.*, 1997). If peptides were included, they were added as for SUV. After the lipids were dried as described above, they were warmed to 70°C in a water bath, and the desired final volume of PBS (800 µl per sample) at 70°C was added and rapidly pipette mixed until no lipid residue was visible on the culture tube. Samples were then covered with Teflon tape, and placed in multitube vortexer at 50°C for 15 min. They were allowed to return to room temperature before use.

To prepare large lamellar vesicles (LUV) used in Chapter 3, the MLV solution was further treated with a minimum of 5 rounds of freeze/thaw in dry ice-acetone. The vesicles were then passed through a mini-extruder (Avanti Polar Lipids) using a 0.1 µm pore filters (Whatman Nucleopore, purchased from Cole-Parmer (Court Vernon Hills, IL) a minimum of 13 times. LUVs were determined to have a hydrodynamic radius and range of 450 ± 100 Å, and a polydispersity of 10-40%. LUV samples were then diluted to 200 µM with PBS and used. Controls were performed with rhodamine-labeled fluorescent lipids and pL_{15} (D10) to determine the amount of lipid and peptide loss during extrusion. These controls showed that extrusion does not lead to a significant loss of either lipid or peptide unless cholesterol is present (data not shown). In the latter case, the net effect is that about 45% of lipid was lost, and the peptide:lipid ratio was decreased by 30% for the DOPC/cholesterol samples in Fig. 3.7.

LUVs used in Chapter 4 were prepared using a different method due to the high cholesterol content. Lipid and when desired peptide solutions were co-dried as for the ethanol dilution vesicles, rehydrated at 70°C to a 2 mM lipid concentration with 800 µl PBS that had been pre-adjusted to a pH of ~ 4 or 10 with either NaOH or acetic acid, respectively. Samples were then mixed for 15 min to form MLVs using a multitube vortexer placed in a 50°C oven. After cooling to room temperature (23°C), the vesicles were subjected to five rounds of freeze-thaw in a dry ice-acetone bath. They were then centrifuged for a minimum of 10 min at 12,000 RPM in a

5415C centrifuge (Eppendorf, Hauppage, NY) (Cheng *et al.*, 2009), to remove MLV. Freeze-thaw lipid yield was typically 10% of initial concentration, with peptide yield of ~6% from initial concentration resulting in a peptide:lipid ratio one half of that of initial. The freeze-thaw vesicles were collected from the supernatant, and then diluted to a nominal concentration of ~20 µM using the appropriately pH-adjusted PBS. Freeze-thaw vesicles with no peptide had an average hydrodynamic radius of 58 nm, with an average polydispersity of 14%, while those with 1 mol% N_2K_2-peptide had an average hydrodynamic radius of 59 nm, with an average polydispersity of 9%.

Osmotic Shrinking Permeability (Pore-Formation) Assay

MLVs were prepared as described above, except at a concentration of 500 µM in 1/10 PBS (1 mM Na_2HPO_4, 15 mM NaCl) pH 7.5 and with lipid containing 5 mol% DOPG. Peptides were included at 1 mol% concentration relative to lipid unless otherwise noted. Hypertonic shock was induced with addition of a 200 µl bolus of 1M glycine into an 800 µl sample. A 200 µl bolus of 1/10 PBS was used as a control for no hypertonic shock. Optical density readings vs. time after bolus addition were made with a Beckman DU-640 UV/VIS absorbance spectrophotometer using a quartz cuvette with 1 cm path length at 550 nm.

Lipid Transleaflet Movement Assay

To determine the rate of lipid flip-flop in our vesicles, we used a modified protocol from (McIntyre & Sleight, 1991). To prepare vesicles with NBD-PC in the outer leaflet only, the desired aliquot of NBD-PC was added to preformed vesicles with or without TM peptides to a final concentration of 0.1 mol% of lipid, i.e a total lipid:NBD-PC ratio of 1,000:1. Vesicles were then incubated with NBD-PC for various time periods (typically 2 or 20 hrs) at room temperature (23°C) to allow NBD-PC to move from the outer leaflet to the inner leaflet. After this incubation, sodium dithionite (NaDt) was added to quench NBD-PC fluorescence by reacting with the NBD group remaining on outer leaflet. A fresh stock of 200 mM NaDt in 1M Tris pH 10 was prepared ~1 h before application and kept on ice until use. Unless stated

otherwise, 8.1 µl of this stock solution was added to the sample-containing cuvette giving a typical final sample NaDt concentration of 2 mM.

NBD-PC fluoresence was measured using a SPEX τ2 Fluorolog exciting at 465 nm and measuring emission at 534 nm. NBD-PC fluoresence was first recorded after the incubation with NBD-PC but before NaDt addition. This defined fluorescence at time = 0. During the first 2 minutes after NaDt addition NBD on the outer leaflet is reduced by NaDt. The residual NBD fluorescence arises from NBD lipid on the inner leaflet at time = 0. However, even after the first two minutes there is continuous slow decrease in NBD fluorescence, due to NaDt leakage into vesicles. This occurs both in vesicles lacking peptide (Armstrong *et al.*, 2003; Langner & Hui, 2000; McIntyre & Sleight, 1991), and those containing peptide (Kol, van Dalen*, et al.*, 2003; Kol, van Laak*, et al.*, 2003; Matsuzaki *et al.*, 1996)). Therefore, NBD fluorescence after the first 2 minutes was extrapolated to time =0 to define the amount of NBD-PC initially on the inner leaflet due to peptide-induced flip. To do this, fluoresence between 3 and 20 mins after NaDt was added was divided by fluorescence at time = 0 to obtain normalized values. Normalized values for samples without peptide were then subtracted from values for samples with peptide. Resultant values were extrapolated back to time = 0. Although the leakage should theoretically follow an exponential time course, a linear fit was found to be sufficient, as previously (Armstrong *et al.*, 2003; McIntyre & Sleight, 1991). Unless otherwise stated, this background (no peptide) flip-flop subtraction was performed for all values presented.

It should be noted, that there were small amounts of impurities remaining in the peptide preparations used for experiments. The major impurities contained extra oxygen, likely due to Trp oxidation, or were low mass reaction off-products. Experiments using HPLC peptide fractions in which the impurities were a predominant fraction of total peptide showed lower activity than fractions that were highly purified (not shown). Therefore, it is very unlikely that the impurities contributed significantly to lipid flip-flop.

A slight modification of the protocol above was needed to investigate the effect of pH upon peptide accelerated lipid flip-flop. DOPC SUV were prepared as above, however prior to NBD-PC addition, sample pH was adjusted with either 1.74M acetic acid or 3.2M Tris base to pH ~4 and

~10, respectively. After incubation, but immediately before NaDt addition, sample pH was adjusted to ~7.5, then initial fluorescence was recorded followed by NaDt addition as described above. This protocol avoided pH-induced variation in the rate of NaDt reactivity with NBD-PC.

Effect of Shifting pH Upon Fluorescence

To determine the speed of interconversion between TM and non-TM inserted states, the pH in samples containing peptides was shifted either from pH ~4 to pH~10 or vice versa (see Chapter 4 Results). Trp Fluorescence was measured using a SPEX τ2 Fluorolog exciting at 280 nm and measuring emission between 310 and 370 nm, at interval of 1nm, reading for 1 sec at each point. The fluoresence spectra for blank sample vesicles created at the same pH and with the same lipid, but lacking peptide, were also recorded. These peptide-lacking spectra were subtracted from the spectra of the peptide-containing samples to calculate peptide fluorescence. From these spectra the λ max was determined. In some instances, the intensity of fluorescence at two emission wavelengths, 345 and 325 nm, was also extracted from these spectra for analysis, as discussed below.

Fluorescent intensity before changing pH (time zero) was also measured at excitation 280 nm, emission at 345 and 325 nm for a total of 12 sec at each wavelength. pH was changed with an aliquot of either 3.2 M Tris base or 1.7 M acetic acid pipeted into the acidic or basic samples, respectively. After mixing with the pipet, intensity was measured as a function of time, with the first reading taken ~10 sec after aliquot addition. Emission readings of 4 sec were made at both 345nm then at 325 nm. This cycle of readings was repeated every 15 sec for 5 min. Additional readings taken as at time zero were made 10, 20, 30 min and at 2 and 20 hrs after aliquot addition (see Table A.2 in Appendix for full data). Similar readings were made on blank samples lacking peptide. Blank readings were subtracted to calculate final fluorescence intensities.

Chapter 3: Effect of Lipid Composition and Amino Acid Sequence Upon Transmembrane Peptide-Accelerated Lipid Transleaflet Diffusion (Flip-Flop).

Abstract:

We examined how hydrophobic peptide-accelerated transleaflet lipid movement (flip-flop) was affected by peptide sequence and vesicle composition and properties. A peptide with a completely hydrophobic sequence had little if any effect upon flip-flop. While peptides with a somewhat less hydrophobic sequence accelerated flip-flop, the half-time remained slow (hours) with substantial (0.5 mol%) peptide in the membranes. It appears that peptide-accelerated lipid flip-flop involves a rare event that may reflect a rare state of the peptide or lipid bilayer. There was no simple relationship between peptide overall hydrophobicity and flip-flop. In addition, flip-flop was not closely linked to whether the peptides were in a transmembrane or non-transmembrane (interfacial) inserted state. Flip-flop was also not associated with peptide-induced pore formation. We found that peptide-accelerated flip-flop is initially faster in small (highly curved) unilamellar vesicles relative to that in large unilamellar vesicles. Flip-flop was also affected by lipid composition, being slowed in vesicles with thick bilayers or those containing 30% cholesterol. Interestingly, these factors also slow spontaneous lipid flip-flop in the absence of peptide. Combined with previous studies, the results are most consistent with acceleration of lipid flip-flop by peptide-induced thinning of bilayer width.

Introduction

As discussed in Chapter 1, we have recently examined the sequence and lipid dependence of the behavior of artificial hydrophobic peptides that form membrane-inserted helices (Caputo & London, 2003a, 2004; Fastenberg *et al.*, 2003; Fujita *et al.*, 2007; Hammond *et al.*, 2002; Lai *et al.*, 2008; Ren, Lew*, et al.*, 1999; Shahidullah *et al.*, 2010). Many of these sequences were found to rapidly equilibrate across the lipid bilayer (Caputo & London, 2004; Hayashibara & London, 2005; Krishnakumar & London, 2007a; Lew *et al.*, 2000; Ren, Kachel*, et al.*, 1999; Rosconi *et al.*, 2004; Shahidullah & London, 2008). In this chapter, we examined the effect of such peptides upon lipid movement across bilayers. We found a peptide-induced acceleration of lipid transverse diffusion that is highly sequence and lipid dependent. Lipid packing and bilayer width appear to modulate the effect of peptides upon lipid flip-flop, but the effect of peptide sequence was complex, and do not support several simple mechanisms such as pore formation or a strict effect of peptide hydrophobicity. Possible models for how membrane-inserted helices accelerate lipid flip-flop are discussed.

Results

NBD-PC Transverse Diffusion Assay Shows Slow Transverse Diffusion of NBD-PC in the Absence of Peptide

To measure the effect of peptide upon transverse diffusion of lipids, we used an NBD-PC protection assay (Fig. 3.1 Left). The basis of the assay is that the NBD group of NBD-PC bound to the external leaflet of a vesicle becomes protected from reduction by externally added sodium dithionite (NaDt), which is only slowly membrane permeable, after the lipid diffuses to the inner leaflet. The reduced NBD group is non-fluorescent, so that residual fluorescence after reduction is proportional to the amount of NBD-PC that has flipped to the inner leaflet of a vesicle. The fraction of protected (inner leaflet) NBD fluorescence is estimated by extrapolation of fluorescence to time zero, which is defined as the time when NaDt is added to the sample. Extrapolation is necessary because the reduction of outer leaflet NBD can take 1-2 min, and some NaDt leakage into the vesicles can occur during this time, which reduces the fluorescence of the inner leaflet NBD.

To confirm the assay was working in the vesicles used in this study, the amount of protection was first measured in vesicles with NBD-PC in both leaflets. When small unilamellar vesicles (SUV) were formed using the ethanol dilution method (Batzri & Korn, 1973) the amount of protected NBD-PC fluorescence was 28% of the fluorescence before NaDt addition (Fig. 3.1 & Fig. 3.2). This agrees well with the expectation that most of the lipid molecules of a SUV are in the outer leaflet, and is consistent with a relatively random distribution of NBD-PC in the vesicles. However, it is possible a small bias towards enrichment of NBD-PC in the outer leaflet may exist. When large unilamellar vesicles (LUV) were prepared with NBD-PC present during their formation we found the amount of protected fluorescence was 45% of the original fluorescence (Fig 3.1 & 3.2). This agrees with the expectation of nearly equal numbers of inner and outer leaflet lipid molecules in LUV. Similar results were found in LUV containing the L15D peptide (Fig 3.2) [found to be the peptide most active at inducing lipid flip, see below],

indicating it had no influence on the initial distribution of NBD-PC lipid.

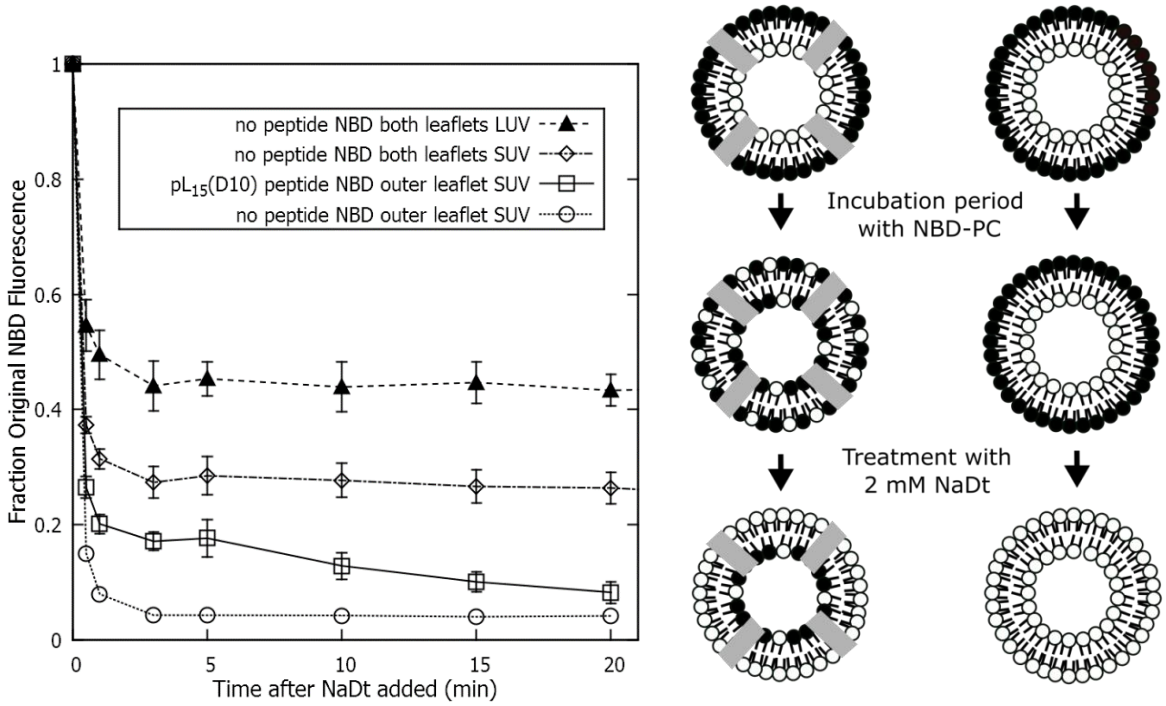

Fig 3.1: NBD-PC protection assay. Left. Schematic diagram of assay. 0.1 mol% NBD-PC (dark headgroups) is added to preformed vesicles prepared with or without TM peptides (grey rectangles). Vesicles are incubated with NBD-PC for various time periods to allow NBD-PC to move from the outer leaflet to the inner leaflet. Then NaDt is added to quench NBD-PC remaining on outer leaflet. NBD-PC in inner leaflet is protected from quenching and still fluoresces. See Methods. Right. Raw data from NBD-PC protection assay. This data used to extrapolate the amount of NBD fluorescence protected at time = 0, as discussed in Methods. Note the higher protection for NBD in SUV in the absence of peptide when its present in both leaflets (open diamond), as compared to outer leaflet only (open circle). Values shown are averages of at least three experiments, with bars representing standard deviation. All experiments here and in following figures were performed at 23^{o}C.

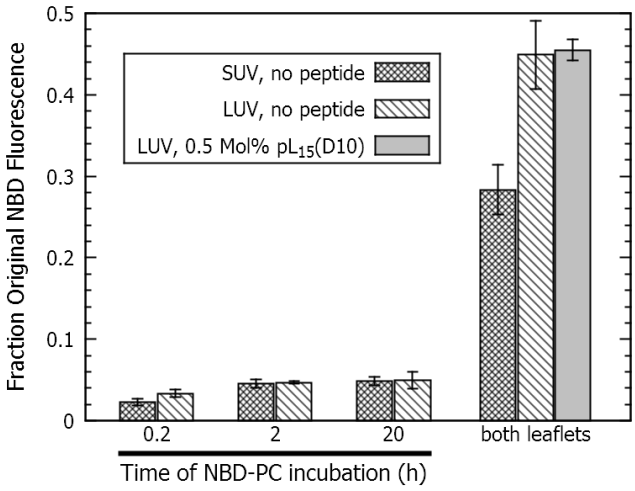

Fig 3.2: Fraction of initial NBD-PC fluorescence protected in vesicles with outer leaflet NBD-PC but lacking peptide after different incubation times, or with NBD-PC in both leaflets. DOPC vesicles were prepared as in Methods. Both leaflet samples had NBD-PC included vesicle formation. Values shown are averages of at least three experiments, with bars representing standard deviation.

To measure the rate of spontaneous lipid flip, NBD-PC was added to preformed SUV so that it should be initially only in the outer leaflet, and prior to NaDt reduction the vesicles were incubated for a set time to allow lipid flip to occur. After incubation of SUV for 20 h this treatment resulted in only 4.5% of initial fluorescence protected, i.e. only 4.5% of total NBD lipid was in the inner leaflet after 20h (Fig 3.1 & 3.2). A similar level of protection was observed using LUV. This slow extent of lipid flip is in agreement with previous studies (John *et al.*, 2002; Kol, van Dalen*, et al.*, 2003; Kol, van Laak*, et al.*, 2003; Langner & Hui, 2000; Matsuzaki *et al.*, 1996). The level of protection was not linear with incubation time. Even after a 100-fold shorter incubation time of 0.2 h (12 min) there was 2-3% protected fluorescence, as compared to initial values. Either there is a small amount of relatively rapid lipid flip, or some NBD lipid initially locates in the inner leaflet by another mechanism. One possibility is that the amount of ethanol introduced together with NBD-PC into the samples dissolves up some small fraction of vesicles which then reassemble into vesicles together with NBD-PC in the inner leaflet.

Addition of Peptide Increases NBD-PC Fluorescence Protection in a Time-Dependent Manner

To investigate the extent to which membrane-inserted peptides accelerate lipid flip-flop we formed vesicles containing hydrophobic peptides, and then assayed the extent of lipid movement across the bilayer with the NBD-PC protection assay. In previous studies, we found a long hydrophobic TM peptide did not accelerate flip-flop appreciably (Cheng *et al.*, 2009). We reasoned that shorter and/or somewhat more hydrophilic sequences might induce a more measurable acceleration of flip-flop. Therefore, we chose several peptides that were shorter than studied previously, and with different degrees of hydrophobicity: pL_{14}, KKGLLLLLLLWLLLLLLLKKA; $p(LA)_6$, KKGLALALAWLALALAKKA; pL_{15}(D10), KKLLLLLLLDWLLLLLLLKK pL_9A_6(D10),KKLALALALDWLLALALALKK. In bilayers with natural acyl chain lengths pL_{14} peptide forms a TM state, while $p(LA)_6$ is membrane bound, but largely in a shallowly-inserted non-TM state close to the bilayer surface (Krishnakumar & London, 2007b). The pL_{15}(D10) and pL_9A_6(D10) peptide primarily form TM states at low pH, at which the Asp residue is protonated, but form a shallowly-inserted state at high pH, at which the Asp residue is ionized (Shahidullah & London, 2008).

Peptide effects were moderately concentration-dependent (Appendix Fig.A.1), and a concentration of 0.5 mol% was generally used because it was sufficient to induce appreciable lipid flip. Fig. 3.3 shows the effect of these peptides upon lipid flip-flop at neutral pH in SUV composed of DOPC. The extent of lipid flip-flop in the absence of peptide has been subtracted from the data shown, as discussed in the Methods. As exemplified in Fig. 3.2, the level of NBD-PC fluorescence in the inner leaflet of vesicles without peptides was generally no more than 5% of total NBD-PC fluorescence. The pL_{14} peptide did not induce NBD-PC flip-flop above the basal level in DOPC SUV after either a 2 h or 20 h incubation. At the other extreme, the pL_{15}(D10) peptide, induced a significant, time-dependent, increase in flip-flop. The level of flip-flop was intermediate for the $p(LA)_6$ and pL_9A_6(D10) peptide. Interestingly, partial substitution of Leu with Ala, which decreases hydrophobicity, decreased flip-flop in peptides containing an Asp residue. Thus, there was no simple relationship between peptide hydrophobicity and flip-flop.

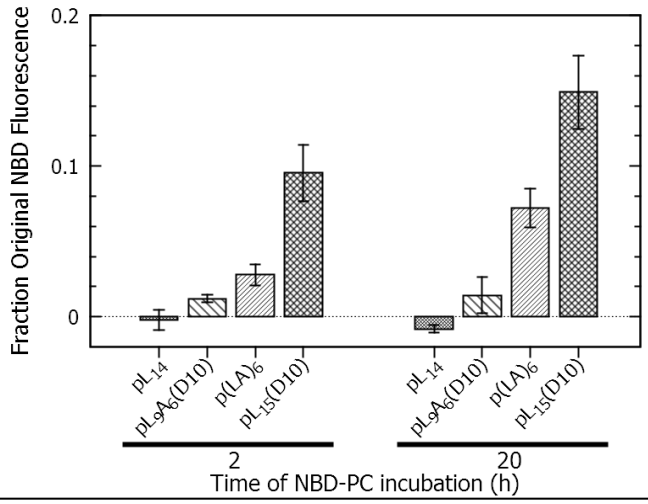

Fig 3.3: Influence of peptide sequence on peptide-accelerated lipid flip-flop. SUV of DOPC were prepared with each peptide included at 0.5 mol%. NBD-PC was added to outer leaflet of vesicles and allowed to incubate at room temperature for either 2 or 20 h. The expected maximum level of fluorescence protection after reaching flip-flop equilibrium would be ~0.33 for SUVs. Values shown are averages of at least three experiments with peptide-free blank values subtracted, with bars representing standard deviation.

Whether vesicle size would affect peptide induced flip-flop was also examined. Although the background level of flip-flop in the absence of peptides was not affected by vesicle size (Fig. 3.2), Fig. 3.4 shows there was a significant difference of flip-flop between SUV and LUV. The initial rate of flip-flop was faster in SUV, while the level of protection after 20h incubation was higher in LUV. The difference in fluorescence protection between SUV and LUV may be explained when the fraction of total lipid in the inner leaflet of SUV (~33% of total lipid molecules) and LUV (~50% of total) is taken into consideration. In the case of LUV, of the 0.1 mol% of total lipid that is NBD-PC, 25.5% is protected in the inner leaflet. The inner leaflet contains half of the total lipid. This gives an NBD-PC concentration of 0.051mol% of the total lipid in the inner leaflet. The analogous calculation for SUV, in which there is 15% protection, gives an NBD-PC concentration of 0.046 mol% in the inner leaflet. Thus, after a 20 h incubation LUV and SUV have a similar mole fraction of NBD-PC in their inner leaflets, and we conclude the difference in % of NBD-PC protection (25.5% vs. 15%) appears to largely reflect the larger percentage of inner leaflet lipid in LUV relative to that in SUV.

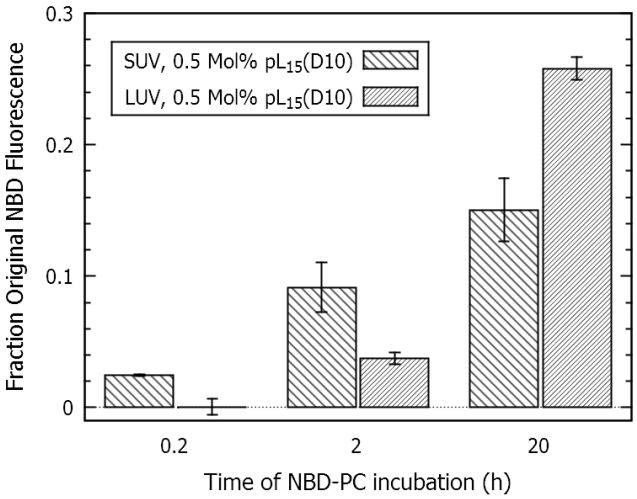

Fig 3.4: Influence of vesicle type on peptide-accelerated lipid flip-flop. SUV and LUV of DOPC were prepared with 0.5 mol% pL_{15}(D10). NBD-PC was added to outer leaflet of vesicles and allowed to incubate at room temperature for various times. The expected maximum level of fluorescence protection after reaching flip-flop equilibrium would be 0.33 for SUVs and ~0.5 for LUVs. Values shown are averages of at least three experiments with peptide-free blank values subtracted, with bars representing standard deviation.

Effect of pH/Peptide Configuration Upon Peptide-Accelerated Flip-Flop

Because the pL_{14} peptide has a TM topography while the $p(LA)_6$ peptide does not (Krishnakumar & London, 2007b), it is possible that peptide acceleration of flip-flop might be affected by the configuration of the peptide in the lipid bilayer. For example, it has been found that spontaneous flip-flop is faster in thinner bilayers (Brown & Conboy, 2013; John *et al.*, 2002; Liu & Conboy, 2005), and that peptides inserted into membranes in a non-TM configuration thin bilayer width to a significant degree (H. W. Huang *et al.*, 2004; Ludtke *et al.*, 1995). Combined these studies would predict fast flip-flop induced peptides in a non-TM state.

To check this, we compared the effect of the pL_{15}(D10) and pL_9A_6(D10) peptides upon lipid flip-flop at low pH (4.0) and high pH (9.9). As noted above, these peptides are in the TM state at low pH, and a non-TM shallowly inserted state at high pH. (Previous work in our lab has shown that the pKa of Asp in these peptides is ~6 in DOPC (Caputo & London, 2004; Shahidullah & London, 2008)). Fig. 3.5 shows the effect of pH upon peptide-accelerated lipid flip-flop for these two peptides and the pL_{14} peptide after 2 h incubation. There was no effect of pL_{14} upon

flip-flop at either high or low pH. (It should be noted that since this peptide lacks and Asp it will not change its TM/non-TM configuration when pH is changed.) For the other peptides, lipid flip-flop was slightly increased at high pH relative to that at low pH (Fig. 3.5). This indicates that flip-flop is accelerated both by peptides in the TM and non-TM states.

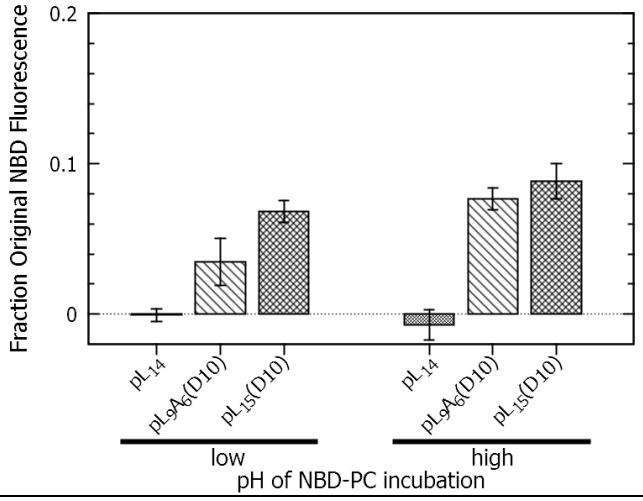

Fig 3.5: Influence of pH on peptide-accelerated lipid flip-flop. DOPC SUV were prepared with each peptide included at 0.5 mol%. Samples were adjusted to given pH, and after NBD-PC was added they were incubated for 2 h. See Methods for details. Values shown are averages of at least three experiments with peptide-free blank values subtracted, with bars representing standard deviation.

Pore Formation by Peptides

It has been observed that some natural peptides (e.g. alamethicin) that accelerate lipid flip-flop also induce pore formation (Hall, 1981; He *et al.*, 1996; Yang *et al.*, 2001). To see if peptide-accelerated flip-flop was associated with pore formation, the ability of the peptides studied here to form pores was examined. An osmotic response assay was used to test for pore formation. In this assay multilamellar vesicles (MLV) are exposed to a hypertonic shock that induces an osmotic pressure gradient across the membranes. This gradient results in an efflux of water from the MLV, and thus vesicle shrinking/contraction which results in an increase in optical density (OD) (Blok *et al.*, 1976; London & Feigenson, 1981).

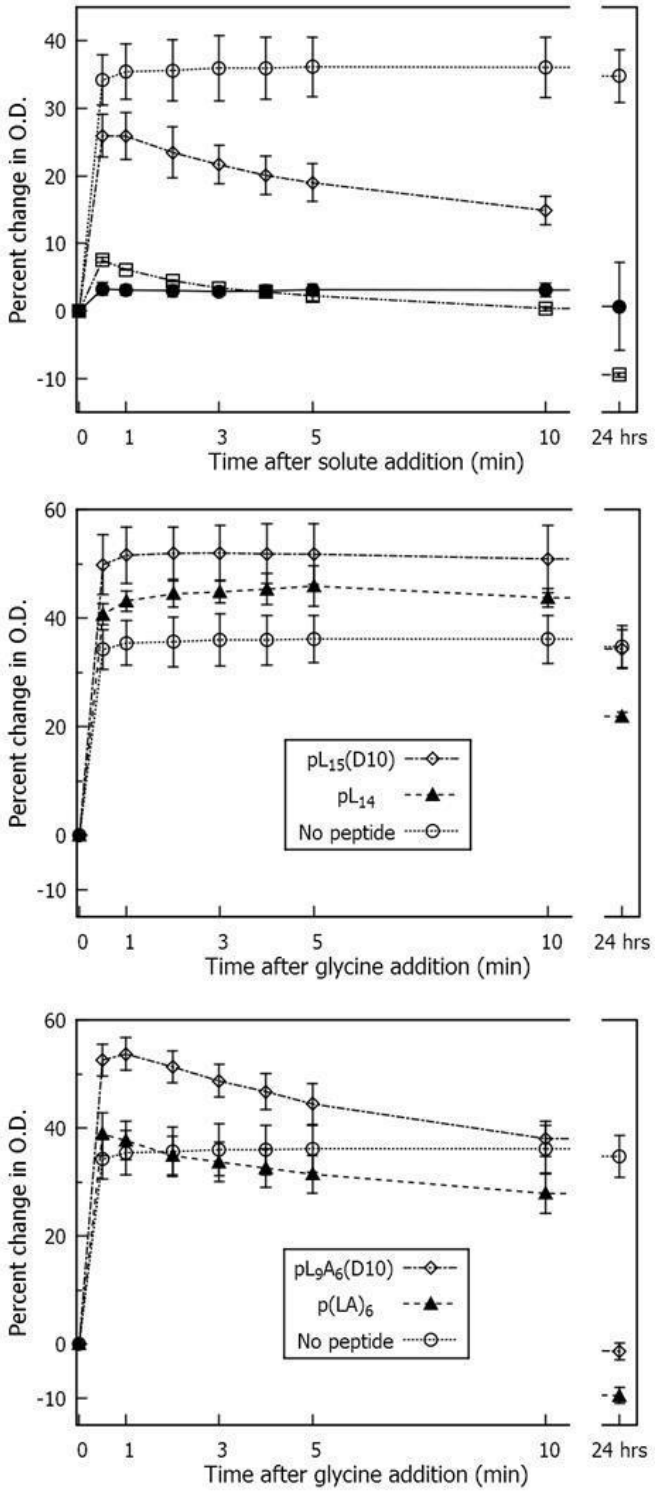

Fig 3.6: MLV pore formation assay. MLV prepared in 1/10 PBS were composed of DOPC with 5 mol% DOPG and either alamethicin, peptides used in flip-flop studies, or no peptide. Optical density was recorded at 550 nm before and after addition of 200 mM glycine. An increase of OD indicates that the MLV contracted due to an osmotic pressure gradient, indicating that no pore was present in the MLVs. **(Top):** Results for 0.5 mol% alamethicin (open diamond), 1 mol% alamethicin (open square) or no peptide (open circle) after glycine additon. Filled circles represent MLVs with no peptide upon addition of 1/10 PBS. **(Middle)** and **(Bottom):** Results for peptides used in flip-flop experiments after glycine addition. Values shown are averages of at least three experiments with peptide-free blank values subtracted, with bars representing standard deviation.

The presence of pores prevents the formation an osmotic pressure gradient and so OD does not change. Fig. 3.6 top (open circles) shows the extent of the osmotic shock induced increase in OD upon addition of an aliquot of hypertonic glycine. There is a lack of OD change upon addition of an aliquot not inducing hypertonic shock (Fig. 3.6 top, filled circles).

As a positive control for pore formation, MLV were prepared including alamethicin. When vesicles included 1 mol% alamethicin a weak, transient contraction was detected, indicating that pores rapidly dissipated the osmotic shock (Fig 3.6 top, open squares). Samples that were prepared including 0.5 mol% alamethicin (Fig. 3.6 top, open diamonds) initially displayed an almost full osmotic shock which mostly dissipated over 10 min, as shown by the decrease in % change in OD after osmotic shock back towards zero. This is consistent with work that has shown full release of vesicle trapped fluorophores seconds after alamethicin addition (Wiedman *et al.*, 2013). These results indicate that the alamethicin in MLV preparations formed pores quickly that allowed glycine to enter the MLV, thus minimizing osmotic contraction.

MLVs were then prepared with 1 mol% of our experimental peptides and the assay was used to determine if they induced pore formation. Results for the pL_{14} and pL_{15}(D10) peptides are very similar those for vesicles lacking peptide, indicating that these peptides do not form pores for glycine to enter the MLVs (Fig. 3.6 top). Vesicles formed with either $p(LA)_6$ or pL_9A_6(D10) show a large initial increase in OD which declines over 10 min (Fig. 3.6 middle), but to a lesser degree than in MLV with 0.5 mol% alamethicin. For all experimental peptides, but not alamethicin, OD responses were above that of peptide-free MLVs, (Fig. 3.6 middle and bottom). This shows that the peptides used in this study were not very effective at pore formation. After 24 h there was a decrease of OD from the maximal value due to osmotic shock in membranes containing $p(LA)_6$ or pL_9A_6(D10), but not pL_{14} or pL_{15}(D10). In addition, note that the most effective peptide for accelerating flip-flop was pL_{15}(D10) (Fig. 3.3), while the peptide showing the most leakage/pore formation (even though a very small amount) was $p(LA)_6$. This indicates that leakage/pore formation is not correlated with the ability of our peptides to accelerate flip-flop. It should also be noted that the 5 mol% DOPG included in the MLV to aid

osmotic response does not affect the extent of peptide-induced flip-flop (see Appendix Figure A.2).

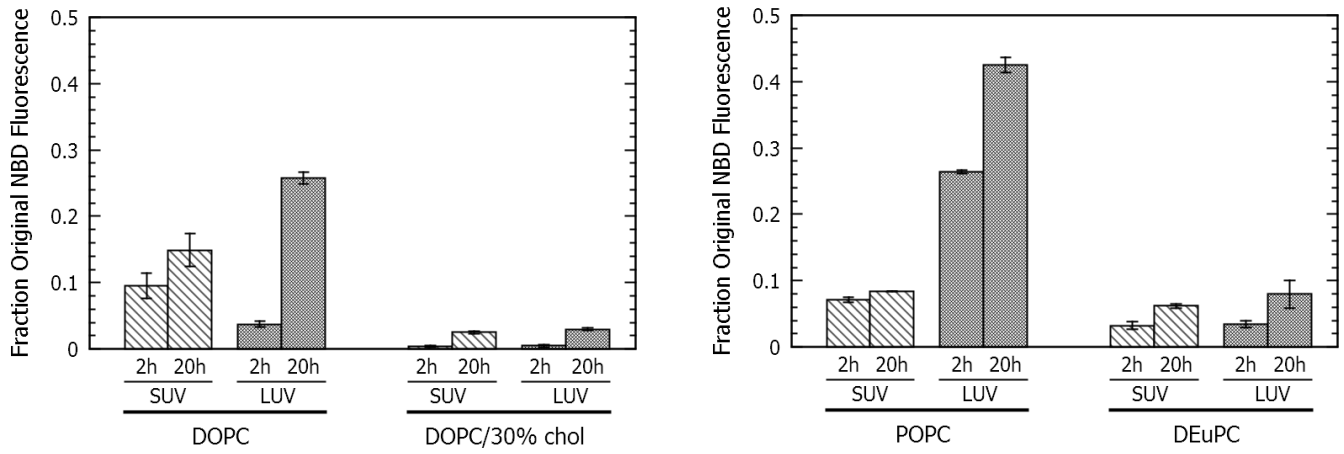

Fig 3.7: Influence of vesicle composition on pL_{15}(D10) acceleration of lipid flip-flop. SUV data represented in hatched bars, LUV data shown in gray bars. Vesicles including 0.5 mol% pL_{15}(D10) peptide were formed with the lipid compositions and vesicle types shown as described in Methods. LUVs including cholesterol had 0.35 mol% pL_{15}(D10) due to peptide loss during sample preparation, see Methods. Values shown are averages of at least three experiments with peptide-free blank values subtracted, and with bars representing standard deviation.

Influence of Lipid Type on Peptide-Accelerated Lipid Flip-Flop

To see if membrane properties influenced the ability of peptides to induce flip-flop (which might provide clues to the mechanism of peptide-induced flip-flop acceleration) the effect of lipid composition upon flip-flop was studied. Spontaneous lipid flip-flop is known to be highly sensitive to lipid composition. Cholesterol and more highly saturated lipids all result in lower flip-flop rates (Armstrong *et al.*, 2003; John *et al.*, 2002; Kol, van Laak*, et al.*, 2003; Langer & Langosch, 2011; Son & London, 2013a). We first tested the effect of cholesterol, a very common plasma membrane lipid (van Meer *et al.*, 2008)**,** upon peptide accelerated flip-flop. Inclusion of 30% cholesterol into DOPC vesicles dramatically reduces pL_{15}(D10) associated NBD-PC protection in both SUV and LUV (Fig 3.7 left). This effect might result either from either

cholesterol's ability to increase the thickness of the membrane (Hung *et al.*, 2007) or from its effect of increasing acyl chain order (Vermeer *et al.*, 2007).

To determine if there was any effect of acyl chain saturation, flip-flop was next assayed on vesicles made of POPC, a common lipid in mammalian membranes. Compared to DOPC, the palmitoyl chain of POPC is two carbons shorter than the oleoyl chain and fully saturated. In SUV pL_{15}(D10)-induced flip-flop in POPC vesicles (Fig. 3.7, right) is less than in DOPC SUV (Fig. 3.7 left). In contrast, POPC LUV with pL_{15}(D10) showed more flip-flop than DOPC LUV (Fig 3.7, left). After a 20 h incubation, POPC LUV with pL_{15}(D10) protected 42% of initial NBD-PC fluorescence. This value approaches the theoretical maximum for full equilibration of inner and outer leaflets, which would be 50% of lipid molecules (Fig. 3.2). To determine the effect of lipid acyl chain length (and therefore bilayer thickness) on peptide accelerated flip-flop, we also studied flip-flop in vesicles composed of phosphatidylcholine with two monounsaturated acyl chains of 22 carbons (DEuPC)(Fig. 3.7, right). Flip-flop was significantly decreased relative to both DOPC and POPC, which form thinner bilayers (Hung *et al.*, 2007; Kucerka *et al.*, 2005; Leftin *et al.*, 2014).

Discussion

Hydrophobic Peptide Accelerated Flip-flop: Sequence and Lipid Dependence

This report shows a variety of hydrophobic helix-forming peptides can accelerate lipid flip-flop. The effect was generally modest, with a half-time on the order of hours even with a considerable peptide concentration in the bilayer, much slower than typical enzyme-catalyzed reactions. Nevertheless, eventual near-equilibration of the inner and outer leaflet was observed in a number of cases. The effect of peptide upon flip-flop was both dependent upon amino acid sequence and lipid type. The effect of varying peptide hydrophobicity was complex. A peptide with a highly hydrophobic all-Leu (except for one Trp) core had no detectable effect upon lipid flip-flop, consistent with previous studies (Cheng *et al.*, 2009). The presence of a single polar Asp residue, in a charged or uncharged state, greatly accelerated flip-flop. However, a peptide with both Asp and substitution of several Leu with Ala showed a decreased

effect upon flip-flop relative to one with Asp in an all Leu hydrophobic core. Thus, decreasing hydrophobicity by itself did not always guarantee increased flip. The effect of peptide orientation was also complex. There was no large difference between the level of flip acceleration for Asp-containing peptides in a TM orientation (Asp uncharged at low pH) or in a non-TM orientation aligned near the membrane surface (Asp ionized at high pH)(Lew *et al.*, 2000).

The effect of lipid composition was somewhat easier to rationalize. Relative to vesicles composed of DOPC, peptide-induced enhancement of flip-flop slowed in the presence of cholesterol or in vesicles composed of DEuPC, which makes thicker bilayers than DOPC. This effect of cholesterol has also been seen in previous studies (Kol, van Laak*, et al.*, 2003; Langer & Langosch, 2011). Interestingly, the effects of lipid structure mirror the effect of these lipids upon spontaneous lipid flip-flop in the absence of peptide (Son & London, 2013a), suggesting that lipid headgroups are exposed to the hydrophobic core of the lipid bilayer when undergoing flip both in the absence and presence of peptide.

We have no simple explanation for the effect of vesicle size upon peptide-enhanced lipid flip. In DOPC vesicles, the extent of peptide-induced flip-flop was greater in SUV (at least over the first 2h) while in POPC vesicles it was greater in LUV. It should be noted that the final extent of flip-flop upon equilibration should be larger in LUV than SUV, due to their having a larger fraction of total lipid in the inner leaflet than SUV. This is consistent with what was observed.

One issue that must be considered is that the effect of peptides was assayed using an NBD-labeled lipid, as in several prior studies (Armstrong *et al.*, 2003; John *et al.*, 2002; Matsuzaki *et al.*, 1996; McIntyre & Sleight, 1991). This means that the measured rate of flip-flop might differ somewhat from that of unlabeled lipid. This is of reduced concern because the aim of this study was to identify factors influencing the relative rate of flip-flop, rather than to define the absolute rate of flip. Furthermore, the greatest barrier to flip-flop, and thus the factor that is rate-limiting for flip-flop, is likely to be the solubility of the charged phosphocholine group of the NBD-PC. In fact, prior studies on the effect of lipid composition upon flip-flop have found similar patterns for NBD-labeled and unlabeled lipids (Brown & Conboy, 2013; Kol, van Laak*, et*

al., 2003; Langer & Langosch, 2011; Son & London, 2013a). In addition, prior studies have shown whether the acyl chain of an NBD lipid was saturated or not had little effect on lipid flip-flop rate (Armstrong *et al.*, 2003).

It is interesting that the sequences studied in this report were able to significantly accelerate lipid flip rate of NBD-PC. Flip rates of NBD lipids in vesicles having membrane-inserted peptide increased in the order NBD-PC ≈ NBD-PS < NBD-PE < NBD-PA for a WALP peptide, and in the order NBD-PC < NBD-PE < NBD-PG for a KALP peptide (Kol, van Laak*, et al.*, 2003). Flip rates for NBD-PC were found to be much slower than NBD-PG either with or without peptides similar to our pL_9A_6(D10) included (Kaihara *et al.*, 2013). Similar results for flipping of NBD labeled lipids (NBD-PC ≈ NBD-PS < NBD-PE) were found when vesicles had inserted TM domains of SNARE peptides (Langer & Langosch, 2011). This order of flip rates was not influenced by the length of the acyl linker to the NBD group (Kol *et al.*, 2001). Interestingly, in lipid bilayers without peptide, lipid flip (using unlabeled lipids) was found to increase in an order (PC ≈ PS < PG ≈ PA) similar to that seen with peptide (Son & London, 2013b). This is consistent with the conclusion that lipid undergoes flip-flop in a similar environment regardless of whether or not peptide is present.

It is also interesting that the pL_{15} (D10) peptide accelerated NBD-PC flip-flop the most. This suggests that a single highly polar residue within the hydrophobic segment is sufficient to flip the most flip-resistant lipid headgroup. In this regard, it has been also been found that flip of NBD-PC can be accelerated with peptides having other ionizable residues in their hydrophobic core (Kaihara *et al.*, 2013)).

Mechanisms of Flip-flop Acceleration by Helical Peptides

We considered several possible mechanisms through which helical peptide-accelerated flip-flop might occur. In the case of the pore-forming peptide alamethicin, one possible mechanism might be movement through a pore with characteristics that allow lipid to pass through (see Introduction). However, the data in this report indicates that for the peptides studied here flip-flop is not associated with pore formation. Not only do the peptides we studied fail to form

pores efficiently, a peptide that did not form pores (pL_{15} (D10)) induced more flip-flop than peptides that have a weak pore-forming ability ($p(LA)_6$ or pL_9A_6(D10)).

A different mechanism for acceleration of flip-flop by peptide is suggested by the observation that the lipid dependence of peptide-accelerated flip-flop shows a pattern similar to that for spontaneous lipid flip. Spontaneous lipid flip is faster for PG and PA than for PE, PS or PC (Son & London, 2013b), as has been has also seen for peptide-accelerated flip in previous studies (Kol *et al.*, 2001; Langer & Langosch, 2011). Spontaneous flip is also faster for bilayers that are thinner (John *et al.*, 2002; Son & London, 2013a), in agreement with our observations. Spontaneous flip is slowed by cholesterol (Bhattacharya & Haldar, 2000; Engberg *et al.*, 2015; Hung *et al.*, 2007; Leftin *et al.*, 2014; Liu *et al.*, 2013; Vermeer *et al.*, 2007), and peptide accelerated flip was found here to be slower in bilayers with cholesterol. All this suggests that the path taken through the membrane by a lipid undergoing a flip event may involve a similar local environment (one at least largely composed of acyl chains) for peptide-free spontaneous and peptide-accelerated flip. (Bhattacharya & Haldar, 2000; Engberg *et al.*, 2015; Hung *et al.*, 2007; Leftin *et al.*, 2014; Vermeer *et al.*, 2007)

A mechanism for peptide-accelerated flip that fits these observations is one in peptide-induced membrane thinning is a major factor that enhances flip. As shown in Appendix Fig. A.3, bilayer thinning would decrease the length of the hydrophobic barrier across which a lipid headgroup has to pass. Hydrophobic peptides that embed in the bilayer in a non-TM state have been shown to thin bilayers (H. W. Huang *et al.*, 2004; Ludtke *et al.*, 1995). Peptides with relatively short hydrophobic sequences that form TM helices, as those in this report, also can locally thin the portion of the bilayer in contact with the peptide (de Planque *et al.*, 2002; de Planque *et al.*, 1998; He *et al.*, 1996; H. W. Huang *et al.*, 2004; Killian, 1998; Krishnakumar & London, 2007a; Ludtke *et al.*, 1995; Yang *et al.*, 2001), and it has already been suggested that this could speed up flip-flop (Nakao *et al.*, 2015). It is possible that the Asp also induces some bilayer thinning even in the TM state. In contrast, a lack of an effect of peptides on bilayer width might explain why PC flip is not accelerated in the presence of long TM helices (Kol *et al.*, 2001).

The effect of peptide is unlikely to simply depend upon the width of the bilayer in the absence of peptide. Vesicles containing DOPC with 30 mol% cholesterol showed less peptide-accelerated lipid flip-flop than in DEuPC vesicles. This result argues against the extent pL_{15}(D10) associated lipid flip-flop being dependent on only bilayer thickness, because the phosphate-to-phosphate distance for DEuPC has been reported as 45 Å (Kucerka *et al.*, 2005) and ~40.5 Å for DOPC with 30% cholesterol (Hung *et al.*, 2007)**.** It is likely that a difference in lipid packing is also a factor in these cases. Tight lipid packing in the presence of cholesterol (Engberg *et al.*, 2015; Leftin *et al.*, 2014; Vermeer *et al.*, 2007) might result in decreased hydration in the core of the bilayer, which would increase the energy penalty for the lipid headgroups in the bilayer core and thus reduce flip-flop. Conversely, loose lipid packing and peptides could increase hydration or even the occurrence of transient water-filled membrane defects, which could also accelerate lipid flip-flop. Consistent with this, lipid flip-flop has been shown to be much faster in highly unsaturated lipid bilayers (Armstrong *et al.*, 2003; Son & London, 2013a).

In addition, the proximity of lipid headgroups to peptide during flip could also decrease the height of the energetic barrier, as suggested previously (Kol *et al.*, 2001). This could reflect a decrease in local lipid packing in the vicinity of the peptide and/or increased local polarity due to the presence of polar groups on the peptide side chains (e.g. the Asp) and backbone.

Chapter 4: Highly hydrophilic segments attached to hydrophobic peptides translocate rapidly across membranes

Abstract

Hydrophilic segments attached to transmembrane helices often cross membranes. In an increasing number of cases, it has become apparent that this occurs in a biologically relevant post-translational event. In this study we investigate whether juxta-membrane (JM) hydrophilic sequences attached to hydrophobic helices are able to rapidly cross lipid bilayers via their ability or inability to block hydrophobic helix interconversion between a transmembrane (TM) and non-TM membrane-associated state. Interconversion was triggered by changing the protonation state of an Asp residue in the hydrophobic core of the peptides, and peptide configuration was monitored by the fluorescence of a Trp residue at in center of the hydrophobic sequence. In POPC vesicles, conversion of the TM to non-TM state at high pH and the non-TM to TM state at low pH was rapid (seconds or less) for KK, KKNN and the KKNNNNNN flanking sequences on both N and C-termini and the KLFAGHQ sequence that flanks the spontaneously TM-inserting 3A protein of polio virus. In vesicles composed of 6:4 (mol:mol) POPC:cholesterol interconversion was still rapid, with the exception of peptide flanked by KKNNNNNN sequences, for which the half time of interconversion slowed to minutes. This behavior suggests that, at least in membranes with low levels of cholesterol, movement of hydrophilic JM segments (and analogous hydrophobic loops in multi-pass TM proteins) across membranes may be more facile than previously thought. This may have important biological implications.

Introduction

In chapter 1, I described work with model peptides that investigated pH-driven self-insertion and what molecular cargoes have been delivered across those membranes. What remains unknown is what are the limits, in charge or size, of polar amino acids that can cross cellular membranes spontaneously. In this chapter we monitored the insertion of model hydrophobic peptides to determine what flanking JM sequences might prevent peptide interconversion between a TM and non-TM state, i.e. what JM sequences cannot rapidly cross lipid bilayers. The TM/non-TM interconversion was triggered by changing the protonation state of an Asp in the center of the hydrophobic sequence, and the position of the peptide was determined by fluorescence of a Trp residue at the center of the hydrophobic sequence. In vesicles lacking cholesterol, TM/non-TM interconversion was observed for all peptide sequences in less than 10 sec, even when the peptide was flanked relatively long and highly hydrophilic N_6K_2 sequences. For the N_6K_2-flanked peptide interconversion in the presence of 40 mol% cholesterol required minutes, but remained very rapid for shorter or less hydrophilic sequences. This has important implications for the plasticity of membrane protein topography.

Results

Peptides for distinguishing TM and non-TM states and measuring TM/non-TM interconversion

Previous work in our lab has investigated the interaction between the sequence of hydrophobic helices and lipid composition (Caputo & London, 2003a, 2004; Krishnakumar & London, 2007a, 2007b; Lew *et al.*, 2003; Lew *et al.*, 2000; Ren *et al.*, 1997; Shahidullah *et al.*, 2010; Shahidullah & London, 2008), including the ability of a membrane-inserted hydrophobic helices ability to exist in the TM configuration (Caputo & London, 2003a, 2004; Krishnakumar & London, 2007a, 2007b; Lew *et al.*, 2000; Ren *et al.*, 1997; Shahidullah *et al.*, 2010; Shahidullah & London, 2008). Under some conditions the TM configuration converts into a non-TM configuration that is still somewhat inserted within polar-non-polar interfacial region of the bilayer. Surprisingly, interconversion between these states can be rapid, even if the hydrophobic sequence is flanked on both termini by two Lys residues (Caputo & London, 2004; Lew *et al.*, 2000; Ren *et al.*, 1997; Shahidullah & London, 2008; Su *et al.*, 2013). To determine if rapid interconversion could be inhibited by even more polar sequences, hydrophobic peptides flanked at both termini by multiple Asn and two Lys residues were studied. Asn residues were chosen to increase the polarity on the peptide termini, while avoiding changing peptide charge.

The peptides used all contained an Asp and Trp near the center of the hydrophobic segment. Previous work has shown that for membrane-associated peptides the wavelength of Trp emission maximum (λ max) of fluorescence is a reliable reporter of the position of the peptide in the bilayer, i.e. whether the peptide is in the TM or membrane-associated interfacial non-TM configuration (Caputo & London, 2003a, 2003b, 2004; Krishnakumar & London, 2007a, 2007b; Lew *et al.*, 2000; Shahidullah *et al.*, 2010; Shahidullah & London, 2008). Trp fluorescence is relatively blue-shifted in the TM state, and relatively red-shifted in the non-TM state (Caputo & London, 2003a, 2003b, 2004; Krishnakumar & London, 2007a, 2007b; Lew *et al.*, 2000; Ren *et al.*, 1997; Shahidullah *et al.*, 2010; Shahidullah & London, 2008). The Asp residue was included in the peptides in order to have a mechanism allowing us to rapidly

control which configuration is thermodynamically favored. Previous work has shown in synthetic (Caputo & London, 2004; Krishnakumar & London, 2007a; Lew *et al.*, 2000; Shahidullah & London, 2008) and natural peptides (Andreev *et al.*, 2010; Fendos *et al.*, 2013; Reshetnyak *et al.*, 2008; Reshetnyak *et al.*, 2007; Weerakkody *et al.*, 2013) that the charge state of an Asp in a TM sequence can determine the location a hydrophobic peptide. The apparent pKa of an Asp in the center of the hydrophobic sequence can fall in the range ~5-8 in bilayers, depending on lipid type (Barrera *et al.*, 2012; Caputo & London, 2004; Fendos *et al.*, 2013; Krishnakumar & London, 2007a; Kyrychenko *et al.*, 2015; Lew *et al.*, 2000; Musial-Siwek *et al.*, 2010; Shahidullah & London, 2008; Weerakkody *et al.*, 2013). At low pH, the Asp is uncharged and the TM configuration is favored, but when the pH is above the Asp pKa the residue is charged, and it is highly unfavorable for a charged residue to reside in the nonpolar environment of the bilayer (Caputo & London, 2004; Krishnakumar & London, 2007a; Lew *et al.*, 2000; Ren *et al.*, 1997; Reshetnyak *et al.*, 2008; Reshetnyak *et al.*, 2007; Shahidullah *et al.*, 2010; Shahidullah & London, 2008), so that the peptide takes on the non-TM configuration. Therefore, we used pH shifts to control the preferred configuration, and then examined how rapidly the peptides switched configurations as a function of the flanking sequences and lipid composition.

All peptides assume two different membrane-inserted states in a pH dependent manner

We first confirmed that the peptides chosen for study could exist in both TM and non-TM configurations. To do this the wavelength of maximum emission (λ max) of the Trp was measured for peptides inserted into vesicles prepared by ethanol dilution and composed of phosphatidylcholine with monounsaturated acyl chains of different lengths. Figure 4.1 shows that at high pH (when Asp is deprotonated and charged) all peptides exhibit a red-shifted λ max in the range 340 ± 5 nm and that was only very weakly dependent on acyl chain length. This λ max is indicative of Trp location in the polar headgroup region of the bilayer (Caputo & London, 2003a, 2003b, 2004; Krishnakumar & London, 2007a, 2007b; Lew *et al.*, 2000; Ren *et al.*, 1997; Shahidullah *et al.*, 2010; Shahidullah & London, 2008), and combined with the weak

dependence on bilayer width is highly characteristic of peptide in the non-TM inserted configuration (Caputo & London, 2003a, 2004; Krishnakumar & London, 2007b; Ren *et al.*, 1997; Shahidullah *et al.*, 2010; Shahidullah & London, 2008). Notice that this was true whether the peptide had zero (N_0K_2-flanked peptide), two (N_2K_2-flanked peptide) or six (N_6K_2-flanked peptide) Asn residues, as well as for a peptide with polar flanking sequences identical to those in the polio 3A protein (see below).

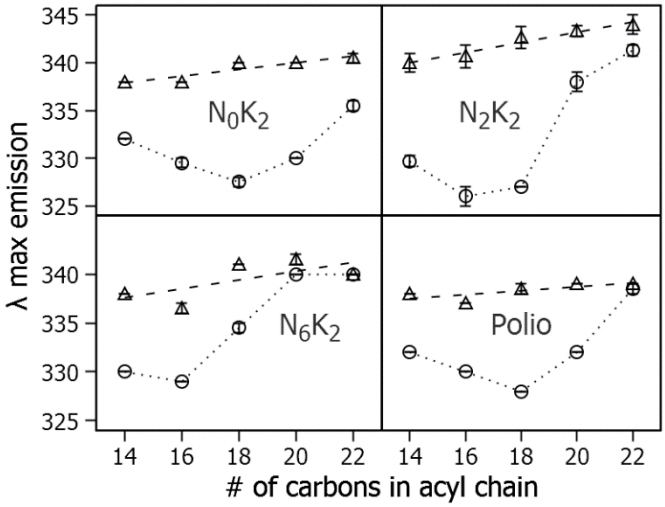

Fig. 4.1. Wavelength of maximum emission (λ max) of peptides in ethanol dilution vesicles composed of phosphatidylcholines with two identical monounsaturated acyl chains with different acyl chain lengths. Vesicles were prepared in PBS below and above the apparent pKa of Asp, at pH ≤ 4 (circles) or pH ~10 (triangles), respectively. Samples contained 200 µM lipid and 2 µM peptide. The peptide present in each sample is noted on the panel. Higher max is equivalent to Trp location in a more polar environment. The dashed line is a linear best fit to λ max obtained in basic conditions; dotted line connects consecutive λ max values under acidic conditions. Values reported are averages from three independent samples, with standard deviation shown as bars. Higher ratio is equivalent to location in a more polar environment.

Figure 4.1 also shows at low pH (when Asp is protonated and uncharged) the λ max of the peptides becomes blue-shifted and highly dependent on the length of the acyl chains. This pattern of λ max dependence upon membrane width has been seen in several studies (Caputo & London, 2003a, 2003b, 2004; Krishnakumar & London, 2007a, 2007b; Ren *et al.*, 1997; Shahidullah *et al.*, 2010; Shahidullah & London, 2008). The shift of λ max in thicker membranes at low pH towards values similar to that at high pH reflects increasing formation of the non-TM state. This destabilization of the TM state is due to the fact that negative hydrophobic

mismatch between the length of the hydrophobic helix and bilayer width increases as bilayer width becomes very large (Caputo & London, 2004; Krishnakumar & London, 2007a, 2007b; Ren, Lew*, et al.*, 1999; Ren *et al.*, 1997; Shahidullah *et al.*, 2010; Shahidullah & London, 2008). The fact that the λ max values at low and high pH tend to match in the thickest bilayer shows that the change in λ max reflects the configuration of the peptide, not a direct effect of whether or not the Asp is protonated (Caputo & London, 2004; Krishnakumar & London, 2007a, 2007b; Ren *et al.*, 1997; Shahidullah & London, 2008). This allows us to interpret changes in λ max in terms of peptide TM/non-TM configuration. Notice that all the same conclusions can be derived from ratio of fluorescence at 345nm to that at 325 nm (Figure 4.2). In the kinetics experiments below, the ratio between emission fluorescence at these two wavelengths was used, as previously, as a proxy to represent changes in λ max (Lew *et al.*, 2003) because it allows more rapid measurements.

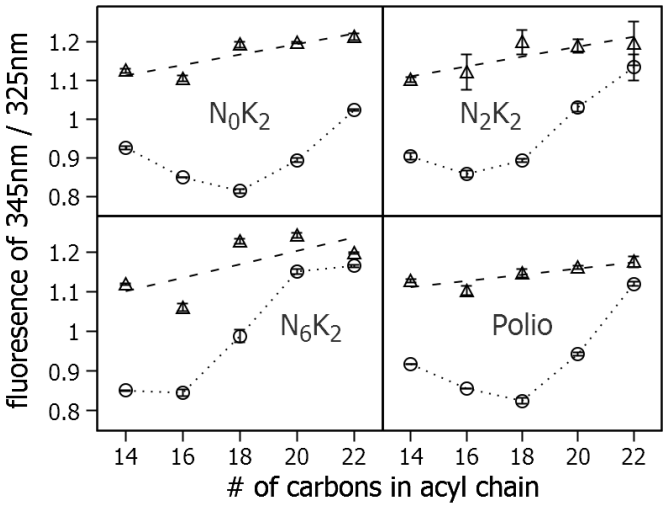

Fig. 4.2. Ratio of intensities measured at 345 and 325 nm of peptides in vesicles composed of phosphatidylcholines with two identical monounsaturated acyl chains. Samples identical to Figure 4.1.

Peptide Flanked by N_0K_2 or N_2K_2 Sequences Undergo Rapid Interconversion Between TM and Non-TM Inserted States

Of the peptides in this study, the N_0K_2-flanked peptide, with only two Lys at each terminus, should have the least limitation on interconversion between TM and non-TM inserted states. When included in the POPC vesicles prepared by ethanol dilution (upper left, Fig. 4.3), at time zero, N_0K_2-flanked peptide showed the same pH dependent difference of 345/325 nm ratio as in Figure 4.2. Next, an aliquot of acid or base was added, to change sample pH from high to low, low or high, respectively. This should induce the protonation of the Asp in the peptide prepared at high pH, and deprotonation of the Asp in the peptide prepared at low pH. The fluorescence ratios for the samples adjusted to high or low pH, shifted to values for samples prepared initially at high or low pH. (The λ max corresponding to the ratios at low and high pH before and after shifting sample pH are given for this and the following peptides in Table A.2iin Appendix). This indicates that the change in ionization was accompanied by rapid conversion of peptide configuration to the non-TM, or TM inserted states, respectively. No further change in fluorescence ratio was observed between 10s and 30 min after shifting pH, indicating interconversion was rapid. Similar results were observed in vesicles prepared by the freeze-thaw method (Fig. 4.3, upper right), except for a small blue shift in fluorescence in the vesicles prepared by freeze-thaw relative to those prepared by ethanol dilution at both low and high pH.

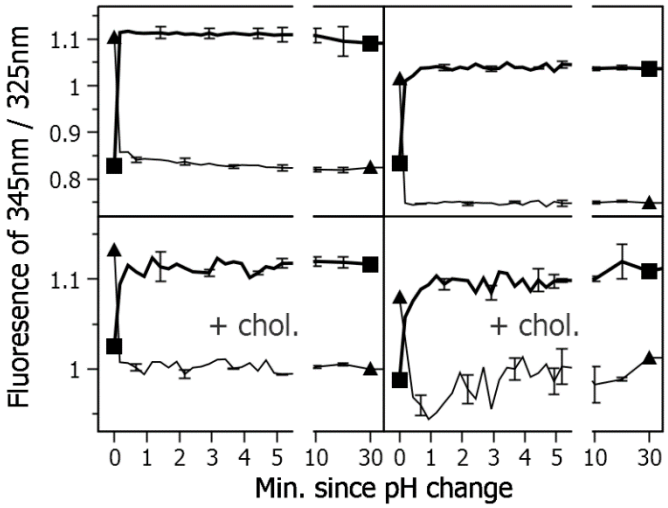

Fig. 4.3. pH-induced interconversion of N_0K_2 flanked peptide between transmembrane inserted and the interfacial non-transmembrane inserted states. In this and the following figures, graphs show ratio of Trp fluorescence emission intensities measured at 345 and 325 nm before and subsequent to pH shifts. Vesicles prepared in PBS at pH ~ 4, and then shifted to pH ~10 at time point zero are represented by heavy line with squares at ends. Triangles connected by thin lines represent vesicles prepared in PBS at pH ~ 10 and then shifted to pH ~4 at time point zero. For the first five minutes readings were taken every 15 s, and the lines connect every data point. Values are from three independent samples, averages are graphed with error bars showing the standard deviation. For clarity, symbols at each reading, and most error bars are omitted. See Appendix Figure A.4 for full data with all error bars explicitly shown. Later readings were taken at 10, 20 and 30 min. Top panels: Vesicles composed of POPC. Bottom panels: vesicles composed of 6:4 POPC:cholesterol (mol:mol). Left panels: ethanol dilution vesicles. Right panels: freeze-thaw vesicles.

The rapid change in configuration upon shifting pH is in agreement with that observed in previous studies with analogous artificial peptides and the pHLIP peptide (Andreev *et al.*, 2010; Caputo & London, 2004; Fendos *et al.*, 2013; Lew *et al.*, 2000; Reshetnyak *et al.*, 2008; Shahidullah & London, 2008; Weerakkody *et al.*, 2013). Very similar results were obtained in ethanol dilution and freeze-thaw vesicles containing POPC with 40mol% cholesterol (Fig. 4.3 lower panels). Cholesterol did red-shift the values of the fluorescence ratios at low pH, indicative of a more polar local environment adjacent to the Trp. This effect of cholesterol was observed for all of the peptides studied. It may represent the presence of a mixture of TM and non-TM inserted states at low pH (see below).

The effect of shifting pH was then examined for the N_2K_2-flanked peptide, which has two additional polar Asn residues added to the termini. The time course of the fluorescence response to shifting pH in ethanol dilution vesicles (Fig. 4.4) was very similar to that for the N_0K_2-flanked peptide. This was true both for samples changed from low to high pH, and high

to low pH, and for samples with or without 40mol% cholesterol. Thus, even four highly hydrophilic residues (two Lys and two Asn) did not block rapid interconversion between TM and non-TM inserted states.

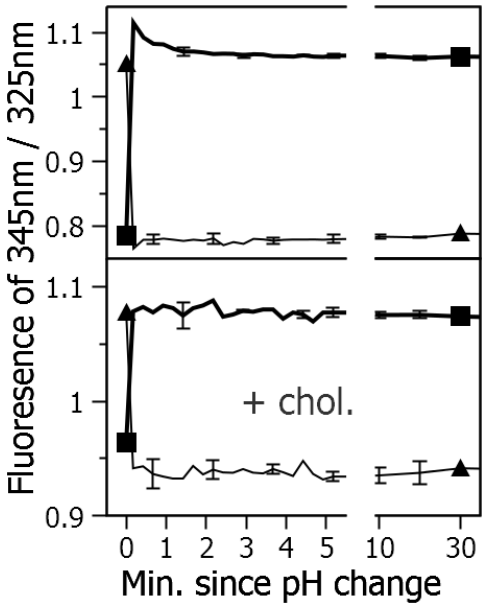

Fig. 4.4. pH-induced interconversion of N_2K_2-flanked peptide between transmembrane inserted and the interfacial non-transmembrane inserted states. Samples contained ethanol dilution vesicles. Top panel: Vesicles composed of POPC. Bottom panel: vesicles composed of 6:4 POPC:cholesterol (mol:mol). Other conditions identical to Figure 4.3.

Peptide Flanked by N_6K_2 Sequences Shows Slow Interconversion Between TM and Non-TM Inserted States Under Some Conditions

The number of Asn was then increased to a total of six at each peptide terminus. Upon changing pH in POPC vesicles prepared by ethanol dilution the N_6K_2-flanked peptide also showed rapid interconversion between the TM and non-TM states. This was mostly complete in less than 10 sec, as for the N_0K_2- and N_2K_2-flanked peptides, (Fig. 4.5, upper left). However, there was a gradual small change in Trp fluorescence ratio at least up to 30 min. This appeared to be similar when shifting to high or low pH. Behavior in vesicles prepared by freeze-thawing was similar (Fig. 4.5 upper right).

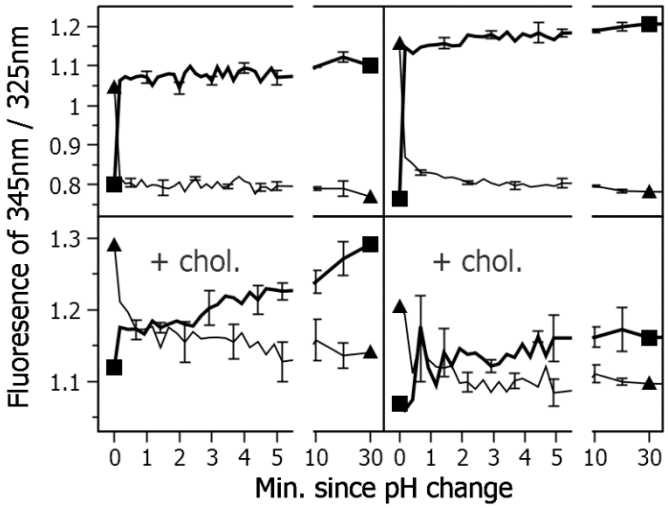

Fig. 4.5. pH-induced interconversion of N_6K_2-flanked peptide between transmembrane inserted and the interfacial non-transmembrane inserted states. Top panels: Vesicles composed of POPC. Bottom panels: vesicles composed of 6:4 POPC:cholesterol (mol:mol). Left panels: ethanol dilution vesicles. Right panels: freeze-thaw vesicles. Other conditions identical to Figure 4.3.

Unlike the other peptides studied, inclusion of 40 mol% cholesterol greatly decreased the speed of interconversion of the N_6K_2-flanked peptide. The half-time both for conversion from the TM to non-TM state when pH is increased, and for conversion from the non-TM to TM state when pH is decreased, slows to minutes. For vesicles prepared by ethanol dilution, upon decreasing pH it took about 5 min for the 345/325 nm ratio approached the value seen for N_6K_2-flanked peptide samples prepared at low pH (Fig. 4.5, lower left panel). The conversion to the TM state was multiphasic, with roughly half of the insertion occurring in the first minute after changing pH. Interestingly, conversion of the N_6K_2-flanked peptide from the TM to non-TM inserted state upon increasing pH appeared to take longer than conversion from the non-TM to TM states, with a half-time of 3-4 minutes. The behavior of the N_6K_2-flanked peptide in freeze-thaw vesicles containing 40mol% cholesterol was generally very similar to that in the ethanol dilution vesicles. The conversion from the TM to non-TM state, was even slower in the freeze-thaw vesicles than in the ethanol dilution vesicles, with a half-time of ~10 min (after overnight incubation the 345/325 nm ratio did reach to near the equilibrium value at high or low pH (Appendix Table A.2)).

Peptide Flanked by Polio 3A Protein C-terminal Sequence Shows Fast Interconversion Between TM and Non-TM Inserted States

In a step necessary for polio virus replication (Fujita *et al.*, 2007) polio 3A protein inserts from solution into membranes in a TM state despite its single hydrophobic sequence that is flanked by a hydrophilic JM sequence (KLFAGHQ). This sequence has charged and/or polar residues that have to cross the membrane upon TM insertion. To see if the rapid insertion of this protein was dependent upon some specific interactions, or if the flanking sequence is always able to pass rapidly through membranes, we studied a peptide with a hydrophobic sequence analogous to those for the peptides discussed above. Fig. 4.6 shows this polio-flanked peptide undergoes rapid interconversion between the TM and non-TM state upon shifting pH using ethanol dilution vesicles. This was true in membrane with and without 40mol% cholesterol. However, in the presence of cholesterol, the interconversion was again biphasic, as in the case for the N_6K_2-flanked peptide. The slow phase was very slow, with a half-time considerably longer than 30 min.

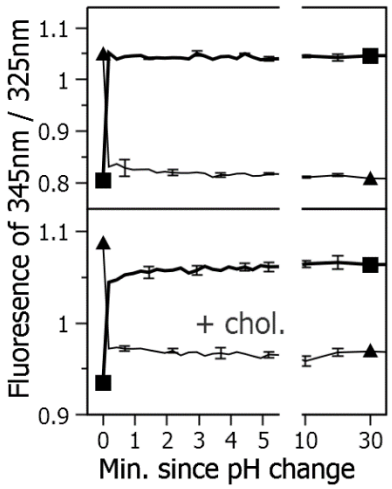

Fig. 4.6. pH-induced interconversion of polio-flanked peptide between transmembrane inserted and the interfacial non-transmembrane inserted states. Samples contained ethanol dilution vesicles. Top panel: Vesicles composed of POPC. Bottom panel: vesicles composed of 6:4 POPC:cholesterol (mol:mol). Other conditions identical to Figure 4.3.

Cholesterol effects the magnitude of the pH dependent shift of fluorescence emission

The data above shows that for the peptides studied the difference in 345/325 ratios at low and high pH is smaller in vesicles containing 40 mol% cholesterol. This largely reflects a smaller blue shift in λ max when pH is decreased in POPC vesicles containing cholesterol than in POPC vesicles lacking cholesterol (Appendix Table A.3). The lesser blue shift in the presence of cholesterol is likely to reflect either formation of a mixture of TM and non-TM states at low pH or a more polar environment of the Trp in the TM state, e.g. due to increased peptide oligomerization in the presence of cholesterol (Lew *et al.*, 2003; Ren, Lew*, et al.*, 1999; Ren *et al.*, 1997). A less likely alternative is that the peptide remains in a non-TM state both at low and high pH, and the lesser blue shift λ max at low pH reflects an effect of Asp protonation. This is ruled out by the observation that when the peptide is incorporated into DEuPC vesicles in which have a very thick bilayer, and so is in the non-TM state both at low and high pH, protonation at low pH induces a much smaller blue shift than seen in the POPC vesicle containing cholesterol (Appendix Table A. 3).

Discussion

Rapid movement of juxtamembrane segments across lipid bilayers.

In this report we studied interconversion between TM and non-TM inserted states of hydrophobic helices to measure whether hydrophilic JM segments sequence affects the ability of JM segments to rapidly translocate across a membrane bilayer. A change in pH sufficient to change the ionization state of an Asp residue in the center of the hydrophobic helix was used to trigger interconversion between the TM and non-TM states and thus JM segment translocation. Given the fact that the translocation of hydrophilic JM segments requires they pass through the hydrophobic core of the lipid bilayer, it was already a surprise in previous studies that Lys-Lys JM sequences at the end of hydrophobic helices were found to rapidly translocate across model membrane bilayers as hydrophobic helices switch between TM and non-TM membrane

inserted states (Caputo & London, 2004; Lew *et al.*, 2000; Ren *et al.*, 1997; Shahidullah & London, 2008; Su *et al.*, 2013). In this report, we find this rapid translocation is not blocked even when JM segments are increased in length and hydrophobicity by the addition of six Asn, a highly hydrophilic residue (Hessa *et al.*, 2005), to the two Lys. Fast translocation of JM segments was also observed for a peptide with JM sequences identical to those in the polio virus 3A protein. It should be noted the hydrophobic core sequence was slightly different for the peptides with Lys-Asn and polio 3A JM sequences. Although unlikely to affect the results in this study, there may be an effect of the sequence of the hydrophobic core of peptides upon the translocation of JM sequences. This would be an interesting topic for future studies.

Presumably, there is a continual fast interconversion between TM and non-TM states both at low and high pH, i.e. that the peptide is continually sampling the TM and non-TM state, with the predominant state being TM at low pH, at which the Asp is uncharged, and non-TM at high pH, at which the Asp is charged. The exact structure of the transition state for interconversion is not known. It seem most likely that the TM segment swings through the lipid bilayer, so that the JM segment is deeply buried in the core of the lipid bilayer in the transition state and that the Asp residue is protonated in the transition state, because the energy of ionizing the Asp in the core of the lipid bilayers would be expected to be very high. The actual ionization or protonation of Asp would be most likely to occur in the non-TM state (Fig. 4.7).

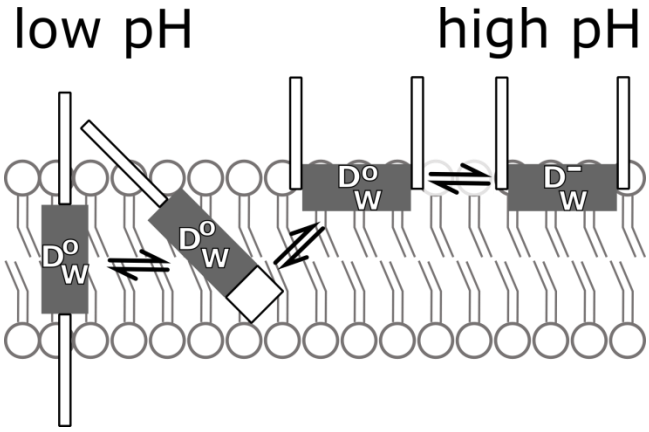

Fig. 4.7. Schematic figure depicting proposed relationship between Asp protonation state and TM/non-TM interconversion for N_6K_2-flanked peptide. Gray rectangle represents the hydrophobic core of 17 residues in an alpha helix, including Trp (W) and Asp (D). The most likely protonation state of Asp is shown. White rectangles represent six Asn, presented here as random coil when not buried within the lipid bilayer. Lipid bilayer shown composed of DOPC. Lipids and peptide are shown approximately to scale. It is most likely that the peptide samples both the TM and the non-TM membrane-associated state. When pH is increased (right) there is Asp deprotonation in the non-TM state traps peptide in the non-TM state. When pH is decreased, Asp protonation shifts the equilibrium to favor the TM state. In the transition state, one flanking sequence may be buried with in the lipid bilayer, perhaps in a helical state (as indicated by its changed dimensions) to reduce its free energy.

There are several possible reasons that hydrophilic JM segments attached to TM helices might pass through membranes so readily. First, attachment to the TM helix increases the local concentration of the JM segments at the bilayer surface relative to a peptide just composed of the JM residues. This would increase the rate of translocation by reducing entropy loss for a translocation JM sequence relative to that for a peptide composed just of JM residues. In addition, the location of the JM peptide at the membrane interfacial zone, with its lower effective dielectric relative to water, might decrease the energetic penalty for the formation of a helix by JM residues. The helical form of the JM residues would be expected to have a much lower free energy than a random coil when passing through the lipid bilayer. Finally, the TM helix itself may aid translocation of JM residues by disrupting local lipid packing, and so reducing the energy penalty due to disrupted lipid packing when a JM residue enters the core of the lipid bilayer.

The ability of JM N_6K_2 segments to cross membranes was slowed significantly in membranes with a high cholesterol concentration. Slow transverse movement of hydrophilic JM Lys-Lys

segments across bilayers with cholesterol was observed previously in POPC-cholesterol bilayers which would exist in the L_o state (Su *et al.*, 2013). In both cases, it is likely that tighter lipid packing and an increase in bilayer width (Bhattacharya & Haldar, 2000; Engberg *et al.*, 2015; Hung *et al.*, 2007; Leftin *et al.*, 2014; Vermeer *et al.*, 2007) slows the translocation of the JM segments. Increased lipid packing, could increase the energy penalty for disruption of lipid packing by a hydrophobic helix and JM segment crossing the bilayer. Increased bilayer width, could increase the energetic barrier for translocation due to the JM segment having a longer distance to translocate across, or by increasing the effective hydrophobicity of the bilayer core. There also could be an influence of cholesterol on the peptide, e.g. increased oligomerization, that somehow slows translocation.

Contrast between rates of transverse movements by hydrophobic peptides with hydrophilic JM segments and phospholipids.

The rapid (sub-sec to sec) transverse of the hydrophilic flanking sequences, including the N_6K_2 sequence, across membranes is in stark contrast to the slow transverse diffusion of hydrophilic headgroups of phospholipids during lipid flip-flop, which can take hours to days in many cases (Armstrong *et al.*, 2003; Son & London, 2013a, 2013b). One possible explanation for this apparent paradox is that the phosphate group of phospholipids has properties that block rapid flip. If true, one function of phosphorylation of short JM segments could be to prevent their transverse movement of hydrophobic helices across the bilayer. Another possible explanation is that a JM segment translocates across the bilayer in a helical form that greatly reduces the energy penalty for its location in the lipid bilayer. This is obviously not possible for lipids. A third possible explanation is that the disruption of lipid packing and increased polarity in the vicinity of TM helices (which have polar peptide bonds) allows hydrophilic flanking sequences to cross membranes more easily. In agreement with this, it should be noted that lipid flip is quite rapid in bilayers composed of highly polyunsaturated lipids, which have much looser lipid packing and reduced hydrophobicity due to the presence of double bonds (Armstrong *et al.*, 2003; Son & London, 2013a).

Biological implications of spontaneous translocation of hydrophilic JM segments across bilayers.

It should be noted that membrane proteins with TM helix anchors flanked at one end by short JM segments are not uncommon (Kalbfleisch *et al.*, 2007; Kutay *et al.*, 1993). The results of this report suggest that it is possible that the TM and short JM segments of such proteins might rapidly interconvert between TM and non-TM forms in which the JM segment has translocated across the bilayer. The spontaneous conversion of the tail of the polio 3A protein into a TM state that we reported previously in model membrane vesicles is an *in vivo* example of such a spontaneous interconversion (Fujita *et al.*, 2007). In the case of tail-anchored proteins, this type of translocation might be involved in the conversion of the non-TM state to the TM state when a protein is released onto a bilayer by the Get3 protein. However, it is as least just as likely that a translocon-like protein is involved in the conversion of the tail-anchored proteins to the TM state.

It is interesting that cholesterol slows the TM/non-TM interconversion. This could mean that this type of interconversion only occurs in organelles with low cholesterol levels, and for plasma membrane proteins at earlier stages in the biosynthetic pathway, i.e. in the endoplasmic reticulum, because cholesterol concentration is low in the endoplasmic reticulum (van Meer *et al.*, 2008). It also could mean that trafficking between the plasma membrane and internal membranes containing lower cholesterol could control when membrane proteins undergo interconversion.

Chapter 5: Conclusions and Future Directions.

Summary of lipid flip studies and their implications

In the work described in Chapter 3, we investigated the ability of hydrophobic peptides to accelerate lipid movement from one leaflet of a lipid bilayer to the other, i.e. lipid flip-flop. The peptides were designed to test the influence on lipid flip-flop of peptides with different total hydrophobicity (poly Leu or Leu-Ala repeat) and presence or absence of an ionizable residue in the TM region. Control experiments showed that 6-NBD-PC did not show a preference for one leaflet or the other, regardless of vesicle curvature. A peptide that did not have an Asp in its poly Leu hydrophobic region (pL_{14}) had no effect on lipid flip-flop, while the introduction of an Asp into the poly Leu sequence (pL_{15}(D10)) induced the greatest amount of flip-flop of the peptides tested. Peptide accelerated lipid flip-flop was time dependent, and generally appeared to progress faster in SUVs. Changing pH, and therefore both the charged state of Asp residue and the orientation of the peptide in the membrane, did not have a clear effect on lipid flip-flop. In contrast to the possible role of pore formation in lipid flip catalyzed by alamethicin, the peptides used in our study did not accelerate flip-flop through pore formation. Membrane thickening, through inclusion of cholesterol or lipids with longer acyl chains, dramatically reduced peptide accelerated lipid flip-flop. This may be a clue to the mechanism of peptide action. We think membrane thinning is the most likely mechanism for peptide-accelerated lipid flip.

Biological relevance of peptide accelerated flip-flop

Membrane proteins may contribute to some extent to lipid equilibration across the ER membrane after lipid synthesis. The location of cholesterol in cells is consistent with this. The work presented in Chapter 3 and discussed in Chapter 1 show that inclusion of cholesterol dramatically retards lipid flip-flop. It is relevant that despite the bulk flow of newly synthesized molecules from ER to the Golgi to various organelles, there exists a specific system to scavenge and concentrate cholesterol in the PM and other organelles; not the ER (Moser von Filseck *et*

al., 2015). This would mean that in the ER membrane proteins would have the greatest effect on lipid flip.

A question that this raises is whether the amount of peptide in ER is enough to influence lipid flip. The lipid:peptide ratio for the work presented in Chapter 3 was 200:1. During an incubation of 12 min, in the presence of this amount of peptide there was ~4% flip of the fluorescently labeled lipid (this represents the total of background plus peptide accelerated lipid flip). Assuming that the lipid flip-flop ability of peptides is additive, in order to flip roughly 50% of labeled lipid over the same 12 minute period, the lipid:peptide ratio would have to decrease to 16:1, or 6 mol% of membrane would need to be helices. While this amount of TM helices is possible, it is more than the ~ 4 mol% TM helices reported in the ER (Quinn *et al.*, 1984). Furthermore, this calculation assumes every TM helix is a monomer, and not a part of a multipass protein. As TM helices group together in a multipass protein, their lipid exposed area decreases and they shield TM polar residues from exposure to bulk lipid (Kauko *et al.*, 2010). Considering that a large fraction of membrane proteins would have this reduced lipid surface area, the mol% of protein would likely have to be even larger if non-specific peptide accelerated flip-flop was to achieve good mixing across the ER membrane. Thus, it seems unlikely that non-specific effects of transmembrane helices can explain all of the lipid flip in ER.

Future experiments on peptide-accelerated lipid flip-flop

A parameter that was not extensively examined in the work described in Chapter 3 is the effect of peptide accelerated flip-flop on phospholipid composition. Eukaryotic plasma membrane is known to have a significant fraction of both PE and PS lipids. Considering the biological implications of PS, both in a signaling aspect and an electrical capacity, the presence of PS on peptide accelerated flip-flop should be examined. PE is known to occur on both leaflets of the PM, and its effect on peptide accelerated lipid flip should be also be investigated. This should be done both for the NBD-PC we studied, and NBD lipids with other polar headgroups.

The work discussed in Chapter 3 utilized a TM peptide with an Asp residue, but other polar residues may also aid lipid flip-flop. The charge state of the Asp, as determined by pH changes, did not seem to have an appreciable effect on lipid flip-flop. Whether uncharged Asn, which has more hydrogen bonding groups than Asp, has a greater effect than Asp could be studied. The effect of a TM Arg and Lys could also yield interesting data. While both are positively charged, the larger side chain of Arg may accelerate flip-flop of negatively charged lipids to a greater extent than that of the smaller Lys residue, as it could swing farther across the membrane while interacting with a lipid. In this way inclusion of a positive TM residue coupled with inclusion of the negatively charged PS may accelerate flip-flop. Alternately, the electrostatic attraction may "lock" the molecules together, decreasing peptide acceleration of flip-flop.

The overall hydrophobicity of the peptide was explored by having TM sequences that were either poly Leu or Leu-Ala repeat. While this addresses hydrophobicity, these sequences were not designed to investigate three dimensional properties. A common hypothesis for peptide accelerated flip-flop is that lipid headgroups might "slide" along the peptide surface. Various TM sequences could be designed that could test this hypothesis. Considering the structure of an alpha helix, a groove in the TM region could be created with different properties than the rest of the helix. This groove could contain small headgroups with Ala residues, increased hydrogen bonding with Ser, or altered flexibility with beta-branched Val and or Gly residues.

Summary of studies of translocation of juxtamembrane residues

In the work described in Chapter 4, we tried to determine the number of JM polar residues required to block peptide TM/non-TM interconversion. This interconversion necessarily requires the translocation of one polar JM end of the peptide through the hydrophobic core of the membrane. The peptides used had an ionizable Asp residue in the middle of the hydrophobic TM sequence, so that the charge state of the Asp could be controlled by changing the pH of the bulk solution. Providing that the sample membranes were not too thick (which

disfavored formation of a TM state), controls indicated that the pH of sample preparation could control whether the peptide was either TM (low pH, uncharged Asp) or non-TM but membrane associated (high pH, charged Asp). The effect of increasing numbers of JM polar residues upon the ability for peptides to interconvert between the TM and non-TM state when pH was changed was then tested. Even a JM sequence of N_6K_2 was able to pass through POPC membranes in less than 10 sec. Inclusion of 40 mol% cholesterol did not hinder interconversion of N_2K_2-flanked peptide or that of a peptide with the JM sequence of the Polio 3A protein, but did hinder N_6K_2-flanked peptide interconversion somewhat. Overall, we were surprised how easily highly polar JM sequences were able to quickly cross membranes.

Why does the number of JM residues outside of TM region affect TM orientation stability?

An interesting observation was as the number of JM Asn increased, the fraction of peptide that was TM at low pH (reported by λ max) decreased in medium and long length lipids. For example, DOPC has an hydrophobic core of 26.8 Å (Kucerka *et al.*, 2005), which should match well with all the peptides. But there was a noticeable difference in λ max between N_2K_2- and N_6K_2-flanked peptide, showing that additional polar JM residues in the interfacial or headgroup region did decrease the amount of peptide in the TM orientation, even for very little hydrophobic mismatch between peptide and lipid. This indicates that although the Asn residues are not in the hydrophobic region, they are still destabilized the TM peptide configuration. It is possible that the hydrophobicity in the polar headgroup region of lipids is sufficiently large to significantly disfavor burial of polar residues. A simple test to determine if this is true would to use a comparable Q_2K_2-flanked peptide. We have shown that in vesicles of C20:1 PC, a significant portion of N_2K_2-flanked peptide is non-TM even at low pH. If this was because of an unfavorable interaction between the charged N_2 residues, the longer sidechain of Gln residues should alleviate this unfavorable interaction, even though Gln has the same polar group as Asn, by allowing the polar amide group to locate farther out into solution and because of the higher hydrophobicity imparted by the extra methylene in Gln, and so the Q_2K_2-flanked peptide should report a lower λ max.

Testing the origin of the effect of cholesterol

Cholesterol has a well-known condensing effect; inclusion of it into membrane causes lipids to become more ordered (Hung *et al.*, 2007), and increases membrane width. This condensing or ordering effect has been shown to affect POPC (Leftin *et al.*, 2014). An interesting question is whether cholesterol ordering of lipids is the property that hinders N_6K_2-flanked peptide interconversion. There are various cholesterol analogues that have been shown to not condense lipids as well as cholesterol (Kim & London, 2015; LaRocca *et al.*, 2013). If it is cholesterol induced increase in order that is hindering interconversion, the inclusion of one of these sterols instead of cholesterol would allow TM/non-TM interconversion to proceed much more quickly than in the presence of cholesterol.

Biological Implications of cholesterol blocking of TM/non-TM interconversion

As discussed in Chapter 1 the ER is the site of biogenesis of most of the structural lipids, including cholesterol. The bulk flow of cholesterol precursors must continue down the biosynthetic pathway, so that synthesis can continue in the Golgi. In addition to this natural flow of cholesterol away from the ER, the eukaryotic cell actively expends energy to remove cholesterol out of the biosynthetic membranes to the PM. The difficulty of the N_6K_2-flanked peptide to interconvert when cholesterol is present may reveal the importance of a very low cholesterol content for ER so that membrane proteins, which often have large polar JM sequences can be synthesized and mature properly.

It would be possible to test this with a dominant negative, inducible, mutation of the protein responsible for the active removal of cholesterol (Moser von Filseck *et al.*, 2015). I would expect that when this mutant was present, there should be an increase in the amount of cholesterol in the ER. This increase might trigger various negative outcomes such as an increase in the unfolded protein response or increased retention of membrane proteins in the ER/cis-Golgi. If so, an increase of cholesterol in the ER may also cause a decrease in the number of folded

membrane proteins in the PM, resulting in decreased sensitivity to a host of extracellular signals.

Properties of JM sequences that block TM/non-TM interconversion

We selected the N_6K_2 JM sequence with the expectation that this sequence would block TM/non-TM interconversion for many hours. However, the interconversion of this sequence was at most hindered, but not blocked, in a lipid mixture commonly used as a eukaryotic model. The experiments with the Polio-flanked sequence shows that the presence of aromatic (Phe), other cyclic polar (His), or highly flexible residues (Gly) also didn't block interconversion. How changes in sequence would alter this behavior is of interest.

Aside from additional experiments varying JM sequence length, there are various questions about the effect of the JM sequence that remain to be probed. The primary property one might expect to control TM/non-TM interconversion is the ability of JM residues to partition between hydrophilic and hydrophobic solvents. A scale for that compares the partitioning of different amino acid residues has already been reported (White & Wimley, 1998). A peptide with a JM sequence of either S_6K_2 or A_6K_2 should, according to Wimley-White scale, interconvert as least as quickly as the N_6K_2 JM sequence. Closely related to this hydrophobic/hydrophilic partition scale, is the total electrical character of the JM sequence. The N_6 portion of the sequence was chosen because although it is polar, but not formally charged. However, the total N_6K_2 sequence carries a charge of 2+. Addition of two Asp or Glu to the JM sequence, which would render the JM sequence to be electrically neutral, could conceivably accelerate TM/non-TM interconversion in 40 mol% cholesterol if net charge slows interconversion. A different consequence of additional charged residues could also be to further hinder TM/non-TM interconversion; this would have to be experimentally determined.

The effect of other structural features of the JM region upon interconversion could be investigated. The Pro sidechain causes a stiff permanent kink in the peptide backbone, while Gly increases backbone dynamics. Inclusion of either residue between the TM and JM region of

a peptide would be expected to effect the bending of the peptide, and possibly interconversion rate.

The ability of individual amino acids to induce, or prevent, formation of a helical structure has been quantified in a helix propensity scale (Pace & Scholtz, 1998). Our selection of Asn as a polar repeating residue renders our JM region ~3.6 kcal/mol less stable as a helix as compared to Ala. Use of a Q_6K_2-flanked sequence would allow to keep the electrical properties of the JM sequence identical to N_6K_2-flanking, but would be 1/3 more likely to maintain a helical structure. This would test if the ability to form a helix helps a JM sequence to cross the membrane. Conversely, a T_6K_2-flanked JM region would have the same helical propensity of N_6K_2-flanked peptide, but a much reduced polarity, and so would be expected to allow even more rapid interconversion.

The Paradox of Polar Groups Moving Through the Hydrophobic Core Quickly for Peptides and Slowly for Lipids

In Chapter 3, we investigated what TM peptide sequences accelerated the movement of lipids through a vesicle membrane. In Chapter 4, we asked what was the maximum limit of polar residues an interconverting peptide could move through a vesicle membrane. Both inquiries were regarding the movement of polar molecules, either headgroups or amino acids, through a hydrophobic bilayer. Surprisingly, our experiments reported movement of 100% N_6K_2-flanked peptide across the membrane in less than 10 sec upon pH shift, yet after 2 hrs of incubation only 25% 6-NBD-PC had with flipped to the interior of POPC LUVs. If lipids moved through the membrane as fast as JM residues seem to, we would measure 50% fluorescence protection (the theoretical maximum) within a minute, not more than 20 hrs.

The simplest explanation is that there is something inherent in lipid structure that normally slows down flip-flop. As discussed in Chapter 1, it is generally thought that the hydrophilic headgroup of lipids is what delays flip-flop. The single most universal and hydrophilic moiety in lipids is the phosphate group. There are now artificial lipids commercially

available that are similar to natural lipids, except that they lack a phosphate linker (similar to 1,2-dioleoyl-sn-glycero-3-succinate). If the phosphate group is what delays lipid flip-flop vesicles an NBD analog of this lipid should show protection in a much shorter incubation time. It is also possible to test the influence of a phosphate group on the ability of a JM sequence to block TM/non-TM interconversion. Peptides can be created that include either Ser or Thr in their JM region. This peptide can be tested for TM/non-TM interconversion, similar to what was proposed above. If designed carefully, this same peptide can serve as a substrate for a kinase to add a phosphate, or more than one, to the JM region. If this modified peptide does not interconvert, then it would be very strong evidence that translocation of phosphate through membranes is very energetically unfavorable.

References:

Abell, B. M., Rabu, C., Leznicki, P., Young, J. C., & High, S. (2007). Post-translational integration of tail-anchored proteins is facilitated by defined molecular chaperones. *J Cell Sci, 120*(Pt 10), 1743-1751. doi: jcs.002410 [pii]

10.1242/jcs.002410

Ahmed, S. N., Brown, D. A., & London, E. (1997). On the origin of sphingolipid/cholesterol-rich detergent-insoluble cell membranes: physiological concentrations of cholesterol and sphingolipid induce formation of a detergent-insoluble, liquid-ordered lipid phase in model membranes. *Biochemistry, 36*(36), 10944-10953. doi: 10.1021/bi971167g

bi971167g [pii]

Alanko, J., & Ivaska, J. (2016). Endosomes: Emerging Platforms for Integrin-Mediated FAK Signalling. *Trends Cell Biol, 26*(6), 391-398. doi: S0962-8924(16)00013-1 [pii]

10.1016/j.tcb.2016.02.001

Andreev, O. A., Dupuy, A. D., Segala, M., Sandugu, S., Serra, D. A., Chichester, C. O., . . . Reshetnyak, Y. K. (2007). Mechanism and uses of a membrane peptide that targets tumors and other acidic tissues in vivo. *Proc Natl Acad Sci U S A, 104*(19), 7893-7898. doi: 0702439104 [pii]

10.1073/pnas.0702439104

Andreev, O. A., Karabadzhak, A. G., Weerakkody, D., Andreev, G. O., Engelman, D. M., & Reshetnyak, Y. K. (2010). pH (low) insertion peptide (pHLIP) inserts across a lipid bilayer as a helix and exits by a different path. *Proc Natl Acad Sci U S A, 107*(9), 4081-4086. doi: 0914330107 [pii]

10.1073/pnas.0914330107

Andrushchenko, V. V., Vogel, H. J., & Prenner, E. J. (2007). Optimization of the hydrochloric acid concentration used for trifluoroacetate removal from synthetic peptides. *J Pept Sci, 13*(1), 37-43. doi: 10.1002/psc.793

Anglin, T. C., & Conboy, J. C. (2009). Kinetics and thermodynamics of flip-flop in binary phospholipid membranes measured by sum-frequency vibrational spectroscopy. *Biochemistry, 48*(43), 10220-10234. doi: 10.1021/bi901096j

Anglin, T. C., Cooper, M. P., Li, H., Chandler, K., & Conboy, J. C. (2010). Free energy and entropy of activation for phospholipid flip-flop in planar supported lipid bilayers. *J Phys Chem B, 114*(5), 1903-1914. doi: 10.1021/jp909134g

Armstrong, V. T., Brzustowicz, M. R., Wassall, S. R., Jenski, L. J., & Stillwell, W. (2003). Rapid flip-flop in polyunsaturated (docosahexaenoate) phospholipid membranes. *Arch Biochem Biophys, 414*(1), 74-82. doi: S0003986103001590 [pii]

Bai, Y., McCoy, J. G., Levin, E. J., Sobrado, P., Rajashankar, K. R., Fox, B. G., & Zhou, M. (2015). X-ray structure of a mammalian stearoyl-CoA desaturase. *Nature, 524*(7564), 252-256. doi: nature14549 [pii]

10.1038/nature14549

Balasubramanian, K., & Schroit, A. J. (2003). Aminophospholipid asymmetry: A matter of life and death. *Annu Rev Physiol, 65*, 701-734. doi: 10.1146/annurev.physiol.65.092101.142459

092101.142459 [pii]

Barrera, F. N., Fendos, J., & Engelman, D. M. (2012). Membrane physical properties influence transmembrane helix formation. *Proc Natl Acad Sci U S A, 109*(36), 14422-14427. doi: 1212665109 [pii]

10.1073/pnas.1212665109

Barrera, F. N., Weerakkody, D., Anderson, M., Andreev, O. A., Reshetnyak, Y. K., & Engelman, D. M. (2011). Roles of carboxyl groups in the transmembrane insertion of peptides. *J Mol Biol, 413*(2), 359-371. doi: S0022-2836(11)00877-1 [pii]

10.1016/j.jmb.2011.08.010

Batzri, S., & Korn, E. D. (1973). Single bilayer liposomes prepared without sonication. *Biochim Biophys Acta, 298*(4), 1015-1019. doi: 0005-2736(73)90408-2 [pii]

Bechinger, B. (1996). Towards membrane protein design: pH-sensitive topology of histidine-containing polypeptides. *J Mol Biol, 263*(5), 768-775. doi: S0022-2836(96)90614-2 [pii]

10.1006/jmbi.1996.0614

Bell, R. M., & Coleman, R. A. (1980). Enzymes of glycerolipid synthesis in eukaryotes. *Annu Rev Biochem, 49*, 459-487. doi: 10.1146/annurev.bi.49.070180.002331

Bevers, E. M., Comfurius, P., & Zwaal, R. F. (1983). Changes in membrane phospholipid distribution during platelet activation. *Biochim Biophys Acta, 736*(1), 57-66. doi: 0005-2736(83)90169-4 [pii]

Bevers, E. M., & Williamson, P. L. (2016). Getting to the Outer Leaflet: Physiology of Phosphatidylserine Exposure at the Plasma Membrane. *Physiol Rev, 96*(2), 605-645. doi: 96/2/605 [pii]

10.1152/physrev.00020.2015

Bhattacharya, S., & Haldar, S. (2000). Interactions between cholesterol and lipids in bilayer membranes. Role of lipid headgroup and hydrocarbon chain-backbone linkage. *Biochim Biophys Acta, 1467*(1), 39-53. doi: S0005-2736(00)00196-6 [pii]

Biswas, A., Gomes, A., Sengupta, J., Datta, P., Singha, S., & Dasgupta, A. K. (2012). Nanoparticle-conjugated animal venom-toxins and their possible therapeutic potential. *J Venom Res, 3*, 15-21.

Blok, M. C., van Deenen, L. L., & De Gier, J. (1976). Effect of the gel to liquid crystalline phase transition on the osmotic behaviour of phosphatidylcholine liposomes. *Biochim Biophys Acta, 433*(1), 1-12.

Bogdanov, M., & Dowhan, W. (1998). Phospholipid-assisted protein folding: phosphatidylethanolamine is required at a late step of the conformational maturation of the polytopic membrane protein lactose permease. *EMBO J, 17*(18), 5255-5264. doi: 10.1093/emboj/17.18.5255

Breyton, C., Haase, W., Rapoport, T. A., Kuhlbrandt, W., & Collinson, I. (2002). Three-dimensional structure of the bacterial protein-translocation complex SecYEG. *Nature, 418*(6898), 662-665. doi: 10.1038/nature00827

nature00827 [pii]

Brown, K. L., & Conboy, J. C. (2013). Lipid flip-flop in binary membranes composed of phosphatidylserine and phosphatidylcholine. *J Phys Chem B, 117*(48), 15041-15050. doi: 10.1021/jp409672q

Callahan, M. K., Williamson, P., & Schlegel, R. A. (2000). Surface expression of phosphatidylserine on macrophages is required for phagocytosis of apoptotic thymocytes. *Cell Death Differ, 7*(7), 645-653. doi: 10.1038/sj.cdd.4400690

Caputo, G. A., & London, E. (2003a). Cumulative effects of amino acid substitutions and hydrophobic mismatch upon the transmembrane stability and conformation of hydrophobic alpha-helices. *Biochemistry, 42*(11), 3275-3285. doi: 10.1021/bi026697d

Caputo, G. A., & London, E. (2003b). Using a novel dual fluorescence quenching assay for measurement of tryptophan depth within lipid bilayers to determine hydrophobic alpha-helix locations within membranes. *Biochemistry, 42*(11), 3265-3274. doi: 10.1021/bi026696l

Caputo, G. A., & London, E. (2004). Position and ionization state of Asp in the core of membrane-inserted alpha helices control both the equilibrium between transmembrane and nontransmembrane helix topography and transmembrane helix positioning. *Biochemistry, 43*(27), 8794-8806. doi: 10.1021/bi049696p

Chen, Y. J., Pornillos, O., Lieu, S., Ma, C., Chen, A. P., & Chang, G. (2007). X-ray structure of EmrE supports dual topology model. *Proc Natl Acad Sci U S A, 104*(48), 18999-19004. doi: 0709387104 [pii]

10.1073/pnas.0709387104

Cheng, H. T., & London, E. (2011). Preparation and properties of asymmetric large unilamellar vesicles: interleaflet coupling in asymmetric vesicles is dependent on temperature but not curvature. *Biophys J, 100*(11), 2671-2678. doi: S0006-3495(11)00526-1 [pii]

10.1016/j.bpj.2011.04.048

Cheng, H. T., Megha, & London, E. (2009). Preparation and properties of asymmetric vesicles that mimic cell membranes: effect upon lipid raft formation and transmembrane helix orientation. *J Biol Chem, 284*(10), 6079-6092. doi: M806077200 [pii]

10.1074/jbc.M806077200

Choe, S., Bennett, M. J., Fujii, G., Curmi, P. M., Kantardjieff, K. A., Collier, R. J., & Eisenberg, D. (1992). The crystal structure of diphtheria toxin. *Nature, 357*(6375), 216-222. doi: 10.1038/357216a0

Cymer, F., von Heijne, G., & White, S. H. (2015). Mechanisms of integral membrane protein insertion and folding. *J Mol Biol, 427*(5), 999-1022. doi: S0022-2836(14)00513-0 [pii]

10.1016/j.jmb.2014.09.014

Daleke, D. L. (2003). Regulation of transbilayer plasma membrane phospholipid asymmetry. *J Lipid Res, 44*(2), 233-242. doi: 10.1194/jlr.R200019-JLR200

R200019-JLR200 [pii]

Daleke, D. L. (2008). Regulation of phospholipid asymmetry in the erythrocyte membrane. *Curr Opin Hematol, 15*(3), 191-195. doi: 10.1097/MOH.0b013e3282f97af7

00062752-200805000-00007 [pii]

Darland-Ransom, M., Wang, X., Sun, C. L., Mapes, J., Gengyo-Ando, K., Mitani, S., & Xue, D. (2008). Role of C. elegans TAT-1 protein in maintaining plasma membrane phosphatidylserine asymmetry. *Science, 320*(5875), 528-531. doi: 320/5875/528 [pii]

10.1126/science.1155847

Davies, A., Lewis, D. J., Watson, S. P., Thomas, S. G., & Pikramenou, Z. (2012). pH-controlled delivery of luminescent europium coated nanoparticles into platelets. *Proc Natl Acad Sci U S A, 109*(6), 1862-1867. doi: 1112132109 [pii]

10.1073/pnas.1112132109

de Kroon, A. I., Rijken, P. J., & De Smet, C. H. (2013). Checks and balances in membrane phospholipid class and acyl chain homeostasis, the yeast perspective. *Prog Lipid Res, 52*(4), 374-394. doi: S0163-7827(13)00027-1 [pii]

10.1016/j.plipres.2013.04.006

De Marothy, M. T., & Elofsson, A. (2015). Marginally hydrophobic transmembrane alpha-helices shaping membrane protein folding. *Protein Sci, 24*(7), 1057-1074. doi: 10.1002/pro.2698

de Planque, M. R., Bonev, B. B., Demmers, J. A., Greathouse, D. V., Koeppe, R. E., 2nd, Separovic, F., . . . Killian, J. A. (2003). Interfacial anchor properties of tryptophan residues in transmembrane peptides can dominate over hydrophobic matching effects in peptide-lipid interactions. *Biochemistry, 42*(18), 5341-5348. doi: 10.1021/bi027000r

de Planque, M. R., Boots, J. W., Rijkers, D. T., Liskamp, R. M., Greathouse, D. V., & Killian, J. A. (2002). The effects of hydrophobic mismatch between phosphatidylcholine bilayers and transmembrane alpha-helical peptides depend on the nature of interfacially exposed aromatic and charged residues. *Biochemistry, 41*(26), 8396-8404. doi: bi0257686 [pii]

de Planque, M. R., Greathouse, D. V., Koeppe, R. E., 2nd, Schafer, H., Marsh, D., & Killian, J. A. (1998). Influence of lipid/peptide hydrophobic mismatch on the thickness of diacylphosphatidylcholine bilayers. A 2H NMR and ESR study using designed transmembrane alpha-helical peptides and gramicidin A. *Biochemistry, 37*(26), 9333-9345. doi: 10.1021/bi980233r

bi980233r [pii]

Delon, C., Manifava, M., Wood, E., Thompson, D., Krugmann, S., Pyne, S., & Ktistakis, N. T. (2004). Sphingosine kinase 1 is an intracellular effector of phosphatidic acid. *J Biol Chem, 279*(43), 44763-44774. doi: 10.1074/jbc.M405771200

M405771200 [pii]

Delos Santos, R. C., Garay, C., & Antonescu, C. N. (2015). Charming neighborhoods on the cell surface: plasma membrane microdomains regulate receptor tyrosine kinase signaling. *Cell Signal, 27*(10), 1963-1976. doi: S0898-6568(15)00197-7 [pii]

10.1016/j.cellsig.2015.07.004

Denks, K., Vogt, A., Sachelaru, I., Petriman, N. A., Kudva, R., & Koch, H. G. (2014). The Sec translocon mediated protein transport in prokaryotes and eukaryotes. *Mol Membr Biol, 31*(2-3), 58-84. doi: 10.3109/09687688.2014.907455

Dicorleto, P. E., & Zilversmit, D. B. (1979). Exchangeability and rate of flip-flop of phosphatidylcholine in large unilamellar vesicles, cholate dialysis vesicles, and cytochrome oxidase vesicles. *Biochim Biophys Acta, 552*(1), 114-119. doi: 0005-2736(79)90250-5 [pii]

Engberg, O., Nurmi, H., Nyholm, T. K., & Slotte, J. P. (2015). Effects of cholesterol and saturated sphingolipids on acyl chain order in 1-palmitoyl-2-oleoyl-sn-glycero-3-phosphocholine bilayers--a comparative study with phase-selective fluorophores. *Langmuir, 31*(14), 4255-4263. doi: 10.1021/acs.langmuir.5b00403

Fadok, V. A., de Cathelineau, A., Daleke, D. L., Henson, P. M., & Bratton, D. L. (2001). Loss of phospholipid asymmetry and surface exposure of phosphatidylserine is required for phagocytosis of apoptotic cells by macrophages and fibroblasts. *J Biol Chem, 276*(2), 1071-1077. doi: 10.1074/jbc.M003649200

M003649200 [pii]

Fadok, V. A., Voelker, D. R., Campbell, P. A., Cohen, J. J., Bratton, D. L., & Henson, P. M. (1992). Exposure of phosphatidylserine on the surface of apoptotic lymphocytes triggers specific recognition and removal by macrophages. *J Immunol, 148*(7), 2207-2216.

Fastenberg, M. E., Shogomori, H., Xu, X., Brown, D. A., & London, E. (2003). Exclusion of a transmembrane-type peptide from ordered-lipid domains (rafts) detected by fluorescence quenching: extension of quenching analysis to account for the effects of domain size and domain boundaries. *Biochemistry, 42*(42), 12376-12390. doi: 10.1021/bi034718d

Fendos, J., Barrera, F. N., & Engelman, D. M. (2013). Aspartate embedding depth affects pHLIP's insertion pKa. *Biochemistry, 52*(27), 4595-4604. doi: 10.1021/bi400252k

Folmer, D. E., van der Mark, V. A., Ho-Mok, K. S., Oude Elferink, R. P., & Paulusma, C. C. (2009). Differential effects of progressive familial intrahepatic cholestasis type 1 and benign recurrent intrahepatic cholestasis type 1 mutations on canalicular localization of ATP8B1. *Hepatology, 50*(5), 1597-1605. doi: 10.1002/hep.23158

Fujita, K., Krishnakumar, S. S., Franco, D., Paul, A. V., London, E., & Wimmer, E. (2007). Membrane topography of the hydrophobic anchor sequence of poliovirus 3A and 3AB proteins and the functional effect of 3A/3AB membrane association upon RNA replication. *Biochemistry, 46*(17), 5185-5199. doi: 10.1021/bi6024758

Futerman, A. H., & Riezman, H. (2005). The ins and outs of sphingolipid synthesis. *Trends Cell Biol, 15*(6), 312-318. doi: S0962-8924(05)00107-8 [pii]

10.1016/j.tcb.2005.04.006

Ghatak, C., Rodnin, M. V., Vargas-Uribe, M., McCluskey, A. J., Flores-Canales, J. C., Kurnikova, M., & Ladokhin, A. S. (2015). Role of acidic residues in helices TH8-TH9 in membrane interactions of the diphtheria toxin T domain. *Toxins (Basel), 7*(4), 1303-1323. doi: toxins7041303 [pii]

10.3390/toxins7041303

Goren, M. A., Morizumi, T., Menon, I., Joseph, J. S., Dittman, J. S., Cherezov, V., . . . Menon, A. K. (2014). Constitutive phospholipid scramblase activity of a G protein-coupled receptor. *Nat Commun, 5*, 5115. doi: ncomms6115 [pii]

10.1038/ncomms6115

Guan, L., & Kaback, H. R. (2006). Lessons from lactose permease. *Annu Rev Biophys Biomol Struct, 35*, 67-91. doi: 10.1146/annurev.biophys.35.040405.102005

Hall, J. E. (1981). Voltage-dependent lipid flip-flop induced by alamethicin. *Biophys J, 33*(3), 373-381. doi: S0006-3495(81)84901-6 [pii]

10.1016/S0006-3495(81)84901-6

Hammond, K., Caputo, G. A., & London, E. (2002). Interaction of the membrane-inserted diphtheria toxin T domain with peptides and its possible implications for chaperone-like T domain behavior. *Biochemistry, 41*(9), 3243-3253. doi: bi011163i [pii]

Han, G. S., Wu, W. I., & Carman, G. M. (2006). The Saccharomyces cerevisiae Lipin homolog is a Mg2+-dependent phosphatidate phosphatase enzyme. *J Biol Chem, 281*(14), 9210-9218. doi: M600425200 [pii]

10.1074/jbc.M600425200

Hartman, I. Z., Liu, P., Zehmer, J. K., Luby-Phelps, K., Jo, Y., Anderson, R. G., & DeBose-Boyd, R. A. (2010). Sterol-induced dislocation of 3-hydroxy-3-methylglutaryl coenzyme A reductase from endoplasmic reticulum membranes into the cytosol through a subcellular compartment resembling lipid droplets. *J Biol Chem, 285*(25), 19288-19298. doi: M110.134213 [pii]

10.1074/jbc.M110.134213

Harzer, U., & Bechinger, B. (2000). Alignment of lysine-anchored membrane peptides under conditions of hydrophobic mismatch: a CD, 15N and 31P solid-state NMR spectroscopy investigation. *Biochemistry, 39*(43), 13106-13114. doi: bi000770n [pii]

Hayashibara, M., & London, E. (2005). Topography of diphtheria toxin A chain inserted into lipid vesicles. *Biochemistry, 44*(6), 2183-2196. doi: 10.1021/bi0482093

He, K., Ludtke, S. J., Heller, W. T., & Huang, H. W. (1996). Mechanism of alamethicin insertion into lipid bilayers. *Biophys J, 71*(5), 2669-2679. doi: S0006-3495(96)79458-4 [pii]

10.1016/S0006-3495(96)79458-4

Heinemann, F. S., & Ozols, J. (2003). Stearoyl-CoA desaturase, a short-lived protein of endoplasmic reticulum with multiple control mechanisms. *Prostaglandins Leukot Essent Fatty Acids, 68*(2), 123-133. doi: S0952327802002624 [pii]

Henneberry, A. L., Wright, M. M., & McMaster, C. R. (2002). The major sites of cellular phospholipid synthesis and molecular determinants of Fatty Acid and lipid head group specificity. *Mol Biol Cell, 13*(9), 3148-3161. doi: 10.1091/mbc.01-11-0540

Hessa, T., Kim, H., Bihlmaier, K., Lundin, C., Boekel, J., Andersson, H., . . . von Heijne, G. (2005). Recognition of transmembrane helices by the endoplasmic reticulum translocon. *Nature, 433*(7024), 377-381. doi: nature03216 [pii]

10.1038/nature03216

Huang, H. W., Chen, F. Y., & Lee, M. T. (2004). Molecular mechanism of Peptide-induced pores in membranes. *Phys Rev Lett, 92*(19), 198304. doi: 10.1103/PhysRevLett.92.198304

Huang, J., & Feigenson, G. W. (1999). A microscopic interaction model of maximum solubility of cholesterol in lipid bilayers. *Biophys J, 76*(4), 2142-2157. doi: S0006-3495(99)77369-8 [pii]

10.1016/S0006-3495(99)77369-8

Hung, W. C., Lee, M. T., Chen, F. Y., & Huang, H. W. (2007). The condensing effect of cholesterol in lipid bilayers. *Biophys J, 92*(11), 3960-3967. doi: S0006-3495(07)71195-5 [pii]

10.1529/biophysj.106.099234

Hunt, J. F., Rath, P., Rothschild, K. J., & Engelman, D. M. (1997). Spontaneous, pH-dependent membrane insertion of a transbilayer alpha-helix. *Biochemistry, 36*(49), 15177-15192. doi: 10.1021/bi970147b

bi970147b [pii]

Jiang, J., Pentelute, B. L., Collier, R. J., & Zhou, Z. H. (2015). Atomic structure of anthrax protective antigen pore elucidates toxin translocation. *Nature, 521*(7553), 545-549. doi: nature14247 [pii]

10.1038/nature14247

John, K., Schreiber, S., Kubelt, J., Herrmann, A., & Muller, P. (2002). Transbilayer movement of phospholipids at the main phase transition of lipid membranes: implications for rapid flip-flop in biological membranes. *Biophys J, 83*(6), 3315-3323. doi: S0006-3495(02)75332-0 [pii]

10.1016/S0006-3495(02)75332-0

Kaihara, M., Nakao, H., Yokoyama, H., Endo, H., Ishihama, Y., Handa, T., & Nakano, M. (2013). Control of phospholipid flip-flop by transmembrane peptides. *Chemical Physics, 419*, 78-83. doi: http://dx.doi.org/10.1016/j.chemphys.2012.12.041

Kalbfleisch, T., Cambon, A., & Wattenberg, B. W. (2007). A bioinformatics approach to identifying tail-anchored proteins in the human genome. *Traffic, 8*(12), 1687-1694. doi: TRA661 [pii]

10.1111/j.1600-0854.2007.00661.x

Karabadzhak, A. G., Weerakkody, D., Wijesinghe, D., Thakur, M. S., Engelman, D. M., Andreev, O. A., . . . Reshetnyak, Y. K. (2012). Modulation of the pHLIP transmembrane helix insertion pathway. *Biophys J, 102*(8), 1846-1855. doi: S0006-3495(12)00332-3 [pii]

10.1016/j.bpj.2012.03.021
Kauko, A., Hedin, L. E., Thebaud, E., Cristobal, S., Elofsson, A., & von Heijne, G. (2010). Repositioning of transmembrane alpha-helices during membrane protein folding. *J Mol Biol, 397*(1), 190-201. doi: S0022-2836(10)00088-4 [pii]

10.1016/j.jmb.2010.01.042
Kihara, A., Sano, T., Iwaki, S., & Igarashi, Y. (2003). Transmembrane topology of sphingoid long-chain base-1-phosphate phosphatase, Lcb3p. *Genes Cells, 8*(6), 525-535. doi: 653 [pii]
Killian, J. A. (1998). Hydrophobic mismatch between proteins and lipids in membranes. *Biochim Biophys Acta, 1376*(3), 401-415. doi: S0304-4157(98)00017-3 [pii]
Kim, J., & London, E. (2015). Using Sterol Substitution to Probe the Role of Membrane Domains in Membrane Functions. *Lipids, 50*(8), 721-734. doi: 10.1007/s11745-015-4007-y
Kodigepalli, K. M., Bowers, K., Sharp, A., & Nanjundan, M. (2015). Roles and regulation of phospholipid scramblases. *FEBS Lett, 589*(1), 3-14. doi: S0014-5793(14)00852-7 [pii]

10.1016/j.febslet.2014.11.036
Kol, M. A., de Kroon, A. I., Rijkers, D. T., Killian, J. A., & de Kruijff, B. (2001). Membrane-spanning peptides induce phospholipid flop: a model for phospholipid translocation across the inner membrane of E. coli. *Biochemistry, 40*(35), 10500-10506. doi: bi010627+ [pii]
Kol, M. A., van Dalen, A., de Kroon, A. I., & de Kruijff, B. (2003). Translocation of phospholipids is facilitated by a subset of membrane-spanning proteins of the bacterial cytoplasmic membrane. *J Biol Chem, 278*(27), 24586-24593. doi: 10.1074/jbc.M301875200

M301875200 [pii]
Kol, M. A., van Laak, A. N., Rijkers, D. T., Killian, J. A., de Kroon, A. I., & de Kruijff, B. (2003). Phospholipid flop induced by transmembrane peptides in model membranes is modulated by lipid composition. *Biochemistry, 42*(1), 231-237. doi: 10.1021/bi0268403
Koriazova, L. K., & Montal, M. (2003). Translocation of botulinum neurotoxin light chain protease through the heavy chain channel. *Nat Struct Biol, 10*(1), 13-18. doi: 10.1038/nsb879

nsb879 [pii]
Krishnakumar, S. S., & London, E. (2007a). The control of transmembrane helix transverse position in membranes by hydrophilic residues. *J Mol Biol, 374*(5), 1251-1269. doi: S0022-2836(07)01370-8 [pii]

10.1016/j.jmb.2007.10.032
Krishnakumar, S. S., & London, E. (2007b). Effect of sequence hydrophobicity and bilayer width upon the minimum length required for the formation of transmembrane helices in membranes. *J Mol Biol, 374*(3), 671-687. doi: S0022-2836(07)01225-9 [pii]

10.1016/j.jmb.2007.09.037
Kucerka, N., Tristram-Nagle, S., & Nagle, J. F. (2005). Structure of fully hydrated fluid phase lipid bilayers with monounsaturated chains. *J Membr Biol, 208*(3), 193-202. doi: 10.1007/s00232-005-7006-8

Kutay, U., Hartmann, E., & Rapoport, T. A. (1993). A class of membrane proteins with a C-terminal anchor. *Trends Cell Biol, 3*(3), 72-75. doi: 0962-8924(93)90066-A [pii]

Kyrychenko, A., Vasquez-Montes, V., Ulmschneider, M. B., & Ladokhin, A. S. (2015). Lipid headgroups modulate membrane insertion of pHLIP peptide. *Biophys J, 108*(4), 791-794. doi: S0006-3495(15)00061-2 [pii]

10.1016/j.bpj.2015.01.002

Lai, B., Zhao, G., & London, E. (2008). Behavior of the deeply inserted helices in diphtheria toxin T domain: helices 5, 8, and 9 interact strongly and promote pore formation, while helices 6/7 limit pore formation. *Biochemistry, 47*(15), 4565-4574. doi: 10.1021/bi7025134

Langer, M., & Langosch, D. (2011). Is lipid flippase activity of SNARE transmembrane domains required for membrane fusion? *FEBS Lett, 585*(7), 1021-1024. doi: S0014-5793(11)00137-2 [pii]

10.1016/j.febslet.2011.02.033

Langer, M., Sah, R., Veser, A., Gutlich, M., & Langosch, D. (2013). Structural properties of model phosphatidylcholine flippases. *Chem Biol, 20*(1), 63-72. doi: S1074-5521(12)00454-1 [pii]

10.1016/j.chembiol.2012.11.006

Langner, M., & Hui, S. (2000). Effect of free fatty acids on the permeability of 1,2-dimyristoyl-sn-glycero-3-phosphocholine bilayer at the main phase transition. *Biochim Biophys Acta, 1463*(2), 439-447. doi: S0005-2736(99)00236-9 [pii]

LaRocca, T. J., Pathak, P., Chiantia, S., Toledo, A., Silvius, J. R., Benach, J. L., & London, E. (2013). Proving lipid rafts exist: membrane domains in the prokaryote Borrelia burgdorferi have the same properties as eukaryotic lipid rafts. *PLoS Pathog, 9*(5), e1003353. doi: 10.1371/journal.ppat.1003353

PPATHOGENS-D-12-03152 [pii]

LeBarron, J., & London, E. (2016). Effect of lipid composition and amino acid sequence upon transmembrane peptide-accelerated lipid transleaflet diffusion (flip-flop). *Biochim Biophys Acta, 1858*(8), 1812-1820. doi: S0005-2736(16)30138-9 [pii]

10.1016/j.bbamem.2016.04.011

Leftin, A., Molugu, T. R., Job, C., Beyer, K., & Brown, M. F. (2014). Area per lipid and cholesterol interactions in membranes from separated local-field (13)C NMR spectroscopy. *Biophys J, 107*(10), 2274-2286. doi: S0006-3495(14)00789-9 [pii]

10.1016/j.bpj.2014.07.044

Leite, N. B., Aufderhorst-Roberts, A., Palma, M. S., Connell, S. D., Ruggiero Neto, J., & Beales, P. A. (2015). PE and PS Lipids Synergistically Enhance Membrane Poration by a Peptide with Anticancer Properties. *Biophys J, 109*(5), 936-947. doi: S0006-3495(15)00768-7 [pii]

10.1016/j.bpj.2015.07.033

Lenoir, G., Williamson, P., & Holthuis, J. C. (2007). On the origin of lipid asymmetry: the flip side of ion transport. *Curr Opin Chem Biol, 11*(6), 654-661. doi: S1367-5931(07)00136-6 [pii]

10.1016/j.cbpa.2007.09.008
Lew, S., Caputo, G. A., & London, E. (2003). The effect of interactions involving ionizable residues flanking membrane-inserted hydrophobic helices upon helix-helix interaction. *Biochemistry, 42*(36), 10833-10842. doi: 10.1021/bi034929i
Lew, S., & London, E. (1997). Simple procedure for reversed-phase high-performance liquid chromatographic purification of long hydrophobic peptides that form transmembrane helices. *Anal Biochem, 251*(1), 113-116. doi: S0003-2697(97)92232-6 [pii]

10.1006/abio.1997.2232
Lew, S., Ren, J., & London, E. (2000). The effects of polar and/or ionizable residues in the core and flanking regions of hydrophobic helices on transmembrane conformation and oligomerization. *Biochemistry, 39*(32), 9632-9640. doi: bi000694o [pii]
Liu, J., Brown, K. L., & Conboy, J. C. (2013). The effect of cholesterol on the intrinsic rate of lipid flip-flop as measured by sum-frequency vibrational spectroscopy. *Faraday Discuss, 161*, 45-61; discussion 113-150.
Liu, J., & Conboy, J. C. (2005). 1,2-diacyl-phosphatidylcholine flip-flop measured directly by sum-frequency vibrational spectroscopy. *Biophys J, 89*(4), 2522-2532. doi: S0006-3495(05)72893-9 [pii]

10.1529/biophysj.105.065672
London, E., & Feigenson, G. W. (1981). Fluorescence quenching in model membranes. 1. Characterization of quenching caused by a spin-labeled phospholipid. *Biochemistry, 20*(7), 1932-1938.
Lu, Y., Turnbull, I. R., Bragin, A., Carveth, K., Verkman, A. S., & Skach, W. R. (2000). Reorientation of aquaporin-1 topology during maturation in the endoplasmic reticulum. *Mol Biol Cell, 11*(9), 2973-2985.
Ludtke, S., He, K., & Huang, H. (1995). Membrane thinning caused by magainin 2. *Biochemistry, 34*(51), 16764-16769.
Mandon, E. C., Ehses, I., Rother, J., van Echten, G., & Sandhoff, K. (1992). Subcellular localization and membrane topology of serine palmitoyltransferase, 3-dehydrosphinganine reductase, and sphinganine N-acyltransferase in mouse liver. *J Biol Chem, 267*(16), 11144-11148.
Martin, S. J., Reutelingsperger, C. P., McGahon, A. J., Rader, J. A., van Schie, R. C., LaFace, D. M., & Green, D. R. (1995). Early redistribution of plasma membrane phosphatidylserine is a general feature of apoptosis regardless of the initiating stimulus: inhibition by overexpression of Bcl-2 and Abl. *J Exp Med, 182*(5), 1545-1556.
Matsuzaki, K., Murase, O., Fujii, N., & Miyajima, K. (1995). Translocation of a channel-forming antimicrobial peptide, magainin 2, across lipid bilayers by forming a pore. *Biochemistry, 34*(19), 6521-6526.
Matsuzaki, K., Murase, O., Fujii, N., & Miyajima, K. (1996). An antimicrobial peptide, magainin 2, induced rapid flip-flop of phospholipids coupled with pore formation and peptide translocation. *Biochemistry, 35*(35), 11361-11368. doi: 10.1021/bi960016v

bi960016v [pii]

McIntyre, J. C., & Sleight, R. G. (1991). Fluorescence assay for phospholipid membrane asymmetry. *Biochemistry, 30*(51), 11819-11827.

Mencarelli, C., & Martinez-Martinez, P. (2013). Ceramide function in the brain: when a slight tilt is enough. *Cell Mol Life Sci, 70*(2), 181-203. doi: 10.1007/s00018-012-1038-x

Menon, I., Huber, T., Sanyal, S., Banerjee, S., Barre, P., Canis, S., . . . Menon, A. K. (2011). Opsin is a phospholipid flippase. *Curr Biol, 21*(2), 149-153. doi: S0960-9822(10)01699-4 [pii]

10.1016/j.cub.2010.12.031

Michel, C., & van Echten-Deckert, G. (1997). Conversion of dihydroceramide to ceramide occurs at the cytosolic face of the endoplasmic reticulum. *FEBS Lett, 416*(2), 153-155. doi: S0014-5793(97)01187-3 [pii]

Mondal, M., Mesmin, B., Mukherjee, S., & Maxfield, F. R. (2009). Sterols are mainly in the cytoplasmic leaflet of the plasma membrane and the endocytic recycling compartment in CHO cells. *Mol Biol Cell, 20*(2), 581-588. doi: E08-07-0785 [pii]

10.1091/mbc.E08-07-0785

Moser von Filseck, J., Vanni, S., Mesmin, B., Antonny, B., & Drin, G. (2015). A phosphatidylinositol-4-phosphate powered exchange mechanism to create a lipid gradient between membranes. *Nat Commun, 6*, 6671. doi: ncomms7671 [pii]

10.1038/ncomms7671

Moshnikova, A., Moshnikova, V., Andreev, O. A., & Reshetnyak, Y. K. (2013). Antiproliferative effect of pHLIP-amanitin. *Biochemistry, 52*(7), 1171-1178. doi: 10.1021/bi301647y

Munk, C., Isberg, V., Mordalski, S., Harpsoe, K., Rataj, K., Hauser, A. S., . . . Gloriam, D. E. (2016). GPCRdb: the G protein-coupled receptor database - an introduction. *Br J Pharmacol, 173*(14), 2195-2207. doi: 10.1111/bph.13509

Musial-Siwek, M., Karabadzhak, A., Andreev, O. A., Reshetnyak, Y. K., & Engelman, D. M. (2010). Tuning the insertion properties of pHLIP. *Biochim Biophys Acta, 1798*(6), 1041-1046. doi: S0005-2736(09)00309-5 [pii]

10.1016/j.bbamem.2009.08.023

Muthusamy, B. P., Raychaudhuri, S., Natarajan, P., Abe, F., Liu, K., Prinz, W. A., & Graham, T. R. (2009). Control of protein and sterol trafficking by antagonistic activities of a type IV P-type ATPase and oxysterol binding protein homologue. *Mol Biol Cell, 20*(12), 2920-2931. doi: E08-10-1036 [pii]

10.1091/mbc.E08-10-1036

Nakao, H., Ikeda, K., Iwamoto, M., Shimizu, H., Oiki, S., Ishihama, Y., & Nakano, M. (2015). pH-dependent promotion of phospholipid flip-flop by the KcsA potassium channel. *Biochim Biophys Acta, 1848*(1 Pt A), 145-150. doi: S0005-2736(14)00336-8 [pii]

10.1016/j.bbamem.2014.10.001

Ohashi, M., Mizushima, N., Kabeya, Y., & Yoshimori, T. (2003). Localization of mammalian NAD(P)H steroid dehydrogenase-like protein on lipid droplets. *J Biol Chem, 278*(38), 36819-36829. doi: 10.1074/jbc.M301408200

M301408200 [pii]
Pace, C. N., & Scholtz, J. M. (1998). A helix propensity scale based on experimental studies of peptides and proteins. *Biophys J, 75*(1), 422-427.
Pirazzini, M., Tehran, D. A., Leka, O., Zanetti, G., Rossetto, O., & Montecucco, C. (2016). On the translocation of botulinum and tetanus neurotoxins across the membrane of acidic intracellular compartments. *Biochim Biophys Acta, 1858*(3), 467-474. doi: S0005-2736(15)00265-5 [pii]

10.1016/j.bbamem.2015.08.014
Pogozheva, I. D., Mosberg, H. I., & Lomize, A. L. (2014). Life at the border: adaptation of proteins to anisotropic membrane environment. *Protein Sci, 23*(9), 1165-1196. doi: 10.1002/pro.2508
Pomorski, T., & Menon, A. K. (2006). Lipid flippases and their biological functions. *Cell Mol Life Sci, 63*(24), 2908-2921. doi: 10.1007/s00018-006-6167-7
Poschner, B. C., Fischer, K., Herrmann, J. R., Hofmann, M. W., & Langosch, D. (2010). Structural features of fusogenic model transmembrane domains that differentially regulate inner and outer leaflet mixing in membrane fusion. *Mol Membr Biol, 27*(1), 1-10. doi: 10.3109/09687680903362044
Preston, G. M., Jung, J. S., Guggino, W. B., & Agre, P. (1994). Membrane topology of aquaporin CHIP. Analysis of functional epitope-scanning mutants by vectorial proteolysis. *J Biol Chem, 269*(3), 1668-1673.
Quinn, P., Griffiths, G., & Warren, G. (1984). Density of newly synthesized plasma membrane proteins in intracellular membranes II. Biochemical studies. *J Cell Biol, 98*(6), 2142-2147.
Ran, S., Gao, B., Duffy, S., Watkins, L., Rote, N., & Thorpe, P. E. (1998). Infarction of solid Hodgkin's tumors in mice by antibody-directed targeting of tissue factor to tumor vasculature. *Cancer Res, 58*(20), 4646-4653.
Rao, L. V., Tait, J. F., & Hoang, A. D. (1992). Binding of annexin V to a human ovarian carcinoma cell line (OC-2008). Contrasting effects on cell surface factor VIIa/tissue factor activity and prothrombinase activity. *Thromb Res, 67*(5), 517-531.
Ren, J., Kachel, K., Kim, H., Malenbaum, S. E., Collier, R. J., & London, E. (1999). Interaction of diphtheria toxin T domain with molten globule-like proteins and its implications for translocation. *Science, 284*(5416), 955-957.
Ren, J., Lew, S., Wang, J., & London, E. (1999). Control of the transmembrane orientation and interhelical interactions within membranes by hydrophobic helix length. *Biochemistry, 38*(18), 5905-5912. doi: 10.1021/bi982942a

bi982942a [pii]
Ren, J., Lew, S., Wang, Z., & London, E. (1997). Transmembrane orientation of hydrophobic alpha-helices is regulated both by the relationship of helix length to bilayer thickness and by the cholesterol concentration. *Biochemistry, 36*(33), 10213-10220. doi: 10.1021/bi9709295

bi9709295 [pii]

Reshetnyak, Y. K., Andreev, O. A., Lehnert, U., & Engelman, D. M. (2006). Translocation of molecules into cells by pH-dependent insertion of a transmembrane helix. *Proc Natl Acad Sci U S A, 103*(17), 6460-6465. doi: 0601463103 [pii]

10.1073/pnas.0601463103

Reshetnyak, Y. K., Andreev, O. A., Segala, M., Markin, V. S., & Engelman, D. M. (2008). Energetics of peptide (pHLIP) binding to and folding across a lipid bilayer membrane. *Proc Natl Acad Sci U S A, 105*(40), 15340-15345. doi: 0804746105 [pii]

10.1073/pnas.0804746105

Reshetnyak, Y. K., Segala, M., Andreev, O. A., & Engelman, D. M. (2007). A monomeric membrane peptide that lives in three worlds: in solution, attached to, and inserted across lipid bilayers. *Biophys J, 93*(7), 2363-2372. doi: S0006-3495(07)71491-1 [pii]

10.1529/biophysj.107.109967

Rosconi, M. P., Zhao, G., & London, E. (2004). Analyzing topography of membrane-inserted diphtheria toxin T domain using BODIPY-streptavidin: at low pH, helices 8 and 9 form a transmembrane hairpin but helices 5-7 form stable nonclassical inserted segments on the cis side of the bilayer. *Biochemistry, 43*(28), 9127-9139. doi: 10.1021/bi049354j

Rothman, J. E., & Dawidowicz, E. A. (1975). Asymmetric exchange of vesicle phospholipids catalyzed by the phosphatidylcholine exhange protein. Measurement of inside--outside transitions. *Biochemistry, 14*(13), 2809-2816.

Sapay, N., Bennett, W. F., & Tieleman, D. P. (2010). Molecular simulations of lipid flip-flop in the presence of model transmembrane helices. *Biochemistry, 49*(35), 7665-7673. doi: 10.1021/bi100878q

Schuldiner, S. (2009). EmrE, a model for studying evolution and mechanism of ion-coupled transporters. *Biochim Biophys Acta, 1794*(5), 748-762. doi: S1570-9639(08)00398-1 [pii]

10.1016/j.bbapap.2008.12.018

Seppala, S., Slusky, J. S., Lloris-Garcera, P., Rapp, M., & von Heijne, G. (2010). Control of membrane protein topology by a single C-terminal residue. *Science, 328*(5986), 1698-1700. doi: science.1188950 [pii]

10.1126/science.1188950

Sessions, A., & Horwitz, A. F. (1983). Differentiation-related differences in the plasma membrane phospholipid asymmetry of myogenic and fibrogenic cells. *Biochim Biophys Acta, 728*(1), 103-111. doi: 0005-2736(83)90442-X [pii]

Shahidullah, K., Krishnakumar, S. S., & London, E. (2010). The effect of hydrophilic substitutions and anionic lipids upon the transverse positioning of the transmembrane helix of the ErbB2 (neu) protein incorporated into model membrane vesicles. *J Mol Biol, 396*(1), 209-220. doi: S0022-2836(09)01414-4 [pii]

10.1016/j.jmb.2009.11.037

Shahidullah, K., & London, E. (2008). Effect of lipid composition on the topography of membrane-associated hydrophobic helices: stabilization of transmembrane topography by anionic lipids. *J Mol Biol, 379*(4), 704-718. doi: S0022-2836(08)00455-5 [pii]

10.1016/j.jmb.2008.04.026
Sharpe, J. C., & London, E. (1999). Diphtheria toxin forms pores of different sizes depending on its concentration in membranes: probable relationship to oligomerization. *J Membr Biol, 171*(3), 209-221. doi: JMEMB098 [pii]
Sharpe, L. J., & Brown, A. J. (2013). Controlling cholesterol synthesis beyond 3-hydroxy-3-methylglutaryl-CoA reductase (HMGCR). *J Biol Chem, 288*(26), 18707-18715. doi: R113.479808 [pii]

10.1074/jbc.R113.479808
Sheng, X., Yung, Y. C., Chen, A., & Chun, J. (2015). Lysophosphatidic acid signalling in development. *Development, 142*(8), 1390-1395. doi: 142/8/1390 [pii]

10.1242/dev.121723
Singer, S. J., & Nicolson, G. L. (1972). The fluid mosaic model of the structure of cell membranes. *Science, 175*(4023), 720-731.
Skach, W. R., Shi, L. B., Calayag, M. C., Frigeri, A., Lingappa, V. R., & Verkman, A. S. (1994). Biogenesis and transmembrane topology of the CHIP28 water channel at the endoplasmic reticulum. *J Cell Biol, 125*(4), 803-815.
Son, M., & London, E. (2013a). The dependence of lipid asymmetry upon phosphatidylcholine acyl chain structure. *J Lipid Res, 54*(1), 223-231. doi: jlr.M032722 [pii]

10.1194/jlr.M032722
Son, M., & London, E. (2013b). The dependence of lipid asymmetry upon polar headgroup structure. *J Lipid Res, 54*(12), 3385-3393. doi: jlr.M041749 [pii]

10.1194/jlr.M041749
Sosunov, E. A., Anyukhovsky, E. P., Sosunov, A. A., Moshnikova, A., Wijesinghe, D., Engelman, D. M., . . . Andreev, O. A. (2013). pH (low) insertion peptide (pHLIP) targets ischemic myocardium. *Proc Natl Acad Sci U S A, 110*(1), 82-86. doi: 1220038110 [pii]

10.1073/pnas.1220038110
Sprong, H., Kruithof, B., Leijendekker, R., Slot, J. W., van Meer, G., & van der Sluijs, P. (1998). UDP-galactose:ceramide galactosyltransferase is a class I integral membrane protein of the endoplasmic reticulum. *J Biol Chem, 273*(40), 25880-25888.
Stachowiak, J. C., Schmid, E. M., Ryan, C. J., Ann, H. S., Sasaki, D. Y., Sherman, M. B., . . . Hayden, C. C. (2012). Membrane bending by protein-protein crowding. *Nat Cell Biol, 14*(9), 944-949. doi: ncb2561 [pii]

10.1038/ncb2561
Stone, S. J., Cui, Z., & Vance, J. E. (1998). Cloning and expression of mouse liver phosphatidylserine synthase-1 cDNA. Overexpression in rat hepatoma cells inhibits the CDP-ethanolamine pathway for phosphatidylethanolamine biosynthesis. *J Biol Chem, 273*(13), 7293-7302.
Stone, S. J., & Vance, J. E. (1999). Cloning and expression of murine liver phosphatidylserine synthase (PSS)-2: differential regulation of phospholipid metabolism by PSS1 and PSS2. *Biochem J, 342 (Pt 1)*, 57-64.

Stone, S. J., & Vance, J. E. (2000). Phosphatidylserine synthase-1 and -2 are localized to mitochondria-associated membranes. *J Biol Chem, 275*(44), 34534-34540. doi: 10.1074/jbc.M002865200

M002865200 [pii]

Su, C. Y., London, E., & Sampson, N. S. (2013). Mapping peptide thiol accessibility in membranes using a quaternary ammonium isotope-coded mass tag (ICMT). *Bioconjug Chem, 24*(7), 1235-1247. doi: 10.1021/bc400171j

Sud, M., Fahy, E., Cotter, D., Brown, A., Dennis, E. A., Glass, C. K., . . . Subramaniam, S. (2007). LMSD: LIPID MAPS structure database. *Nucleic Acids Res, 35*(Database issue), D527-532. doi: gkl838 [pii]

10.1093/nar/gkl838

Takamori, S., Holt, M., Stenius, K., Lemke, E. A., Gronborg, M., Riedel, D., . . . Jahn, R. (2006). Molecular anatomy of a trafficking organelle. *Cell, 127*(4), 831-846. doi: S0092-8674(06)01400-0 [pii]

10.1016/j.cell.2006.10.030

Tam, P. C., Maillard, A. P., Chan, K. K., & Duong, F. (2005). Investigating the SecY plug movement at the SecYEG translocation channel. *EMBO J, 24*(19), 3380-3388. doi: 7600804 [pii]

10.1038/sj.emboj.7600804

Tanaka, Y., Sugano, Y., Takemoto, M., Mori, T., Furukawa, A., Kusakizako, T., . . . Tsukazaki, T. (2015). Crystal Structures of SecYEG in Lipidic Cubic Phase Elucidate a Precise Resting and a Peptide-Bound State. *Cell Rep, 13*(8), 1561-1568. doi: S2211-1247(15)01179-1 [pii]

10.1016/j.celrep.2015.10.025

Tang, X., Halleck, M. S., Schlegel, R. A., & Williamson, P. (1996). A subfamily of P-type ATPases with aminophospholipid transporting activity. *Science, 272*(5267), 1495-1497.

Thevenin, D., An, M., & Engelman, D. M. (2009). pHLIP-mediated translocation of membrane-impermeable molecules into cells. *Chem Biol, 16*(7), 754-762. doi: S1074-5521(09)00204-X [pii]

10.1016/j.chembiol.2009.06.006

Utsugi, T., Schroit, A. J., Connor, J., Bucana, C. D., & Fidler, I. J. (1991). Elevated expression of phosphatidylserine in the outer membrane leaflet of human tumor cells and recognition by activated human blood monocytes. *Cancer Res, 51*(11), 3062-3066.

van den Eijnde, S. M., van den Hoff, M. J., Reutelingsperger, C. P., van Heerde, W. L., Henfling, M. E., Vermeij-Keers, C., . . . Ramaekers, F. C. (2001). Transient expression of phosphatidylserine at cell-cell contact areas is required for myotube formation. *J Cell Sci, 114*(Pt 20), 3631-3642.

van Meer, G., Voelker, D. R., & Feigenson, G. W. (2008). Membrane lipids: where they are and how they behave. *Nat Rev Mol Cell Biol, 9*(2), 112-124. doi: nrm2330 [pii]

10.1038/nrm2330

Veneziano, R., Rossi, C., Chenal, A., Devoisselle, J. M., Ladant, D., & Chopineau, J. (2013). Bordetella pertussis adenylate cyclase toxin translocation across a tethered lipid bilayer. *Proc Natl Acad Sci U S A, 110*(51), 20473-20478. doi: 1312975110 [pii]

10.1073/pnas.1312975110

Vermeer, L. S., de Groot, B. L., Reat, V., Milon, A., & Czaplicki, J. (2007). Acyl chain order parameter profiles in phospholipid bilayers: computation from molecular dynamics simulations and comparison with 2H NMR experiments. *Eur Biophys J, 36*(8), 919-931. doi: 10.1007/s00249-007-0192-9

Vitrac, H., Bogdanov, M., & Dowhan, W. (2013). In vitro reconstitution of lipid-dependent dual topology and postassembly topological switching of a membrane protein. *Proc Natl Acad Sci U S A, 110*(23), 9338-9343. doi: 1304375110 [pii]

10.1073/pnas.1304375110

Vitrac, H., MacLean, D. M., Jayaraman, V., Bogdanov, M., & Dowhan, W. (2015). Dynamic membrane protein topological switching upon changes in phospholipid environment. *Proc Natl Acad Sci U S A, 112*(45), 13874-13879. doi: 1512994112 [pii]

10.1073/pnas.1512994112

Wan, H. C., Melo, R. C., Jin, Z., Dvorak, A. M., & Weller, P. F. (2007). Roles and origins of leukocyte lipid bodies: proteomic and ultrastructural studies. *FASEB J, 21*(1), 167-178. doi: fj.06-6711com [pii]

10.1096/fj.06-6711com

Waugh, M. G. (2015). PIPs in neurological diseases. *Biochim Biophys Acta, 1851*(8), 1066-1082. doi: S1388-1981(15)00050-5 [pii]

10.1016/j.bbalip.2015.02.002

Weerakkody, D., Moshnikova, A., Thakur, M. S., Moshnikova, V., Daniels, J., Engelman, D. M., . . . Reshetnyak, Y. K. (2013). Family of pH (low) insertion peptides for tumor targeting. *Proc Natl Acad Sci U S A, 110*(15), 5834-5839. doi: 1303708110 [pii]

10.1073/pnas.1303708110

White, S. H., & Wimley, W. C. (1998). Hydrophobic interactions of peptides with membrane interfaces. *Biochim Biophys Acta, 1376*(3), 339-352. doi: S0304-4157(98)00021-5 [pii]

Wiedman, G., Herman, K., Searson, P., Wimley, W. C., & Hristova, K. (2013). The electrical response of bilayers to the bee venom toxin melittin: evidence for transient bilayer permeabilization. *Biochim Biophys Acta, 1828*(5), 1357-1364. doi: S0005-2736(13)00034-5 [pii]

10.1016/j.bbamem.2013.01.021

Williams, J. M., & Tsai, B. (2016). Intracellular trafficking of bacterial toxins. *Curr Opin Cell Biol, 41*, 51-56. doi: S0955-0674(16)30069-2 [pii]

10.1016/j.ceb.2016.03.019

Woodall, N. B., Yin, Y., & Bowie, J. U. (2015). Dual-topology insertion of a dual-topology membrane protein. *Nat Commun, 6*, 8099. doi: ncomms9099 [pii]

10.1038/ncomms9099

Wu, C., Miloslavskaya, I., Demontis, S., Maestro, R., & Galaktionov, K. (2004). Regulation of cellular response to oncogenic and oxidative stress by Seladin-1. *Nature, 432*(7017), 640-645. doi: nature03173 [pii]

10.1038/nature03173

Yamaoka, S., Miyaji, M., Kitano, T., Umehara, H., & Okazaki, T. (2004). Expression cloning of a human cDNA restoring sphingomyelin synthesis and cell growth in sphingomyelin synthase-defective lymphoid cells. *J Biol Chem, 279*(18), 18688-18693. doi: 10.1074/jbc.M401205200

M401205200 [pii]

Yang, L., Harroun, T. A., Weiss, T. M., Ding, L., & Huang, H. W. (2001). Barrel-stave model or toroidal model? A case study on melittin pores. *Biophys J, 81*(3), 1475-1485. doi: S0006-3495(01)75802-X [pii]

10.1016/S0006-3495(01)75802-X

Yasuda, S., Nishijima, M., & Hanada, K. (2003). Localization, topology, and function of the LCB1 subunit of serine palmitoyltransferase in mammalian cells. *J Biol Chem, 278*(6), 4176-4183. doi: 10.1074/jbc.M209602200

M209602200 [pii]

Yasuda, T., Tsuchikawa, H., Murata, M., & Matsumori, N. (2015). Deuterium NMR of raft model membranes reveals domain-specific order profiles and compositional distribution. *Biophys J, 108*(10), 2502-2506. doi: S0006-3495(15)00386-0 [pii]

10.1016/j.bpj.2015.04.008

Zhang, W., Bogdanov, M., Pi, J., Pittard, A. J., & Dowhan, W. (2003). Reversible topological organization within a polytopic membrane protein is governed by a change in membrane phospholipid composition. *J Biol Chem, 278*(50), 50128-50135. doi: 10.1074/jbc.M309840200

M309840200 [pii]

Zhang, W., Campbell, H. A., King, S. C., & Dowhan, W. (2005). Phospholipids as determinants of membrane protein topology. Phosphatidylethanolamine is required for the proper topological organization of the gamma-aminobutyric acid permease (GabP) of Escherichia coli. *J Biol Chem, 280*(28), 26032-26038. doi: M504929200 [pii]

10.1074/jbc.M504929200

Zinser, E., Sperka-Gottlieb, C. D., Fasch, E. V., Kohlwein, S. D., Paltauf, F., & Daum, G. (1991). Phospholipid synthesis and lipid composition of subcellular membranes in the unicellular eukaryote Saccharomyces cerevisiae. *J Bacteriol, 173*(6), 2026-2034.

Appendix:

Below is the program “processSPEX.py” to be executed through free-libre open source (FLOSS)

program Python (32 bit, V3.3.0)

```
# -*- coding: utf-8 -*-
"""
Spyder Editor

This temporary script file is located here:
C:\Program Files\WinPython-32bit-3.3.0.0beta2\settings\.spyder2\.temp.py
"""

"""
FILE HISTORY:
  created ~2013/03/25 by J. LeBarron
  2013/06/19 JL : improved comments, made result columns tab delimited
  2014/03/28 JL : fixed header size bug, added 2 aquMode list for MultiGroup
  2014/07/02 JL : now handles ? numbers other than two
"""
class cSPEX:
  def __init__(self, arguments): #,master):
    pass
    """ how to use in sepereate file:
    from imp import reload
    import fSPEX
    a = fSPEX.cSPEX()
    filename = r'the R really needs to be there'
    a.readSPEX(filename)
    """

  def readCommands(self,filename):
    '''
    Reads command file containing path for all data files and how to proccess
    them. Reads command file, opens data files and smooths if requested,
    returns all processed curves at end of command file given in vertical
    columns. Currently only smooths files and subtracts.
    Command format: data\filename\string (with ?? signifing # to be replaced)
                  : Num1 func Num2
    '''

    from os.path import normpath
    thingy = open(normpath(filename), mode='tr+')
    f = thingy.readlines()

    prefix = f[0].split()[0]  #strip off return carriage off file names
    numQuest = prefix.count('?')
    comList = []              #create empty list, will hold commands
    finalList=[]              #holds all result data, loop through to print



    #values to pass to Savitsky_Golay filter, when used
    SG_window = int(21) # to match SPEX window most used
    SG_strength = int(7)#match SPEX apparent filtering polynomial used, or 5?

    """
    Every element of comList is at most a 3tuple of files to maniputlate.For
    every 3tuple, open two files, check for consistency, possibly smooth
    values, and do math. Save all to append to command filename later
    """
```

```
    for i in f[1:]:
      if len(i) > 1 :
        comList.append(i.split())

    for i in comList:

      #if no smoothing wanted, set first file name
      if len(i[0]) == numQuest:
        file1=prefix.replace(numQuest*'?',i[0])
        data1 = self.readSPEX(file1)

      #if s in front first filename (wants smoothing)
      elif (len(i[0])==numQuest+1) and i[0][0].lower() == 's':
        file1 = prefix.replace(numQuest*'?',i[0][1:])
        data1 = self.readSPEX(file1)
        smoothed = self.savitzky_golay(data1[-1],SG_window,SG_strength)

        #typecast smoothed and instert to data1: array->list->tuple
        hold = []
        for j in smoothed: hold.append(j)
        data1[-1] = tuple(hold)

      else: file1= 'Error_Type_1. File_attempt'+str(i[0])

      #If 2nd filename exists in this command, w/o smoothing, set filename
      if len(i) >= 3:
        if len(i[2]) == numQuest:
          file2 = prefix.replace(numQuest*'?',i[2] )
          data2 = self.readSPEX(file2)

        #2nd filename exists, and wants smoothing. Treat as fn1 smoothed.
        elif (len(i[2])==numQuest+1) and i[2][0].lower() == 's':
          file2 = prefix.replace(numQuest*'?',i[2][1:])
          data2 = self.readSPEX(file2)
          smoothed = self.savitzky_golay(data2[-1],SG_window,SG_strength)

          hold = []
          for j in smoothed: hold.append(j)
          data2[-1] = tuple(hold)

        else: file2= 'Error_Type_2 File_attempt'+str(i[2])

      """
      create list of data that will be output to command list file. Most data
      is passed from 1st data file, but actual values need to be computed.
      _SOME_ consistancy checking b/w 1st and 2nd data file performed.
      """
      """
      i = commands for this line of command list. Cast command tuple to
      string, add to end of 1st data file data. _CURRENTLY_ only supports
      subtraction b/w files, but can be smoothed at any point.
      """

      il =''
      for element in i:
          il = il+str(element)
      preresult = [data1[0],data1[1],data1[2],data1[3],data1[4],
                           data1[5],data1[6],str(data1[7])+' sec,
'+data1[8],il]

      #file substraction, enforcing same length
      if (len(i) >= 3) and (i[1]=='-') and (data1[0:3]==data2[0:3]):
```

```
        resultdata=[]

        #subtract two datas, which are individually already smoothed, if
wanted
        for k in range(len(data1[-1])):
          resultdata.append(data1[-1][k]-data2[-1][k])

        #smooth subtraction result, if wanted
        if len(i) == 4 and i[3][0].lower() == 's':
          subSmooth = self.savitzky_golay(resultdata,SG_window,SG_strength)
          holder = []
          for j in subSmooth: holder.append(j)
          resultdata = holder

        #add results to preresult, then add to output data
        preresult.extend(resultdata)
        finalList.append(preresult)

      #for one file in i =commands, pass data to finallist
      if len(i) ==1:
        resultdata=[]

        for k in range(len(data1[-1])):
          resultdata.append(data1[-1][k])

        preresult.extend(resultdata)
        finalList.append(preresult)

    '''
    Done with all file commands, now print. get largest non-whitespace entry
    using split, pad the rest of the entries to the same str length. then for
    range(len(comlist)), print data going down.

    Cycle through all the file manipultations (len(finalList)), get longest
    string from all entries (len (finalList x y)).
    '''
    padlength = -1
    test = finalList[0][:3],len(finalList[0])

    for x in range(len(finalList)):
      if (finalList[x][:3],len(finalList[x])) != test:
        test = 0

      for y in range(len(finalList[x])):
        padlength = max(padlength, len(str(finalList[x][y])))
    padlength = padlength +1

    #empty line between file input and output
    thingy.write('\n')

    '''
    cycle through created data, build output string, write string to file
    if test passed(set to !0) means all data same. Build x axis array to
    hold x positions for all
    '''

    #for test values, make X axis, vert. pad for preresult, and skip 3
entries
    startPt = 0
    if test != 0:
      startPt = 3
      xPad = len(finalList[0])-startPt-finalList[0][2] #vertical padding
xaxis
      xAxis = ['-'* len(str(finalList[0][0]+finalList[0][1]*1))] #pad with
```

```
      xAxis = xAxis*xPad

      for i in range(finalList[0][2]): #[0][2] is num of steps
        xAxis.append(str(finalList[0][0]+finalList[0][1]*i))
        #x value = startX +step*numSteps

    #loop through vert. entries, gathering xaxis, and all other data
    for y in range(startPt,len(finalList[0])): #for individual entries
      outline=''
      if (test !=0):    # and (y >= len(finalList[0])-test[0][2]):
        outline=outline+str(xAxis.pop(0))+"\t"

      for x in range(len(finalList)):
        outline=outline+str(finalList[x][y]).rjust(padlength)+"\t"

      thingy.write(outline+'\n')

    thingy.close()
    #return finalList #data1,data2,resultdata

  def readSPEX(self,datafile):
      '''
      reads in filename(.spt) that contains SPEX data, returns:
          [startX,incX, numX, date,expmtType,sType,scanDim, intTime,
           aquMode,titleX,titleY,titleZ,output]
      '''
      from struct import unpack
      from string import printable
      import os

      #usefull commands; os.path.normpath(r"string")
      #baseDIR=os.path.normpath("E:\London_Lab\Curves_for_Testing")

      #read data into bytearray, then discard datafile
      thingy = open(os.path.normpath(datafile),mode = "rb")
      data = thingy.read()
      del thingy

      #get firmware version, set what kind of expermint created data file
      Hard_Software  = list(data[0:11])
      expmtType = ["Excitation scan","Emission scan","Time base measurement",
             "Temperature scan","Simple scan","CCD array detector scan",
             "Cation measurement","Phos. Excitation scan","Phos Emission
scan",
             "Phos. Synchronous scan","Phos. Lifetime base scan","Multi-
group",
             "PDA"]
      expmtType = expmtType[Hard_Software[2] -1]

      #get time when expmt performed, stack into usefull form
      year = str(data[34]) + str(data[35])
      month = str(data[36]).rjust(2,str(0))
      day = str(data[37]).rjust(2,str(0))

time=str(data[38]).rjust(2,str(0))+str(":")+str(data[39]).rjust(2,str(0))
      date = str(year)+'/'+str(month)+'/'+str(day)+' '+str(time)

      spectrumTitle = str(data[40:70])

      """take position of monochromoters from file, (each position stored as
      double (=8 bytes)). struct.unpack unpacks 8 bytes to one double (d) #.
      This returns tuple of one value, must extract THAT to single (float)
      number. Only ex1 and em1 are used/ in our machine, apparently.
      """
```

```
        ex1 = unpack('d', data[74:82])[0]
        #ex2 = unpack('d', data[82:90])[0]
        em1 = unpack('d', data[90:98])[0]
        #em2 = unpack('d', data[98:106])[0]
        #grooveDensity = unpack('4f', data[204:220]) #ex1 ex2 em1 em2

        #take movement of monochromoters during experiment.
        #SHOULD cross reference with Hard_Software values.
        ex1Move = unpack('d', data[106:114])[0]
        #ex2Move = unpack('d', data[114:122])[0]
        em1Move = unpack('d', data[122:130])[0]
        #em2Move = unpack('d', data[130:138])[0]
        #mChromUsed = bin(data[139]) #bit flags, XXXX em2 em1 ex2 ex1

        #determine type of expmt from what moved
        if ex1Move == 0:   sType = 'Excite at '+str(ex1)
        elif em1Move == 0: sType = 'Emission at '+str(em1)
        else: print('Error with excitation/emission readings')

        #get unit measured, start of X axis, size and # of increments
        scanDim =["Nanometer","Angstrom","Wavenumbers","Delta_Wavenumbers",
            "eV","Microns"]
        scanDim =scanDim[data[138]-1]
        startX=unpack('d', data[142:150])[0]
        incX = unpack('d', data[150:158])[0]
        numX = unpack('H', data[158:160])[0]

        #integration time (sec) per inrement, & acquistion mode (byte 164 ONLY)
        intTime = unpack('f',data[160:164])[0]
        aquMode=['S','R','S/R','S&R','(S1/R1)/(S2/R2)','S1/R1 & S2/R2',
                 'S1,R1,S2 &R2','Live array detector scan',
                 'Accumulated array detector scan','S1','R1','S1/R1','S1&R1',
                 'S2','R2','S2/R2','S2&R2','S1/S2','S1&S2','R1&R2',
                 'Polarization','Anisotropy','Raw polarization',
                 'Vert. Polarization','Horiz. Polarization','p35 Polarization',
                 'p55 Polarization','num27','num28','num29','num30','num31',

'num32','num33','num34','num35','num36','num37','num38','num39',

'num40','num41','num42','num43','num44','num45','num46','num47',
                 'num48','num49','num50','all S/R inputs']
        aquMode=aquMode[data[164]]

        #high voltage setting for photomultiplier
        voltSettings = unpack('4h', data[244:252])

        #create empty axis titles, pull from file
        titleX = titleY = titleZ = ''
        for a in data[266:286]:
          if chr(a) in printable:
            titleX = titleX + chr(a)
        for a in data[286:306]:
          if chr(a) in printable:
            titleY = titleY + chr(a)
        for a in data[306:326]:
          if chr(a) in printable:
            titleY = titleY + chr(a)

        #possibly collect comments from file
        anyComments =''
        for a in data[432:512]:
          if chr(a) in printable:
            anyComments = anyComments + chr(a)
```

```
      """   FIXED
      hard code header offset in bytes which sets where collected data
starts.
      Should be variable in data[140:142], but values there don't make sense
      """
      #headerOffset = int(512)
      headerOffset = unpack('H', data[140:142])[0]
      if (len(data)-headerOffset) /4 == numX:
        output = unpack(str(numX)+'f', data[headerOffset:len(data)])
      return [startX,incX, numX, date,expmtType,sType,scanDim,
              intTime,aquMode,titleX,titleY,titleZ,output]

  def savitzky_golay(self, y, window_size, order, deriv=0, rate=1):
    r"""Smooth (and optionally differentiate) data with aSavitzky-Golay
filter.
    The Savitzky-Golay filter removes high frequency noise from data.It has
the
    advantage of preserving the original shape and features of the signal
    better than other types of filtering approaches, such as moving averages
    techniques. http://www.scipy.org/Cookbook/SavitzkyGolay
    """
    # limit help info to paragraph above
    """
    Parameters
    ----------
    y : array_like, shape (N,)
        the values of the time history of the signal.
    window_size : int
        the length of the window. Must be an odd integer number.
    order : int
        the order of the polynomial used in the filtering.
        Must be less then `window_size` - 1.
    deriv: int
        the order of the derivative to compute(default =0 means only
smoothing)
    Returns
    -------
    ys : ndarray, shape (N)
        the smoothed signal (or it's n-th derivative).
    Notes
    -----
    The Savitzky-Golay is a type of low-pass filter, particularly
    suited for smoothing noisy data. The main idea behind this
    approach is to make for each point a least-square fit with a
    polynomial of high order over a odd-sized window centered at
    the point.
    Examples
    --------
    t = np.linspace(-4, 4, 500)
    y = np.exp( -t**2 ) + np.random.normal(0, 0.05, t.shape)
    ysg = savitzky_golay(y, window_size=31, order=4)
    import matplotlib.pyplot as plt
    plt.plot(t, y, label='Noisy signal')
    plt.plot(t, np.exp(-t**2), 'k', lw=1.5, label='Original signal')
    plt.plot(t, ysg, 'r', label='Filtered signal')
    plt.legend()
    plt.show()
    References
    ----------
    .. [1] A. Savitzky, M. J. E. Golay, Smoothing and Differentiation of
       Data by Simplified Least Squares Procedures. Analytical
       Chemistry, 1964, 36 (8), pp 1627-1639.
    .. [2] Numerical Recipes 3rd Edition: The Art of Scientific Computing
       W.H. Press, S.A. Teukolsky, W.T. Vetterling, B.P. Flannery
```

```
       Cambridge University Press ISBN-13: 9780521880688
    """
    import numpy as np
    from math import factorial, fabs
    try:
        window_size = np.abs(np.int(window_size))
        order = np.abs(np.int(order))
    except ValueError :#, msg:
        raise ValueError("window_size and order have to be of type int")
    if window_size % 2 != 1 or window_size < 1:
        raise TypeError("window_size size must be a positive odd number")
    if window_size < order + 2:
        raise TypeError("window_size is too small for the polynomials order")
    order_range = range(order+1)
    half_window = (window_size -1) // 2

    # precompute coefficients
    b = np.mat([[k**i for i in order_range] for k in range(-half_window,
half_window+1)])
    m = np.linalg.pinv(b).A[deriv] * rate**deriv * factorial(deriv)

    """
    pad the signal at the extremes with values taken from the signal itself
    this >>> firstvals = y[0] - np.abs( y[1:half_window+1][::-1] - y[0] ) <<<
    from online doesn't work, reverse engineered firstvals & lastvals myself
    """

    firstvals = []
    for i in  y[1:half_window+1][::-1]:
      thing = y[0] - fabs(i-y[0])
      firstvals.append(thing)

    #lastvals = y[-1] + np.abs(y[-half_window-1:-1][::-1] - y[-1])
    lastvals=[]
    for i in y[-half_window-1:-1][::-1]:
      thing = y[-1] - fabs(i-y[-1])
      lastvals.append(thing)

    y = np.concatenate((firstvals, y, lastvals))
    return np.convolve( m[::-1], y, mode='valid')

if __name__ == '__main__':
    import sys
    from os.path import exists
    for i in sys.argv[1:]:
      if exists(i):
        bob = cSPEX(i)
        bob.readCommands(i)
      else:
        print(r'filename --> '+i+' does not exist,try again')

'''Then, from a shell,

$ convertImage.py the_image_file.png
/var/www/uploads/tmp/the_image_file.png
'''
```

Supplemental Materials to Chapter 3

Effect of Lipid Composition and Amino Acid Sequence Upon Transmembrane Peptide-Accelerated Lipid Transleaflet Diffusion (Flip-Flop)

Figure A.1:

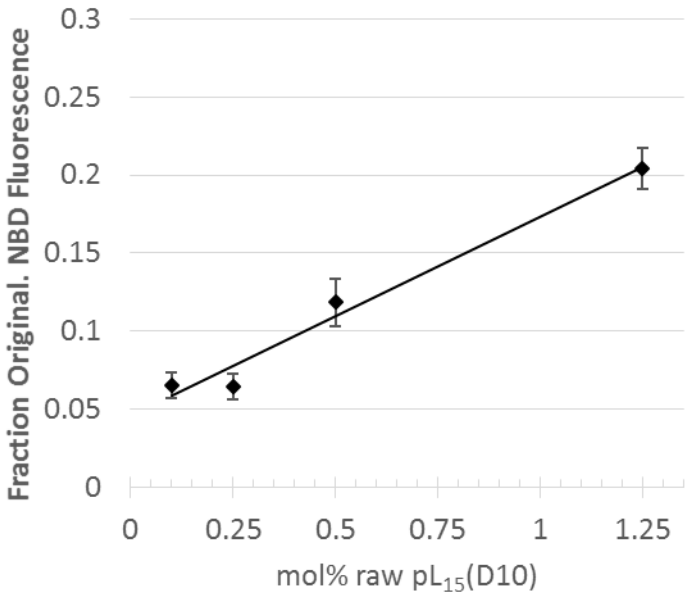

Fig A.**1:** Dependence of peptide-accelerated lipid flip-flop upon concentration of pL_{15}(D10). DOPC LUV were prepared as described in Methods with different mol% pL_{15}(D10) included in vesicles. NBD-PC was added to preformed vesicles and samples then incubated at room temp for 2 h prior to NaDt addition. Data processed as in Methods. Values shown are averages of three experiments with peptide-free blank values subtracted, and with bars representing standard deviation. Unpurified (about 85% pure) pL_{15}(D10) was used in these experiments.

Figure A.2:

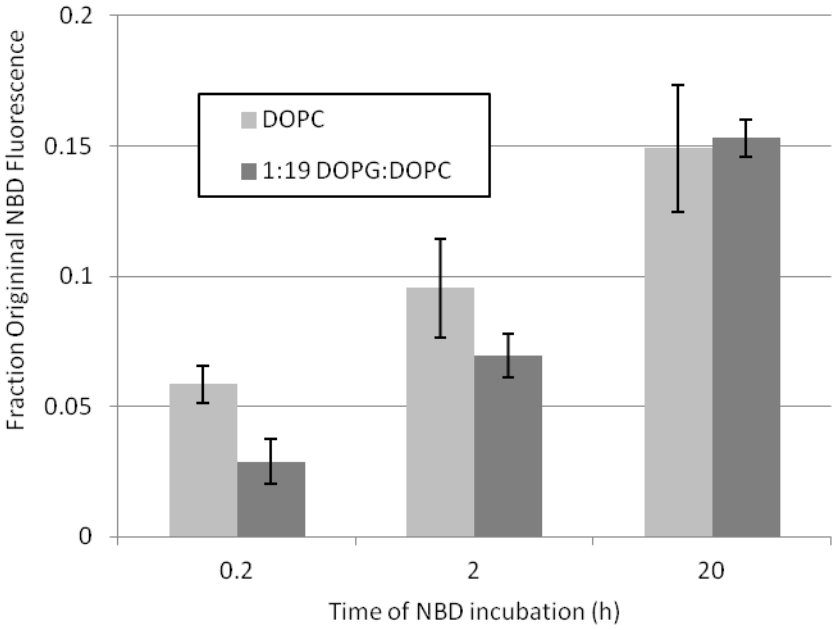

Fig A.2: Comparison of pL_{15}(D10) accelerated flip-flop in SUV composed of DOPC or DOPC with 5 mol% DOPG (plus peptide). Data processed as described in Methods. Values shown are averages of three experiments with peptide-free blank values subtracted, and with bars representing standard deviation. Unpurified pL_{15}(D10) (about 85% pure) was used in these experiments.

Figure A.3:

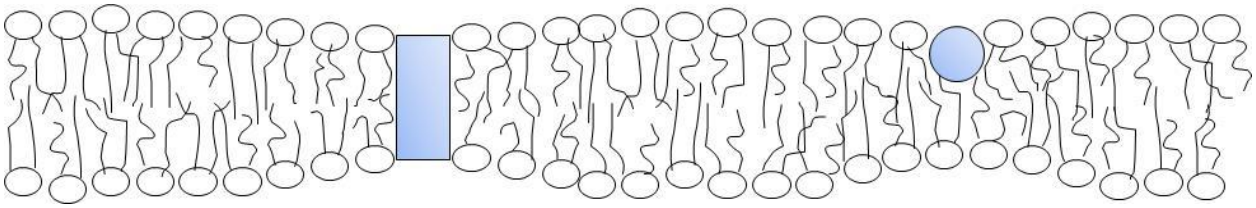

Fig A.3: Schematic figure illustrating membrane thinning by alpha helices for a short transmembrane (blue rectangle) or shallowly-inserted non-transmembrane (blue circle representing helix seen end on) states.

Supplemental Materials for Chapter 4

Highly hydrophilic segments attached to hydrophobic peptides translocate rapidly across membranes

	Rh (nm)		Poly Disp (%)	
	Avg	**SD**	**Avg**	**SD**
blank	15.4	1.8	27.4	5.0
N_0K_2	20.8	2.3	41.2	10.9
N_2K_2	57.3	22.1	32.9	9.7
N_6K_2	63.3	6.5	22.5	9.8
Polio	22.3	5.4	45.0	9.9

Table A.1. Dynamic light scattering-determined size of vesicles prepared by ethanol dilution. Vesicles containing 200 μM POPC with 1 mol% peptide were diluted 14-fold before measuring dynamic light scattering. Values are averages/standard deviations of for independent samples. Avg = average; SD = standard deviation.

A:

N_0K_2 -flanked peptide			0	12 sec	5 min	30 min	20 hr
EtOH vesicles 100% POPC	3.9 → 9.3	Ratio	0.83 ± 0.003	1.11 ± 0.014	1.11 ± 0.015	1.09 ± 0.038	1.08 ± 0.041
		λ max	**329**			**338**	**337**
	9.1 → 3.7	Ratio	1.10 ± 0.003	0.86 ± 0.005	0.82 ± 0.006	0.82 ± 0.006	0.83 ± 0.031
		λ max	**338**			**328**	**328**
EtOH vesicles 60% POPC 40% chol	3.9 → 9.3	Ratio	1.03 ± 0.005	1.09 ± 0.009	1.12 ± 0.005	1.12 ± 0.012	
		λ max	**334**			**339**	
	8.8 → 3.5	Ratio	1.13 ± 0.004	1.01 ± 0.003	0.99 ± 0.001	1.00 ± 0.001	
		λ max	**339**			**335**	
Freeze-thaw 100% POPC	4.2 → 9.9	Ratio	0.83 ± 0.001	1.01 ± 0.005	1.05 ± 0.007	1.04 ± 0.001	1.03 ± 0.014
		λ max	**328**			**337**	**334**
	9.2 → 3.7	Ratio	1.02 ± 0.004	0.75 ± 0.011	0.75 ± 0.006	0.75 ± 0.004	0.75 ± 0.003
		λ max	**335**			**326**	**324**
Freeze-thaw 60% POPC 40% chol	3.6 → 9.9	Ratio	0.99 ± 0.001	1.06 ± 0.005	1.10 ± 0.002	1.11 ± 0.042	1.26 ± 0.311
		λ max	**334**			**337**	**343**
	9.3 → 3.7	Ratio	1.08 ± 0.008	1.03 ± 0.041	1.00 ± 0.020	1.01 ± 0.007	0.99 ± 0.023
		λ max	**337**			**334**	**333**

B:

N_2K_2 -flanked peptide			0	12 sec	5 min	30 min	20 hr
EtOH vesicles 100% POPC	3.6→ 9.8	Ratio	0.78 ± 0.006	1.11 ± 0.003	1.06 ± 0.004	1.06 ± 0.004	1.03 ± 0.007
		λ max	325			336	335
	9.9→ 3.9	Ratio	1.05 ± 0.004	0.76 ± 0.010	0.78 ± 0.007	0.79 ± 0.009	0.76 ± 0.005
		λ max	335			325	324
EtOH vesicles 60% POPC 40% chol	3.9 → 9.6	Ratio	0.96 ± 0.003	1.08 ± 0.006	1.08 ± 0.004	1.07 ± 0.008	1.05 ± 0.020
		λ max	332			337	337
	10.1 → 3.5	Ratio	1.08 ± 0.006	0.94 ± 0.003	0.93 ± 0.004	0.94 ± 0.009	0.93 ± 0.030
		λ max	**337**			**331**	**331**

C:

N_6K_2 -flanked peptide			0	12 sec	5 min	30 min	20 hr
EtOH vesicles 100% POPC	3.9 → 9.5	Ratio	0.80 ± 0.001	1.06 ± 0.012	1.07 ± 0.018	1.10 ± 0.002	
		λ max	**327**			**340**	
	9.4 → 4.0	Ratio	1.05 ± 0.006	0.82 ± 0.018	0.80 ± 0.011	0.77 ± 0.005	
		λ max	**336**			**325**	
EtOH vesicles 60% POPC 40% chol	9.5 → 3.9	Ratio	1.29 ± 0.008	1.21 ± 0.014	1.13 ± 0.028	1.14 ± 0.017	
		λ max	**342**			**338**	
	4.0 → 9.5	Ratio	1.12 ± 0.007	1.18 ± 0.019	1.23 ± 0.012	1.29 ± 0.011	
		λ max	**338**			**342**	
Freeze-thaw 100% POPC	4.2 → 10.0	Ratio	0.76 ± 0.002	1.15 ± 0.026	1.18 ± 0.009	1.21 ± 0.014	1.20 ± 0.015
		λ max	**325**			**339**	**340**
	8.7 → 3.7	Ratio	1.16 ± 0.009	0.87 ± 0.006	0.80 ± 0.012	0.78 ± 0.002	0.76 ± 0.011
		λ max	**340**			**325**	**324**
Freeze-thaw 60% POPC 40% chol	3.9 → 9.7	Ratio	1.07 ± 0.012	1.06 ± 0.052	1.12 ± 0.019	1.16 ± 0.004	1.28 ± 0.064
		λ max	**337**			**339**	**342**
	10.0 → 3.5	Ratio	1.20 ± 0.008	1.19 ± 0.090	1.12 ± 0.025	1.10 ± 0.005	1.07 ± 0.022
		λ max	**341**			**338**	**338**

D:

Polio-flanked peptide			0	12 sec	5 min	30 min	20 hr
EtOH vesicles 100% POPC	3.6 → 9.9	Ratio	0.80 ± 0.001	1.05 ± 0.005	1.04 ± 0.004	1.05 ± 0.007	1.06 ± 0.003
		λ max	**328**			**336**	**337**
	9.6 → 3.7	Ratio	1.05 ± 0.003	0.83 ± 0.003	0.82 ± 0.002	0.81 ± 0.003	0.80 ± 0.001
		λ max	**336**			**327**	**327**
EtOH vesicles 60% POPC 40% chol	3.5→ 9.9	Ratio	0.93 ± 0.012	1.04 ± 0.007	1.06 ± 0.005	1.06 ± 0.007	1.08 ± 0.011
		λ max	**332**			**337**	**336**
	9.7 → 3.8	Ratio	1.09 ± 0.001	0.97 ± 0.009	0.97 ± 0.003	0.97 ± 0.003	0.95 ± 0.010
		λ max	**337**			**333**	**332**

Table A.2. Values for 345/325 and emission lambda max from experiments shown in Figure 4.3-6 before and after shifting pH. A. N_0K_2 -flanked peptide; B. N_2K_2 -flanked peptide; C. N_6K_2 -flanked peptide; D. Polio-flanked peptide.

N_6K_2- flanked peptide

	pH	λ Max.	Δ λ Max.
POPC	3.6	327	14
	9.8	341	
POPC 40 mol% chol	3.6	335	8
	9.6	343	
DEuPC	3.6	337	2
	9.8	339	
DEuPC 40 mol% chol	3.6	338	2
	9.9	340	

Polio-flanked peptide

POPC	3.5	328	9
	9.7	337	
POPC 40 mol% chol	3.6	330	7
	9.7	337	
DEuPC	3.5	336	3
	9.8	339	
DEuPC 40 mol% chol	3.9	336	2

TableA.3. Comparison of effect of lipid composition on the wavelength of maximum fluorescence emission for peptides as a function of and pH. Peptides were incorporated during the formation of ethanol dilution vesicles at either pH ~4 or ~10 with lipid compositions shown. Fluorescence intensity and wavelength of maximum Trp emission (λ max) was recorded. Δ λ max is the difference between λ max at acidic and basic pH. Values shown are averages from three samples. λ max values are reproducible to ±1 nm. -It should be noted that DEuPC, a lipid with 22 carbon acyl chains, forms a bilayer too thick for the TM state form for the peptides of the type used in this study (Caputo & London, 2004; Krishnakumar & London, 2007a, 2007b; Ren *et al.*, 1997; Shahidullah *et al.*, 2010; Shahidullah & London, 2008) (and see Figure 1). The data shows that, at least for the N_6K_2-flanked and polio-flanked peptides, changing pH in DEuPC vesicles has a much smaller effect on λ max than in POPC vesicles, with or without cholesterol.

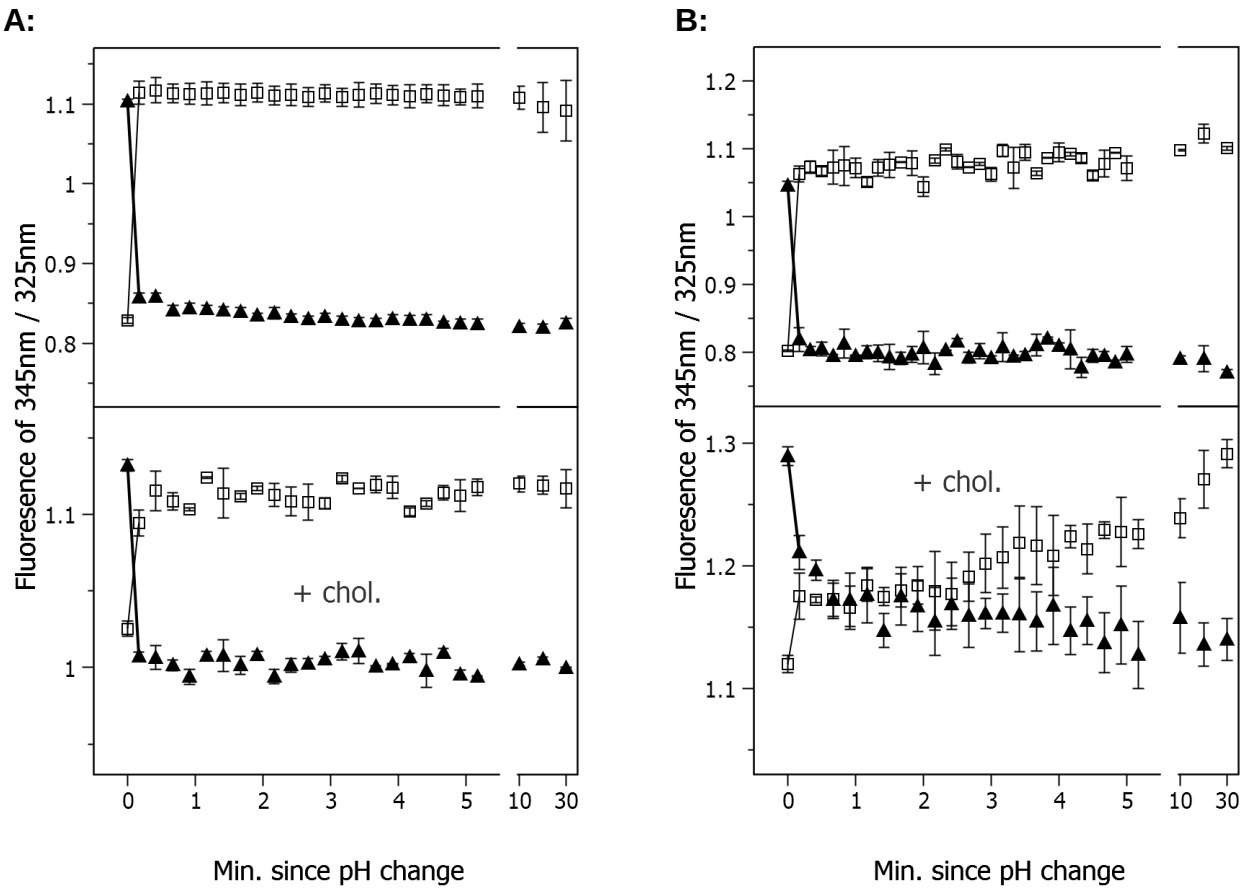

Figure A.4: Full data for pH-induced interconversion of Asn flanked peptide. Re-graph of data for ethanol dilution vesicles with all time points shown for Figures 4.3 and 4.5. The ratio of Trp fluorescence emission intensities at 345 and 325 nm before and subsequent to pH shifts is shown. Vesicles prepared at pH ~4 and shifted to pH ~10 represented by open squares. Filled triangles represent ethanol dilution vesicles prepared at pH ~10 and shifted to pH ~4. Other conditions identical to Figure 3. **A:** Vesicles containing 1 mol% N_0K_2-flanked peptide. **B:** Vesicles containing 1 mol% N_6K_2-flanked peptide.